Statistical Field Spectral Calculations in Some Problems of Anisotropic Turbulence

A thesis submitted in
partial fulfillment of the requirements
for the degree of

DOCTOR OF PHILOSOPHY

by

Kishore Dutta

Department of Physics
Indian Institute of Technology Guwahati

February 2010

Certificate

This is to certify that the work contained in this thesis, entitled **"Statistical Field Spectral Calculations in Some Problems of Anisotropic Turbulence"** has been carried out by Kishore Dutta under my supervision and that this work has not been submitted elsewhere for a degree.

Dr. Malay K. Nandy
Associate Professor
Depertment of Physics
I.I.T. Guwahati
India

Dedicated
to
"MY SOURCE OF INSPIRATION"

Acknowledgements

I would like to express my profound appreciation to my supervisor, Dr. Malay K. Nandy, Associate Professor, IIT Guwahati, for his careful guidance in the area of theoretical aspects of turbulence, encouragement on creative thinking, teaching, and fruitful discussions.

I Sincerely thank Professors A. Khare, C. Y. Kadolkar, M. Pandey, and D. C. Dalal of IIT Guwahati for their valuable academic advice and generous help in carrying out my research work smoothly. I would like to thank everybody in the Department of Physics, Indian Institute of Technology Guwahati, for providing me a sound research environment. I take this oppertunity to thank all my current and previous teachers throughout my entire student carreer for their teaching, enlightening guidance, inspiration and encouragement.

Kishore Dutta

Synopsis

In this research work we apply the "standard" perturbative methods to some anisotropic cases of fluid turbulence and obtain information about the effect of anisotropy within such frameworks. As a matter of fact, the anisotropy makes the problems much more complex than the corresponding isotropic cases, and we hope that such a study will have both academic and practical relevance.

Homogeneous shear turbulence has been studied in great details in the last few decades. The cases of anisotropic turbulence have been mostly dealt with $SO(3)$ decomposition [102]. However, we take alternative routes to the problems of anisotropic turbulence and hence we are interested in tackling directly the anisotropic terms appearing in the dynamical equations by means of "standard" perturbative methods. In practical applications, what one is interested in is the effect of turbulence on the mean flow and on transport, which is parametrized in terms of eddy-viscosities and eddy-diffusivities. In some cases, in order to calculate these quantities, information about the turbulent energy spectrum is necessary, and the universal Kolmogorov spectrum with scaling law $E(k) = C\,\varepsilon^{2/3}k^{-5/3}$ is usually assumed. Here k is the wavenumber, ε is the energy flux, and C the universal Kolmogorov constant.

Since most flows occurring in nature are inherently anisotropic, the dynamics of anisotropic turbulent shear flow has attracted much attention, mostly experimental, during the last few decades. Persistence of small scale anisotropy in high Reynolds-number turbulence subject to imposed large scale anisotropy has been demonstrated experimentally [141]. A number of numerical and experimental investigations in shear flow turbulence have shown that the anisotropy appears not only at higher order moments, but also at second

order moments. We carried out a perturbative analysis along the lines suggested by Leslie [90] for homogeneous shear turbulence where the isotropic background field is strained by the uniform shear. We make a perturbative expansion of the velocity correlation tensor, which has contributions due to isotropy as well as due to imposed anisotropy. Through direct calculations, we obtain anisotropic correction to the equal-time velocity correlation tensor, which is of the form $Q_{ij}^{(1)}(\mathbf{k},0) = S_{ab}\left[P_{ia}(\mathbf{k})P_{jb}(\mathbf{k}) + P_{ja}(\mathbf{k})P_{ib}(\mathbf{k})\right] R^{(1,1)}(k) + S_{lm}\dfrac{k_l k_m}{\mathbf{k}^2} P_{ij}(\mathbf{k})\, R^{(1,3)}(k)$. It may be noted that, this form of anisotropic velocity correlation tensor is derived rather than it is conjectured. In this expression, the factors $R^{(1,1)}(k)$ and $R^{(1,3)}(k)$, the integrands of which involve isotropic correlation and response functions, are found to be of the form $R^{(1,1)}(k) = A\ \varepsilon^{1/3}k^{-13/3}$ and $R^{(1,3)}(k) = B\ \varepsilon^{1/3}k^{-13/3}$, where A and B are two non-dimensional universal numbers. We calculate A and B using inputs from renormalization group calculations. Our calculated values of A and B are $A = -0.13$ and $B = -0.48$. These values are comparable with the experimental values $A \approx -0.17$ and $B \approx -0.45$ [164]. Thus, we note that, our calculated values, specifically the value of B, is quite better than earlier theoretical results and it is found to be very close to the experimental values as well as direct numerical simulation (DNS) values [61, 185].

There is an another class of problems, namely, stratified turbulence, where the scalar (density or temperature) field is coupled to the momentum equation by an imposed buoyancy force ($N\psi\hat{e}_3$ term in the momentum equation). In addition, an extra term (namely, $-Nu_3$) appears in the advection equation for the scalar field (N is the Brunt-Väisälä frequency). When we apply Leslie's perturbation method to this problem, it is found that information about the passive scalar dynamics is necessary and we treat the problem in the Heisenberg approximation.

For passive scalar convection, a scaling law, similar to the Kolmogorov's, holds for the mean-square scalar given by $\mathcal{E}(k) =$ Ba $\chi\ \varepsilon^{-1/3}\ k^{-5/3}$, where Ba is the Batchelor constant and χ is the scalar flux. We derive analytic expressions for eddy-viscosity and eddy-diffusivity from the transfer integrals

of energy and mean-square scalar implementing Heisenberg's approximation. In the same scheme, we evaluate the flux integrals for energy and mean-square scalar. These procedures allow for the evaluation of relevant amplitude ratios, from which we calculate the universal numbers, namely, Batchelor constant (Ba) and turbulent Prandtl number (σ), under two different schemes (with ϵ expansion and without ϵ expansion). Our calculations yield $\sigma = 0.7179$ and Ba $= 1.0311$. These results are comparable with other theoretical calculations, namely, Yakhot-Orszag's renormalization group calculation (Ba $= 1.16$ and $\sigma = 0.7179$) [183] and experimental investigations (Ba ≈ 1.0 and $\sigma \approx 0.7 - 0.9$) [111, 70]. As a byproduct, we obtain a relation between Kolmogorov constant (C), Batchelor constant (Ba) and turbulent Prandtl number (σ), namely, Ba $= \sigma\ C$, which is consistent with that of Yakhot and Orszag's (derived from Pao's formulations) [184, 183]. We also carried out calculations of these universal numbers in arbitrary space dimensions. To compare our results with the experimental values, we calculated Batchelor constant in one dimension, leading to Ba$' = 0.62$. As stated earlier, these universal numbers are found to be useful because they occur in our calculations of the universal numbers occurring as coefficients in various anisotropic spectra associated with stratified turbulence.

To carry out the problem further, we perform Leslie's perturbative treatment [90] on stably stratified turbulence, where the terms $N\psi\hat{e}_3$ and $-Nu_3$ in the corresponding dynamical equations are treated as perturbations against the isotropic background fields. Thereby, we make perturbation expansions of the velocity and scalar fields. This enables us to evaluate the corresponding corrections to various correlation functions, namely, velocity-velocity, temperature-temperature, and velocity-temperature correlations. The resulting anisotropic corrections to the velocity-velocity and temperature-temperature correlations turn out to be of the forms $C_1N^2P_{i3}(\mathbf{k})P_{j3}(\mathbf{k})k^{-5}$ and $C_2N^2P_{33}(\mathbf{k})k^{-5}$, and the velocity-temperature correlation function of the form $C_3NP_{i3}(\mathbf{k})k^{-13/3}$, where $P_{ij}(\mathbf{k}) = \delta_{ij} - k_ik_j/\mathbf{k}^2$. It is found that the prefactors C_1, C_2 and C_3 depend on ε, χ, C, Ba, and σ, and hence they are

calculable. It is obvious that the above calculations yield the anisotropic part of energy and mean-square scalar spectra as k^{-3} and the anisotropic buoyancy spectrum as $k^{-7/3}$. We note that, at sufficiently large scales, the anisotropic k^{-3} spectrum would dominate over the isotropic $k^{-5/3}$ spectrum. Thus we expect a k^{-3} power law behavior of energy spectrum at sufficiently large scales. It may be noted that this scenario is similar to the analysis of experimental investigations by Nastrom and Gage [115, 116], who analysed the atmospheric data (upper troposphere and lower stratosphere) collected by NASA instrumented commercial Boeing 747 airliners, and found that the atmospheric energy spectra follow the -3 power law in the synoptic scales and the $-5/3$ power law in the mesoscales with a smooth transition in between. Following this, various hypotheses on the origin of the spectra have been proposed, such as 2D turbulence with two sources [92], internal gravity waves [35, 55]. Calculation of third order structure function [29] suggested a forward cascade with $k^{-5/3}$ spectrum in the mesoscale range. To explain the spectra of stably stratified turbulence, there followed various attempts such as direct energy cascade in a two-layer quasigeostrophic (QG) model [167], surface QG models [165, 150], stratified turbulence simulations [18], and spectral condensation of the inverse cascade in 2D turbulence [180, 181]. However, our results support the additive spectrum previously proposed by Tung and Orlando [167] although we follow a different route.

We further make perturbation expansion similar to Kraichnan's direct interaction approximation (DIA) to study the above problem of stably stratified turbulence. We find that the corresponding corrections to velocity-velocity, temperature-temperature, and velocity-temperature correlation functions acquire new terms in addition to those which were obtained in our previous Leslie type perturbation calculations. The prefactors associated with these universal scaling laws are calculated within this framework which are found to be dependent on ε, χ, C, Ba, and σ in a more complicated fashion than the results following from our previous Leslie type calculations.

For the case of stratified turbulence with stable temperature stratification,

we further carried out a dynamic renormalization group (RG) analysis up to one-loop order to achieve a coarse-grained description of turbulent flow field via successive elimination of small shells of modes, yielding the flow equations for the renormalized coupling constants. Due to the presence of anisotropy, the perturbative RG treatment of this problem involves many extra Feynman diagrams along with those of Yakhot and Orszag's [183]. We find that, apart from the usual isotropic viscosity and diffusivity terms ($\nu_0 k^2$ and $\kappa_0 k^2$), there appear different terms ($\nu_3 k_3^2$ and $\kappa_3 k_3^2$) corresponding to the vertical motion. This gives rise to a very complicated RG analysis. However, in the limit of weak stratification, the stability analysis of the flow equations can be performed with less difficulty. It is found that the Kolmogorov scaling regime exists and thus it is expected that the energy cascade at small scales would follow the Kolmogorovian scaling law as conjectured by Kolmogorov.

Contents

List of Figures

Chapter 1

Introduction

> "*Observe the motion of the water surface, which resembles that of hair, that has two motions: one due to the weight of the shaft, the other to the shape of the curls; thus water has* ***eddying motions****, one part of which is due to the* ***principal current****, the other to the random and reverse motions.*"
>
> —*Leonardo da Vinci (1510)*

Most of the macroscopic physical processes in nature are generally non-equilibrium processes. A system can be regarded to be in equilibrium if the macroscopic processes occurring in the system are slow compared to the time scale of observation. After more than one hundred years of study, the equilibrium statistical physics is almost perfect. However, nonequilibrium statistical physics as an independent discipline has been paid great attention only in the last forty to fifty years, and it is still in the developing stage. There are a number of problems which have the common characteristics that complex microscopic behavior underlies macroscopic effects. In simple cases, as in hydrodynamics for example, the microscopic fluctuations average out when larger scales are considered, and the averaged quantities satisfy classical continuum equations. Unfortunately, there is a much more difficult class of problems where fluctuations persist out to macroscopic wavelengths, and fluctuations on all intermediate length scales are important too. Fully developed turbulent fluid flows [160, 90, 111], critical phenomena [63], surface growth [10], and

elementary particle physics turn out to be in this category. Theorists have difficulties with these problems because they involve very many coupled degrees of freedom.

In fully developed turbulence in the atmosphere, global air circulation becomes unstable, leading to eddies on a scale of thousands of kilometers. These eddies break down into smaller eddies, which in turn break down, until chaotic motions to all length scales down to millimeters are excited. Around the scale of millimeters, viscosity damps out the turbulent fluctuations and no smaller scales in the dissipation region are important.

In quantum field theory, the "elementary" particles are interpreted as excitations of fields interacting via the exchange of gauge Bosons. The fields have to be treated to all scale sizes down to zero. As a result, ultraviolet divergences appear in the perturbative treatment of the theory. These divergences, however, can be removed by way of renormalization leading to the renormalization of mass and charge. Thus, the mass and charge of an elementary particle becomes scale dependent.

Computers can extend the capabilities of theorists, but even high-end computers are incapable of handling the huge number of degrees of freedom that are required for the simulation of fully developed turbulence. For instance, a direct-numerical simulation of the Earth atmosphere from the planetary scale (several thousands of kilometers horizontally and tens of kilometers vertically) to the scale of millimeters would require about 10^{25} degrees of freedom to put on the computer. Thus, it is not possible to simulate explicitly all the scales of motion from the largest to the smallest.

Non-equilibrium situations can be extremely difficult to deal with in any rigorous manner, and we are able to explore only some of the simpler phenomenological approximations that are available. Non-linear field equations describing a system with friction, non-linearity and a driving noise have received much attention. Two prime examples are the Navier-Stokes equation [111, 45] and the KPZ equation [67, 108].

In elementary particle physics, excellent results have been obtained using

diagrammatic perturbation methods and renormalization group (RG) techniques. Extrapolation of these quantum field theoretic methods have had success in the theory of critical phenomena [177, 36]. Examples of such problems are the liquid-gas transition, paramagnetic-ferromagnetic transition, where fluctuations to all scales interact among themselves. It has been found that the renormalization group (RG) procedure can successfully handle the enormous number of interacting fluctuations. This procedure of RG has been adopted to the problem of turbulence [43, 34, 184, 170, 187]. The idea is to integrate out fluctuations starting with fluctuations near the smallest scale, and then moving successively to larger scales. This results in a correction to the viscosity at each stage of the elimination process. The process is repeated recursively. This generates a renormalized (scale dependent) viscosity.

In this dissertation, we shall explore a few problems of non-equilibrium statistical physics governed by non-linear stochastic field equations, such as the noise driven Navier-Stokes equation. To be more specific, we shall be considering the noise driven dynamics of homogeneous shear flow and stably stratified turbulence where the Navier-Stokes dynamics is augmented by extra nonlinear terms. In particular, we employ some "standard" perturbation methods akin to those developed by Kraichnan [78, 81] and Leslie [90] for the above problems, and we eventually employ the dynamic RG method to one of those problems. In the following section, we shall briefly summarize the salient features and conceptual issues of these problems.

1.1 Physical Nature of Turbulence

"Turbulence is the last great unsolved problem of classical physics."

—Richard P. Feynman

Turbulent flows have mystified people for ages, as evidenced by Leonardo da Vinci's sketches of the turbulent wakes downstream of some bridge columns [37]. The last quarter of the 19th century was a remarkable time in human history of fluid science and engineering as modern scientific methodologies were

formally introduced into turbulent studies through the pioneering works of various scientists, motivated principally by engineering applications. Among these pioneering contributions, Osborne Reynold's famous experiment [134] was a milestone for discovering the laminar and turbulent states of a flow. Beginning with careful experimental studies of flows under various experimental conditions [134, 133] and with the formulation of the Navier-Stokes equation [117, 156], turbulence became a subject of thorough scientific inquiry. Although one hundred and twenty years have passed since the beginning of modern turbulence studies, the nature of turbulence is still far from being unveiled. Unlike many other branches of physics, a standard research methodology for the study of turbulence has not yet been well established. The problem of turbulence still remains one of the most elusive yet fascinating unsolved puzzles of science.

The importance of the study of turbulence comes from the fact that most flows occurring in nature and in engineering applications are turbulent. The boundary layers in the Earth's atmosphere, jet streams in the upper troposphere, the water current below the surface of the oceans, the flow of water in rivers and canals, the wakes of ships, submarines, and aircrafts, the gulf stream, the photosphere of the Sun and similar stars, interstellar gas clouds, the wake of the Earth in the solar wind, all are in turbulent motion. There is vital interest, both scientific and commercial, in understanding and reducing the detrimental effects of enhanced turbulent drag in a wide range of applications. Our modern interests in energy-efficient transportation, in accurate weather forecasting, in the prediction of large scale oceanic movements, in global climate modeling, and in nuclear fusion, attach an even greater importance to the problem of turbulence.

Direct numerical simulation of turbulent flows using the instantaneous Navier-Stokes equation poses a great challenge. Since an overwhelmingly large number of degrees of freedom are excited in turbulent motions of high Reynolds number, the numerical procedure requires resolution of the smallest scales of turbulent eddies. The number of grid points required is proportional to the

nine-fourth power of the flow Reynolds number [87]. The computer resources needed are thus too large even with the largest modern supercomputer.

From the physical point of view, turbulent flow is time and space dependent with a very large number of spatial degrees of freedom. The dynamics of turbulence involves all scales and are superimposed in the flow, with smaller ones living inside the larger ones, that is, it consists of a sea of eddies of many sizes in which smaller eddies are more numerous than the larger eddies. Random interactions among the eddies are responsible for a cascade of energy from the largest to the smallest eddies. Although, due to randomness, turbulence is unpredictable in detail, its statistical properties are supposed to be reproducible and it is fruitful to consider averages and probability distributions of flow quantities [45]. In fact, this is the reason why the spectral analysis of turbulence in a statistical framework is so useful.

A measure of smallness of viscous effects on the large scales of turbulence is provided by the flow Reynolds number, $\mathrm{Re} = UL/\nu$, where U is the characteristic velocity scale corresponding to the length scale L representing the order of size of the large scales and ν is the kinematic viscosity of the fluid. Re is typically high for turbulent flows ($\sim 10^6$ to 10^{10}), implying little direct effect of viscosity on the large scales. The generation of velocity fluctuations is due to the nonlinear terms in the equation of motion. However, viscous effects play an important role in the dynamics of the smallest scales where dissipation occurs smoothing out the velocity fluctuations. One might expect that for large Re the relative magnitude of viscosity is so small that viscous effect in a flow tends to become vanishingly small. The nonlinear terms in the Navier-Stokes equation counteract this threat by generating motions at scales small enough to be affected by viscosity. There seems to be no way of doing away with viscosity: as soon as the flow field becomes so large that viscosity effects could conceivably be neglected, the flow creates small-scale motion, thus keeping viscosity effects at a finite level.

Since small-scale motions tend to have fast time scales, one may assume that these motions are statistically independent of the relatively slower large-

scale motions. If these assumptions make sense, the small-scale motion should depend only on the rate at which it is supplied with energy by the large-scale motion, and on the kinematic viscosity. It is reasonable to assume that the rate of energy input should be equal to the rate of dissipation. Thus, there is a flow of energy from the largest scales to the smallest scales. Since the intermediate scales are far from both the energy input scales and the dissipation scales, their statistical properties are independent of those scales. This is the basis for what is called Kolmogorov's universal equilibrium theory [74].

A common source of energy for turbulent velocity fluctuations is shear in the mean flow [90, 163] which produces a disturbance and sets the fluid into macroscopic motion causing deviations from the equilibrium steady state. In a real flow, the shear is always created by the presence of a wall. Shear flow is therefore intimately connected with near wall turbulence dynamics. Nevertheless, many features can be understood in the idealized case of a uniform mean shear in the absence of boundaries, in the context of homogeneous anisotropic turbulence.

In fact, the equilibrium state is modified not only by the existence of mean shear flow but also by external forces such as buoyancy or magnetic field. One very interesting and challenging problem in geophysics and astrophysics is turbulence in stably stratified fluid [126, 89], in which the fluid is driven by buoyancy forces. Density stratification in atmospheric boundary layers [147, 162] and salt stratification in oceanic mixed layers [54] may be considered to be stable in which the vertical mixing is reduced leading to the development of structural anisotropy. Despite its significantly intriguing nature and practical significance, namely in numerical weather prediction [148, 149], stably stratified turbulence has not received much attention. This might be attributed to the lack of adequate field or laboratory measurements, to the inevitable difficulties in numerical simulations and to the intrinsic complexity in its dynamics. In order to improve the understanding of stably stratified turbulence and to explore some of its inherent characteristics, we make use of "standard" perturbation methods and perform statistical field theoretical

spectral calculations for the case of stably stratified turbulence.

1.2 Mathematical Description of Turbulence

1.2.1 Dynamical Equations

The equation of motion for a fluid can be expressed as [87]

$$\frac{\partial v_i}{\partial t} + v_j \frac{\partial v_i}{\partial x_j} = \frac{1}{\rho} \frac{\partial}{\partial x_j} \sigma_{ij} \tag{1.1}$$

where $v_i(\mathbf{x}, t)$ is the instantaneous velocity field, $\rho(\mathbf{x}, t)$ is the density field, and $\sigma_{ij}(\mathbf{x}, t)$ is the stress tensor. Since the fluid mass is conserved, the fluid motion obeys the equation of continuity

$$\frac{\partial \rho}{\partial t} + \frac{\partial}{\partial x_i}(\rho v_i) = 0 \tag{1.2}$$

We shall henceforth consider only incompressible flows for which the equation of continuity reduces to

$$\frac{\partial v_i}{\partial x_i} = 0 \tag{1.3}$$

In the case of a Newtonian fluid (obeying linear stress-strain law), the stress tensor σ_{ij} is given by

$$\sigma_{ij} = -p\delta_{ij} + 2\mu s_{ij} \tag{1.4}$$

where δ_{ij} is the Kronecker delta, p is the hydrodynamic pressure and μ is the dynamic viscosity. The rate of strain is defined by

$$s_{ij} = \frac{1}{2}\left(\frac{\partial v_i}{\partial x_j} + \frac{\partial v_j}{\partial x_i}\right) \tag{1.5}$$

When Eq. (1.4) is substituted into Eq. (1.1) and the incompressibility condition (1.3) is invoked, the Navier-Stokes equation (1.1) is obtained as

$$\frac{\partial v_i}{\partial t} + v_j \frac{\partial v_i}{\partial x_j} = -\frac{1}{\rho}\frac{\partial p}{\partial x_i} + \nu \frac{\partial^2 v_i}{\partial x_j \partial x_j} \tag{1.6}$$

where $\nu (= \mu/\rho)$ is the kinematic viscosity.

1.2.2 Reynolds Decomposition

To study turbulent flows, Reynolds decomposition [133, 160, 58] was proposed through the decomposition of the flow into mean and turbulent motions. The full velocity field $v_i(\mathbf{x}, t)$ can be decomposed into the mean flow $U_i(\mathbf{x})$ and the velocity fluctuations $u_i(\mathbf{x}, t)$ as

$$v_i = U_i + u_i \tag{1.7}$$

Since $\overline{v_i} = U_i$, the mean value of the fluctuating velocity is zero; $\overline{u_i} = 0$. Further, the mean value of the spatial derivative of a variable is equal to the corresponding spatial derivative of the mean value of that variable. For example

$$\overline{\frac{\partial v_i}{\partial x_j}} = \frac{\partial U_i}{\partial x_j}, \quad \overline{\frac{\partial u_i}{\partial x_j}} = \frac{\partial}{\partial x_j}\overline{u}_i = 0$$

The pressure p and the stress σ_{ij} are also decomposed into mean and fluctuating components. Averages of the product are computed as

$$\overline{v_i v_j} = \overline{(U_i + u_i)(U_j + u_j)} = U_i U_j + \overline{u_i u_j} + \overline{U_i u_j} + \overline{U_j u_i} = U_i U_j + \overline{u_i u_j}$$

where the terms consisting of product of a mean value and fluctuation vanish if they are averaged, because the average of a fluctuating quantity is zero.

If we apply the decomposition given by Eq. (1.7) to the incompressibility condition (1.3), we obtain

$$\frac{\partial v_i}{\partial x_i} = \frac{\partial}{\partial x_i}(U_i + u_i) = 0 \tag{1.8}$$

On averaging this equation, we readily obtain that the mean flow and the fluctuating parts are separately incompressible.

The equation of motion for the mean flow U_i is obtained by substituting Eq. (1.7) into Eq. (1.1) and taking the average of all terms in the resulting equation. This yields

$$U_j \frac{\partial U_i}{\partial x_j} + \overline{u_j \frac{\partial u_i}{\partial x_j}} = \frac{1}{\rho}\frac{\partial}{\partial x_j}\Sigma_{ij} \tag{1.9}$$

where Σ_{ij} denotes the mean value of σ_{ij} and is given by

$$\Sigma_{ij} = -P\delta_{ij} + 2\mu S_{ij} \tag{1.10}$$

with the mean pressure P, and the mean strain

$$S_{ij} = \frac{1}{2}\left(\frac{\partial U_i}{\partial x_j} + \frac{\partial U_j}{\partial x_i}\right) \tag{1.11}$$

Further, using the incompressibility condition, we can write the second term on the left hand side of Eq. (1.9) as

$$\overline{u_j \frac{\partial u_i}{\partial x_j}} = \frac{\partial}{\partial x_j}\overline{u_i u_j} \tag{1.12}$$

where $\overline{u_i u_j}$ is the Reynolds stress tensor. This yields the Reynolds momentum equation as

$$U_j \frac{\partial U_i}{\partial x_j} = \frac{1}{\rho}\frac{\partial}{\partial x_j}\tau_{ij} \tag{1.13}$$

where the total mean stress τ_{ij} is given by

$$\tau_{ij} = \Sigma_{ij} - \rho\overline{u_i u_j} = -P\delta_{ij} + 2\mu S_{ij} - \overline{\rho u_i u_j} \tag{1.14}$$

Thus, the equation of mean flow looks like

$$U_j \frac{\partial U_i}{\partial x_j} + \frac{\partial}{\partial x_j}\overline{u_i u_j} = \frac{1}{\rho}\frac{\partial P}{\partial x_i} + \nu\frac{\partial^2 U_i}{\partial x_j \partial x_j} \tag{1.15}$$

Applying Reynolds decomposition on the full Navier-Stokes equation (1.6) and then subtracting the equation for the mean flow given by Eq. (1.15), we get the dynamical equation for the fluctuating velocity field $u_i(\mathbf{x}, t)$ as

$$\frac{\partial u_i}{\partial t} + U_j\frac{\partial u_i}{\partial x_j} + u_j\frac{\partial U_i}{\partial x_j} + u_j\frac{\partial u_i}{\partial x_j} = f_i - \frac{1}{\rho}\frac{\partial p}{\partial x_i} + \frac{\partial \overline{u_i u_j}}{\partial x_j} + \nu\frac{\partial^2 u_i}{\partial x_j \partial x_j} \tag{1.16}$$

For the simple case of homogeneous shear turbulence, we consider the general form of mean velocity

$$U_i = S_{ij}x_j \tag{1.17}$$

where the strain S_{ij} is assumed to be uniform in space and constant in time and $S_{ii} = 0$ due to incompressibility. We consider this problem in Chapter 2, where we evaluate the anisotropic correction to the equal-time velocity correlation tensor.

1.2.3 Turbulence Phenomenology

Since we assume that the flow is incompressible, the Laplacian of the pressure field is related to the divergence of the advective term, and therefore, the pressure field can be eliminated. The evolution of the flow is governed by two forces, each with different characteristic time scales. These are the inertial force, represented by the advective term (with pressure included), and the dissipative force, represented by the viscous term. The inertial force describes self-advection of the flow with time scales $\tau_e = l/u$, where u and l are the characteristic velocity and length scales of the flow. In fact, turbulence consists of hierarchy of such scales and it is useful to think of the flow as a hierarchy of eddies of different scales. Consequently, if u is the characteristic flow velocity of the eddies of scale l, τ_e is the time scale of that eddy. The flow is a superposition of many eddies of different scales. The evolving flow becomes random because the transfer of energy between scales constantly changes the configuration of the eddies. Motion at a given scale loses coherence due to advection by other eddies and within the time scale τ_e the energy is transferred to other eddies. This energy transfer process is conservative, causing no loss of energy, only transfer of energy from motion in one scale to motion in other scales. An equal distribution of energy in this energy transfer process leads to a self-similar energy cascade. The turbulent flow velocity at each scale adjusts itself so that the energy transfer rate u^2/τ_e is invariant for all scales in which viscosity has a negligible effect on the dynamics [74].

The effect of viscosity is quantified by the viscous dissipation rate $\tau_d^{-1} = \nu/l^2$, the rate at which the energy of fluid motion is dissipated and converted to heat. Because viscous dissipation is diffusive (giving the l^2 factor in the denominator of τ_d^{-1}), at smaller scales, dissipation rate increases faster than the turbulent decorrelation (eddy turnover) rate τ_e. Therefore, at large scales the condition $\tau_d^{-1} < \tau_e^{-1}$ is satisfied and energy is transferred between scales with negligible dissipation, establishing the self-similar energy cascade. At smaller scales the relation $\tau_d^{-1} > \tau_e^{-1}$ is satisfied and energy is dissipated

before advection can pass it to other scales, terminating the cascade. In three-dimensional (3D) Navier-Stokes turbulence, energy is injected at large scales (where $\tau_d/\tau_e \gg 1$) and it is transferred to successively smaller scales by the cascade. This process continues until the cascade reaches the Kolmogorov scale (η) at which $\tau_d = \tau_e$, whereupon the cascade ceases and the energy is converted into heat. The ratio τ_d/τ_e evaluated for the flow velocity U at the largest scale L defines the flow Reynolds number $\mathrm{Re} = UL/\nu$, which for turbulent motion is necessarily much larger than unity. Scales in the range $L \gg l \gg \eta$ are referred to as the inertial range.

1.2.4 Kolmogorov Theory and Universality

Kolmogorov [74] proposed his famous universal scaling law for the inertial-range energy spectrum of locally isotropic three-dimensional turbulence. The energy spectrum is thought to be composed of three distinct wavenumber regions: a region of energy injection (provided by external forcing) at the largest scales, an intermediate inertial range characterized by zero forcing and zero dissipation and, at the very smallest scales, a region dominated by viscosity. The energy cascades from higher to lower wavenumbers due to the nonlinear term in the Navier-Stokes equation. The energy cascade is eventually terminated at the Kolmogorov microscale $\eta = (\nu^3/\varepsilon)^{1/4}$, where dissipation due to viscosity begins to become important (ν is the kinematic viscosity of the fluid).

In this phenomenological picture, which has been critically analyzed and carefully explained in various classic texts [87, 11, 111, 90, 45, 89, 160, 144], the essential qualitative idea is a cascade of energy from large scales to small scales due to the nonlinear terms in the Navier-Stokes equation with an eventual dissipation of the energy by viscosity at the smallest scales. Now one dynamical quantity, namely ε, plays a key role. The quantity ε determines the rate at which energy is fed into the fluid. It is also the rate at which energy is transferred from large to small scales by the nonlinear term in the Navier-Stokes equation. Moreover, it equals the average rate of energy dissipation at the smallest length scales. Thus ε can be regraded as the energy flux and the

inertial range is characterized by a constant energy flux ε.

This discussion suggests that the parameters governing the small-scale motion include at least the dissipation rate ε ($\mathrm{m^2sec^{-3}}$) and the kinematic viscosity ν ($\mathrm{m^2sec^{-1}}$). With these parameters, one can construct length, time and velocity scales as

$$\eta \equiv (\nu^3/\varepsilon)^{1/4}, \quad \tau \equiv (\nu/\varepsilon)^{1/2}, \quad v \equiv (\nu\varepsilon)^{1/4}$$

These scales are referred to as the Kolmogorov microscales of length, time and velocity.

On the basis of purely dimensional reasoning, Kolmogorov found the scaling law for the energy spectrum as [74, 120]

$$E(k) = C\varepsilon^{2/3}k^{-5/3} \tag{1.18}$$

Here $E(k)$ is the energy density at wave number k and C is the universal Kolmogorov constant. C is found experimentally to lie in the range 1.4–1.7 [53, 125]. Similar dimensional analysis gives the eddy-viscosity as

$$\nu(k) = \alpha\varepsilon^{1/3}k^{-4/3} \tag{1.19}$$

where α is a constant. This phenomenology has had an overwhelming influence on theoretical and experimental investigations of the physics of turbulence, and has been a mater of discussion for a long while as evidenced in the classic texts [87, 11, 111, 90, 45, 89, 160, 144].

1.3 Theories Based on Dynamical Equations

The inertial range turbulence has been modelled by the randomly driven Navier-Stokes equation

$$\frac{\partial u_i}{\partial t} + u_j\frac{\partial u_i}{\partial x_j} = f_i - \frac{1}{\rho}\frac{\partial p}{\partial x_i} + \nu_0\frac{\partial^2 u_i}{\partial x_j \partial x_j} \tag{1.20}$$

along with the incompressibility condition

$$\frac{\partial u_i}{\partial x_i} = 0 \tag{1.21}$$

where f_i is a random stirring force field. In $(d+1)$ dimensional Fourier space, these equations become

$$\left(-i\omega + \nu_0 k^2\right) u_i(\mathbf{k},\omega) = f_i(\mathbf{k},\omega) + \frac{i}{2} P_{ijl}(\mathbf{k}) \int \frac{d^d p}{(2\pi)^d} \int_{-\infty}^{\infty} \frac{d\omega_1}{(2\pi)} u_j(\mathbf{p},\omega_1) u_l(\mathbf{q},\omega_2) \qquad (1.22)$$

with incompressibility condition

$$k_i u_i(\mathbf{k},\omega) = 0 \qquad (1.23)$$

where $\mathbf{p}+\mathbf{q} = \mathbf{k}$, and $\omega_1 + \omega_2 = \omega$, $P_{ijl}(\mathbf{k}) = k_j P_{il}(\mathbf{k}) + k_l P_{ij}(\mathbf{k})$ with $P_{ij}(\mathbf{k}) = \delta_{ij} - k_i k_j/\mathbf{k}^2$.

The random stirring force $f_i(\mathbf{k},\omega)$, is assumed to have a Gaussian white-noise statistics with correlation

$$\langle f_i(\mathbf{k},\omega) f_j(\mathbf{k}',\omega')\rangle = F(k) P_{ij}(\mathbf{k}) [2\pi]^d \delta^d(\mathbf{k}+\mathbf{k}') [2\pi] \delta(\omega+\omega') \qquad (1.24)$$

in the Fourier space. The transverse projection operator $P_{ij}(\mathbf{k}) = \delta_{ij} - k_i k_j/\mathbf{k}^2$ appears on the right hand side due to the assumption of statistical isotropy. A case which has been much studied in the literature [43, 34, 44, 184, 183] is the power law force spectrum

$$F(k) = 2D_0 k^{-d+4-\epsilon} \qquad (1.25)$$

where the exponent is written in the given form for later convenience. The choice $\epsilon = 2-d$ was studied by Forster, Nelson and Stephen [43] as "Model A". If the noise strength is chosen by the fluctuation-dissipation relation $D_0 = (\nu_0/\rho) k_B T$, then the force in Model A represents molecular noise and the equation is a realistic model of fluctuations in an equilibrium fluid at absolute temperature T. The general case for arbitrary ϵ was first proposed for study by DeDominicis and Martin [34], who realized that the model has a strong-coupling fixed point for small ϵ in any dimension d, which may be studied perturbatively. For $\epsilon = 4$ the constant D_0 has units of energy dissipation and the energy spectrum is obtained as $k^{1-2\epsilon/3}$ giving the Kolmogorov spectrum $k^{-5/3}$ for $\epsilon = 4$.

From Navier-Stokes equation, we can derive an equation for energy transport amongst the Fourier modes. This is obtained by adding the two equations; one obtained by multiplying the Navier-Stokes equation for $u_i(\mathbf{k},t)$ by $u_n(-k,t)$ and the other by multiplying the Navier-Stokes equation for $u_n(-\mathbf{k},t)$ by $u_i(\mathbf{k},t)$. Averaging the result, we obtain

$$\left(\frac{\partial}{\partial t}+2\nu_0 k^2\right)\langle u_i(\mathbf{k},t)u_n(-\mathbf{k},t)\rangle = \langle u_n(-\mathbf{k},t)f_i(\mathbf{k},t)\rangle + \langle u_i(\mathbf{k},t)f_n(-\mathbf{k},t)\rangle - \frac{i}{2}P_{ijl}(\mathbf{k})\int\frac{d^dq}{[2\pi]^d}\langle u_j(\mathbf{q},t)u_l(\mathbf{p},t)u_n(-\mathbf{k},t)\rangle - \frac{i}{2}P_{njl}(-\mathbf{k})\int\frac{d^dq}{[2\pi]^d}\langle u_j(-\mathbf{q},t)u_l(-\mathbf{p},t)u_i(\mathbf{k},t)\rangle \tag{1.26}$$

We express the second-order velocity correlation tensor as

$$\langle u_i(\mathbf{k},t)u_j(\mathbf{k}',t')\rangle = Q_{ij}(\mathbf{k};t,t')[2\pi]^d\delta^d(\mathbf{k}+\mathbf{k}') \tag{1.27}$$

The velocity correlation tensor takes the form

$$Q_{ij}(\mathbf{k};t,t') = Q(k;t,t')P_{ij}(\mathbf{k}) \tag{1.28}$$

due to the assumption of isotropy. The turbulent energy density $E(k)$ is defined as

$$\frac{1}{2}\langle u^2(\mathbf{x},t)\rangle = \int_0^\infty E(k)dk \tag{1.29}$$

The quantity $Q(k;t,t)$ is related to the turbulence energy density $E(k;t,t)$ as

$$E(k;t,t) = \frac{d-1}{2}\frac{S_d}{[2\pi]^d}k^{d-1}Q(k;t,t) \tag{1.30}$$

where S_d is the surface area of a unit sphere embedded in the d-dimensional space. Making a substitution of Eq.(1.27) in Eq.(1.26), taking the trace of the entire expression, and then substituting Eq.(1.30), we get the energy balance equation representing the turbulent kinetic energy transport between Fourier modes

$$\left(\frac{\partial}{\partial t}+2\nu_0 k^2\right)E(k;t,t) = T(k;t,t)+W(k;t,t) \tag{1.31}$$

where $T(k;t,t)$ represents the non-linear transfer term, $W(k;t,t)$ is the rate of energy input due to forcing, and $2\nu k^2E(k;t,t)$ is the dissipation term. Eq. (1.31) tells us about the energy balance at each mode k.

Integrating the entire expression over all k-space, we obtain

$$\frac{\partial E}{\partial t} + \int 2\nu_0 k^2 E(k;t,t)dk = \int W(k;t,t)dk + \int T(k;t,t)dk \tag{1.32}$$

Here $\int W(k;t,t)dk$ is the rate of work done by the external forcing term and $\int 2\nu_0 k^2 E(k;t,t)dk$ is the rate at which energy is lost from the system due to viscous dissipation. The total spectral energy E is constant for a steady state. The last term, which represents the action of the nonlinear term, is conservative

$$\int T(k;t,t)dk = 0. \tag{1.33}$$

1.4 Passive Scalar Turbulence

When a dynamically passive scalar field, for example pollutants (as in the familiar case of smoke diffusing in air), heat (when a hot object is cooled in the flow), or a dye, is mixed by a turbulent flow, a spectrum of fluctuations of the scalar field is produced. The scale of these fluctuations range from the scale of the energy containing eddies to the smallest scale that depends on the ratio of diffusivities (Prandtl number, Schmidt number, etc.). Many of the concepts that were used to elucidate the form of the kinetic energy spectrum can also be applied to the spectra of the passive scalar fields. If the Reynolds number is large enough for an equilibrium range to exist in the kinetic energy spectrum, there is also an equilibrium range in the spectrum of scalar variance exhibiting local isotropy. Moreover, the scalar cascade is similar to that of the energy cascade.

The time evolution of a passive scalar field $\psi(\mathbf{x},t)$ transported by an incompressible velocity field $\mathbf{u}(\mathbf{x},t)$, is governed by the advection-diffusion equation

$$\frac{\partial \psi}{\partial t} + (\mathbf{u}\cdot\nabla)\,\psi = \kappa\nabla^2\psi \tag{1.34}$$

where κ is the molecular diffusivity. The mean-square scalar $\langle\psi^2(\mathbf{x},t)\rangle$ is related to the spectrum of passive scalar $\mathcal{E}(k)$ as

$$\langle\psi^2(\mathbf{x},t)\rangle = \int_0^\infty \mathcal{E}(k)dk \tag{1.35}$$

Kolmogorov's argument was extended to the case of passive scalar turbulence by Obukhov and Corrsin [120, 33]. The Kolmogorov-Obukhov-Corrsin theory states that the dissipation rate of scalar variance is independent of molecular diffusivity. Because dissipation occurs only at small scales, a constant scalar variance flux must pass through the "inertial range" comprising all scales intermediate between the initial injection scale L' and the final dissipation scale η'. In the case of passive scalar convection, a scaling law similar to Eq. (1.19) holds for three-dimensional mean-square scalar. It is given by [120, 12, 33]

$$\mathcal{E}(k) = \text{Ba}\ \chi\ \varepsilon^{-1/3}\ k^{-5/3} \tag{1.36}$$

where χ is the scalar flux and Ba is the well-known Batchelor (or Obukhov-Corrsin) constant. The universal number Ba has been measured in several experiments [151, 99, 18]. Moreover, there have been extensive studies to validate the spectrum in Eq. (1.36) by numerical simulations and by experiments.

We take up the problem of turbulent diffusion of a passive scalar in Chapter 3. Using the Heisenberg approximation, we calculate the associated universal numbers, namely the Batchelor constant Ba and the turbulent Prandtl number σ. We evaluate these constants in all space dimensions d.

1.5 Anomalous Scaling

The subject of anomalous scaling in turbulence has gained a great deal of attention in the past few decades. The numerical values of these exponents, as well as the physical mechanism which is responsible for the anomalous scaling, have been the target of an extensive experimental, numerical, and theoretical research. On the theoretical side, important progress was made by studying Kraichnan's model of passive scalar advection [84]. This model describes the advection of a passive scalar field by a synthetic, solenoidal velocity field with a Gaussian, white-in-time statistics. The linearity of the equations for the passive scalar field and the white-in-time statistics of the velocity field make it

possible to write down a closed set of equations for the equal-time correlation functions of the passive scalar [84]. It was shown that the solution of these equations can lead to anomalous scaling [49, 28]. The key point is that the homogeneous solutions of these equations are scale invariant with non-trivial anomalous scaling exponents, which are different from the dimensional scaling exponents that characterize the inhomogeneous, forced solutions. Being usually smaller than the dimensional scaling exponents, the anomalous exponents dominate the small-scale statistics of the passive scalar field. The homogeneous solutions are commonly referred to as zero modes, and have been calculated to first-order perturbatively in Refs. [49, 28] for the fourth-order structure function and for all even structure functions in Ref. [13]. Exact computer-assisted calculations of the exponents of the third-order structure functions were presented in [48]. Besides suggesting an elegant mechanism for anomalous scaling, Kraichnan's model also provided an example in which the scaling of the anisotropic parts of structure functions is different from the isotropic scaling. In Ref. [41], it was shown how such a thing can happen, by expanding the second-order structure function of the passive field in terms of spherical harmonics $Y_{jm}(\hat{r})$. It was found that this expansion leads to a set of decoupled j-dependent equations for the expansion prefactors. These equations can be easily solved by a power law whose exponent is an increasing function of j . These exponents are universal in the sense that they are independent of the forcing and boundary conditions.

1.6 Homogeneous Shear Turbulence

Turbulent shear flows have been of interest for a long time as demonstrated by various classic texts [163, 128, 58]. The local isotropy postulate of Kolmogorov together with the assumption that developed turbulence in the inertial range is independent of the viscous cutoff, shape, and size of boundary conditions, creates a basis that is difficult to accept for a satisfactory understanding of the full complexity of turbulence. In this phenomenology, the effect of any

anisotropy imposed at the large scales is expected to diminish rapidly due to successive loss of memory as the energy cascade takes place from larger to smaller scales of motion. Surprisingly enough, recent experimental and numerical findings [137, 142, 138] have detected the survival of anisotropic turbulent fluctuations down to the Kolmogorov scale η. In all realistic flows, there always exists some anisotropy at all scales; the statistical properties of the velocity field are effected by the geometry of the boundaries or the driving mechanism, which are never rotationally invariant [142, 85]. For example, all geophysical flows are subjected to the rotation of the globe, which introduces anisotropy via the Coriolis forces [20, 46]. Therefore, a realistic description of turbulence cannot be purely isotropic and must contain some anisotropic elements. Yet the problem is that once we take anisotropy into account, we face a drastic increase in the complexity of the theory. As a consequence of these inherent difficulties, the existing anisotropic effects were simply ignored in many of the theoretical and simulational studies of statistical turbulence. This attitude gave rise to ambiguous assessments of important fundamental issues like the universality of the scaling exponents in turbulence. Thus a central challenge in the theory of anisotropic turbulence is the construction of an efficient mathematical language to describe it. The study of anisotropic turbulence is therefore not only of theoretical but also of practical interest.

Considerable attention has been paid during the last few decades in experimental anisotropic turbulence [47, 141] and numerical homogeneous shear flows [130, 129], to investigate the persistence of anisotropy in the small scales [100]. Various formal approaches to the analysis of this phenomenon has been proposed [85, 52]. The deviations of the statistical behavior of fully developed turbulence from the isotropic statistics, confirmed by a variety of experiments and computer simulations, may be induced by the interactions of fluctuating fields with the mean flow gradients or external fields. A number of numerical and experimental investigations in shear flow turbulence have shown that anisotropy appears not only in second order moments but also in higher order moments. Measurement of structure functions in shear turbulence [153]

indicated that the large scale shear persists down to the smallest scales. This observed effect of anisotropy in small scale turbulence is a challenge in both theoretical and experimental domains.

For the simplest case of homogeneous shear flow, Leslie [90] offered a perturbation procedure and applied it to study his simple model on the basis of Kraichnan's closure formulations [78, 79, 80]. A different formulation was offered by Ishihara et al. [61, 185] in which they conjectured a form of the anisotropic part of the correlation tensor. Using direct numerical simulation (DNS) as well as Lagrangian renormalized approximation (LRA) scheme [66], they carried out an analysis of the anisotropic property of the velocity correlation tensor and evaluated the non-dimensional universal numbers associated with it. Although their DNS values for these universal numbers were in good agreement with the experimental values [164], their LRA values were not in good agreement.

In the recent past, employing the invariance of the equations of fluid mechanics to all rotations, various efforts have been made to understand the effects of anisotropy through an $SO(3)$ decomposition of the structure functions and other tensorial objects [102, 16]. This method offers a transparent way of determining the degree of anisotropy in turbulence statistics. This device allows a discussion of the scaling properties of the statistical objects in well-defined sectors of the symmetry group, each of which is determined by the angular momenta sector (j, m). The exponents appear universal in each sector, and again strictly increasing as a function of j.

Recently [14], a finite dimensional inertial range approximation of the anisotropic two-point, second-order velocity correlation tensor

$$R_{ij}(\mathbf{x}, \mathbf{r}) = \langle u_i(\mathbf{x}) u_j(\mathbf{x} + \mathbf{r}) \rangle \tag{1.37}$$

was constructed in real space in terms of three linearly independent structure tensors proposed earlier by Kassinos et al. [68]. It contains information about the structure of the anisotropy. They noted that, unlike the $SO(3)$ representation, the linear representation in terms of structure tensors is not a complete

basis for $R_{ij}(\mathbf{r})$. The number of degrees of freedom in this model is reduced by imposing continuity and self-consistency constraints, and the inertial-range assumption led to a power law dependence in r.

Here we take a route to the problem of homogeneous anisotropic turbulence entirely different from the above methods. Basically, we are interested in tackling directly the anisotropic terms appearing in the dynamical equations by means of "standard" perturbative methods. Considering a general form of mean velocity

$$U_i = S_{ij} x_j$$

with a uniform strain S_{ij}, and using Reynolds decomposition [160, 58], we obtain the Fourier transform of the equation of motion for the fluctuating part of velocity field, namely Eq. (1.16), as

$$\begin{aligned} \left(-i\omega + \nu_0 k^2\right) u_i(\mathbf{k},\omega) \;+\; & \frac{i}{2} P_{ijl}(\mathbf{k}) \int \frac{d^3p}{(2\pi)^3} \int_{-\infty}^{\infty} \frac{d\omega_1}{(2\pi)} u_j(\mathbf{p},\omega_1) u_l(\mathbf{q},\omega_2) \\ = \; & f_i(\mathbf{k},\omega) + \lambda \hat{N}_{ij}(\mathbf{k}) u_j(\mathbf{k},\omega) \end{aligned} \tag{1.38}$$

The anisotropic operator

$$\hat{N}_{ij}(\mathbf{k}) = -S_{ij} + 2\frac{k_i k_l}{\mathbf{k}^2} S_{lj} + \delta_{ij} k_l S_{lm} \frac{\partial}{\partial k_m}$$

consists of pure strain (the first term), rapid pressure (second term) and wave vector space deformation (last term). An expansion parameter λ $(= 1)$ is inserted with $\hat{N}_{ij}$ in order to make a Leslie-type perturbation expansion about the isotropic background field [90]. The forcing term $f_i(\mathbf{k},\omega)$ is introduced in order to maintain a steady state for the isotropic background field $u_i^{(0)}(\mathbf{k},\omega)$. Through direct calculations free from any conjectures, we derive the form of the anisotropic part of the equal-time velocity correlation tensor and find

$$\begin{aligned} Q_{ij}^{(1)}(\mathbf{k},0) = S_{ab} \left[P_{ia}(\mathbf{k}) P_{jb}(\mathbf{k}) + P_{ja}(\mathbf{k}) P_{ib}(\mathbf{k})\right] R^{(1,1)}(k) \\ + S_{lm} \frac{k_l k_m}{\mathbf{k}^2} P_{ij}(\mathbf{k}) R^{(1,3)}(k) \end{aligned} \tag{1.39}$$

In this expression, the factors $R^{(1,1)}(k)$ and $R^{(1,3)}(k)$, the integrands of which involve correlation and response functions, are found to be

$$R^{(1,1)}(k) = A\, \varepsilon^{1/3} k^{-13/3} \tag{1.40}$$

$$R^{(1,3)}(k) = B\ \varepsilon^{1/3} k^{-13/3} \tag{1.41}$$

where A and B are two non-dimensional universal numbers. We calculate A and B using inputs from renormalization group (RG) calculations. The details of calculations are presented in Chapter 2.

1.7 Stably Stratified Turbulence

Stable stratification plays a crucial role on turbulent motion in the atmosphere and oceans [126, 89]. Such flows are mainly driven by buoyancy forces and gravity breaks the isotropy and acts at all scales. The flow is inherently anisotropic due to the presence of stratification.

The dynamics of freely evolving turbulence under the influence of buoyancy forces is of great importance to the understanding of atmospheric and oceanic turbulence [126]. Stratification induces a certain degree of decoupling between the various fluid masses resulting in the existence of additional types of motion.

1.7.1 Buoyancy Effects

In a stable configuration, heavier fluid parcels lie below the lighter ones. If the fluid is incompressible and if it is displaced vertically from z to $z + h$, the displaced parcel of volume V retains its former density despite a slight pressure change, and at that new level, a buoyancy force appears because of the density difference. Thus the Newton's law yields

$$\rho(z) V \frac{d^2 h}{dt^2} = g\left[\rho(z+h) - \rho(z)\right] V$$

For the case of geophysical fluids, the density variations, although sufficient to drive or affect motions, are nonetheless relatively small compared to the average or reference density of the fluid. This was the essence of the Boussinesq approximation [87, 24]. This fact allows us to replace $\rho(z)$ on the left hand side of above equation by the reference density ρ_0 and to use a Taylor expansion to approximate the density difference by

$$\rho(z+h) - \rho(z) \simeq \frac{d\rho}{dz} h$$

Thus the equation of motion becomes

$$\frac{d^2h}{dt^2} - \frac{g}{\rho_0}\frac{d\rho}{dz}h = 0 \tag{1.42}$$

which clearly shows that two different cases can arise. If

$$N^2 = -\frac{g}{\rho_0}\frac{d\rho}{dz} \tag{1.43}$$

is positive, that is, if $d\rho/dz < 0$, the solution to Eq. (1.42) has an oscillatory character. This means that, when the parcel is displaced upwards, being heavier than its surroundings, it feels a downward restoring force and eventually descends. In this process the fluid parcel acquires a downward velocity; upon reaching its original level the particle's inertia causes it to go further downward and to become surrounded by the heavier fluid. The parcel, now buoyant, is pushed upward. Thus oscillation persists about the equilibrium level with oscillation frequency given by N, commonly known as stratification frequency, or Brunt-Väisälä frequency [31].

On the other hand, if N^2 is negative (i.e., $d\rho/dz > 0$, corresponding to a top heavy fluid configuration), the solution exhibits exponential growth and indicates one kind of instability. The parcel displaced upward is surrounded by heavier fluid, finds itself buoyant, and moves farther and farther upward from its initial position. Obviously, small perturbations will ensure not only that the single displaced parcel will depart from its initial position, but that all other fluid parcels will likewise participate in a general overturning of the fluid until it is finally stabilized, with the lighter fluid lying above the heavier fluid.

In a compressible fluid, such as the air of our planetary atmosphere, density can change in one of two ways: by pressure change or by internal energy changes. Out of these, the internal energy changes are dynamically important as it often occurs because of heat flux (such as heating in the tropic and cooling at high latitudes, or according to the diurnal cycle) or because of variation in air composition (such as water vapour). Such variations among fluid parcels occur despite adiabatic compression or expansion and cause density difference

that drives motion. The separation of density leads to the concept of potential density.

If we consider a neutral (adiabatic) atmosphere consisting of all air parcels having the same internal energy and behaving as a single ideal gas, we can write the equation-of-state and the adiabatic equation as

$$p = \rho\ R\ T, \qquad \frac{p}{p_0} = \left(\frac{\rho}{\rho_0}\right)^{\gamma} \tag{1.44}$$

where p, ρ, and T are respectively the pressure, density, and absolute temperature, $R = C_p - C_v$, and $\gamma = C_p/C_v$ are the constants of an ideal gas. p_0 and ρ_0 are the reference pressure and density characterizing the level of internal energy of the fluid; the corresponding reference temperature of the fluid is given by $T_0 = p_0/R\rho_0$. Expressing both pressure and density in terms of the temperature, we obtain

$$\frac{p}{p_0} = \left(\frac{T}{T_0}\right)^{\gamma/(\gamma-1)} \tag{1.45}$$

$$\frac{\rho}{\rho_0} = \left(\frac{T}{T_0}\right)^{1/(\gamma-1)} \tag{1.46}$$

Using these expressions, we can express the static equilibrium condition ($dp/dz = -\rho g$) as

$$\frac{dT}{dz} = -\frac{\gamma-1}{\gamma}\frac{g}{R} = -\frac{g}{C_p} \tag{1.47}$$

This temperature gradient, commonly known as adiabatic lapse rate, implies that lower parcels are under grater pressure than the higher parcels and thus have higher densities and temperatures. However, departure from this adiabatic lapse rate takes place in a compressible fluid such as in atmospheric motions.

If we consider a fluid parcel at a height z of a vertically stratified gas, and if it is displaced adiabatically upwards over a small distance h, then according to the hydrostatic equation, this results in a pressure change $\delta p = -\rho g h$, which causes density and temperature changes under the adiabatic constraints given by Eqs. (1.44) and (1.45) as $\delta\rho = -\rho g h/\gamma RT$ and $\delta T = -(\gamma-1)gh/\gamma R$. Thus the new density is $\rho' = \rho + \delta\rho = \rho - \rho g h/\gamma RT$. But at that new level, the

ambient density is given by the stratification $\rho(z+h) \simeq \rho(z) + (d\rho/dz)h$. The net force exerted on the parcel is the difference between its own weight and the weight of the displaced fluid at the new location, which is

$$F = g\left[\rho(z+h) - \rho'\right] \simeq g\left(\frac{d\rho}{dz} + \frac{\rho g}{\gamma RT}\right) h \tag{1.48}$$

As the ideal gas law holds everywhere, using ideal gas equation and hydrostatic balance condition, we can rewrite the above expression in terms of temperature gradient as

$$F \simeq -\frac{\rho g}{T}\left(\frac{dT}{dz} + \frac{g}{C_p}\right) h \tag{1.49}$$

Thus, if

$$N^2 = -\frac{g}{\rho}\left(\frac{d\rho}{dz} + \frac{\rho g}{\gamma RT}\right) = \frac{g}{T}\left(\frac{dT}{dz} + \frac{g}{C_p}\right) \tag{1.50}$$

is a positive quantity, than the stratification is stable. Further, it is also clear that the relevant quantity is not the actual temperature gradient but its departure from the adiabatic gradient g/C_p.

In order to avoid the systematic subtraction of the adiabatic gradient from the temperature gradient, the concept of potential temperature (a scalar θ) is introduced which is defined as the temperature that the fluid parcel would have if it were brought adiabatically to a given reference pressure. From Eq. (1.45), we have

$$\frac{p}{p_0} = \left(\frac{T}{\theta}\right)^{\gamma/(\gamma-1)}$$

which gives

$$\theta = T\left(\frac{p}{p_0}\right)^{-(\gamma-1)/\gamma} \tag{1.51}$$

The corresponding density is called the potential density σ given by

$$\sigma = \rho\left(\frac{p}{p_0}\right)^{-1/\gamma} \tag{1.52}$$

The definition of the stratification frequency now takes the more compact form

$$N^2 = -\frac{g}{\sigma}\frac{d\sigma}{dz} = +\frac{g}{\theta}\frac{d\theta}{dz} \tag{1.53}$$

Comparison with earlier definition, given by Eq. (1.43), immediately shows that the substitution of potential density for density allows us to treat compressible fluids as incompressible.

The Brunt-Väisälä frequency N plays an important role in the dynamics of stratified fluids. For a stratified fluid of height H and stratification frequency N flowing horizontally at a speed U, we can construct a dimensionless number called Froude number Fr, defined as $\mathrm{Fr} = U/(NH)$, which is a measure of the importance of stratification. Thus, if $\mathrm{Fr} \leq 1$, stratification effects in turbulence can not be neglected. For large Fr, the kinetic energy is much larger than the potential energy changes across a height of order H. For small Fr, the stratification suppresses the vertical motion because a substantial fraction of kinetic energy must be converted to potential energy when a parcel moves in the vertical direction.

1.7.2 Phenomenological Considerations

Early theories for stably stratified turbulence were mainly based on dimensional arguments. Lumley [101] assumed spectral dependence on energy flux ε and considered the case $|\varepsilon/(\partial\varepsilon/\partial k)| \ll 1$, where $|\varepsilon/(\partial\varepsilon/\partial k)|$ is a measure of wavenumber bandwidth over which appreciable variation in ε occurs. He applied this reasoning to the case of stably stratified fluid and made an estimate (on dimensional grounds) for the buoyancy spectrum as

$$\zeta(k) = -C_1 N^2 \varepsilon(k)^{1/3} k^{-7/3} \tag{1.54}$$

where

$$\varepsilon(k) = \varepsilon_0 \left[1 + \left(\frac{k_B}{k}\right)^{4/3}\right]^{3/2} \tag{1.55}$$

Here $k_B = (C_1/2)^{3/4}(N^3/\varepsilon)^{1/2}$, with the Brunt-Väisälä frequency N given by $N^2 = (g/T_0)\partial T_0/\partial z$, and g and T_0 are the acceleration due to gravity and mean temperature respectively. This led him to suggest the energy spectrum in the form

$$E(k) = C\ \varepsilon_0^{2/3} \left[1 + (k/k_B)^{-4/3}\right] k^{-5/3} \tag{1.56}$$

Thus $E(k) \sim N^2 k^{-3}$ for large scales ($k_B/k \gg 1$) whence $\varepsilon(k)$ tends to ε_0. Further, Lumley made a rough estimate for the constant C in terms of Prandtl number σ and found that $C = 2\sigma^{-1}$. The underlying physical hypotheses are

delineated by Phillips [127], who derived a theoretical temperature spectra in the buoyancy subrange as

$$B(k) \sim \phi(k)\varepsilon_0^{-1/3}\left[1+(k_B/k)^{4/3}\right]^{-1/2}k^{-5/3} \tag{1.57}$$

where the scale dependent mean square density flux $\phi(k)$ is defined in terms of buoyancy spectra $\zeta(k)$ as

$$\phi(k) = \phi_0 + N^2\int_k^\infty dq\zeta(q) \tag{1.58}$$

where ϕ_0 is the value of $\phi(k)$ in the inertial subrange. This in turn produces the well-known Batchelor-Obukhov scaling law [121], namely $B(k) \sim \ \phi_0\,\varepsilon^{-1/3}k^{-5/3}$ in the inertial subrange. By introducing a conditional speculation that $\phi(k) \sim \phi_0$ in the buoyancy subrange ($k_B/k \ \gg 1$), Phillips obtained the density spectra as $B(k) \sim \phi_0 N^{-1}k^{-1}$, which was not consistent with observations. Following carefully Phillips' derivation, Weinstock [176] derived the temperature spectrum as

$$B(k) \sim N^2\varepsilon_0^{2/3}\left[1+(k_B/k)^{4/3}\right]k^{-5/3} \tag{1.59}$$

In the Boussinesq approximation, temperature fluctuation could be regarded as proportional to the density fluctuation [87]. Thus, in the $k_B/k \ \gg 1$ limit, he obtained $B(k) \sim N^4k^{-3}$. Though using quite different hypotheses, Holloway [59] obtained the kinetic energy and potential energy spectra showing the same functional form as Lumley's kinetic energy spectrum, with a radically distinct physical interpretation. Ramsden and Holloway [132] investigated the nonlinear interactions among internal gravity waves by direct numerical experiments in 2D and 3D Navier-Stokes turbulence and found that the transfer of kinetic energy (KE) from large to small scales is less efficient than the transfer of potential energy (PE). The imbalance between these transfers lead to a characteristic buoyancy flux spectrum which is negative (KE to PE) at large scales and positive (PE to KE) at small scales.

1.7.3 Dynamical Equations

The dynamics of stratified turbulence is governed by the Navier-Stokes equations. In the presence of a gravitational field **g**, Navier-Stokes equation takes

the form [126, 87]

$$\frac{\partial \mathbf{u}}{\partial t} + (\mathbf{u} \cdot \nabla)\,\mathbf{u} = -\frac{\nabla p}{\rho} + \nu_0 \nabla^2 \mathbf{u} + \mathbf{g} \tag{1.60}$$

The thermal convection equation can be written as

$$\frac{\partial T}{\partial t} + (\mathbf{u} \cdot \nabla)\,T = \kappa_0 \nabla^2 T \tag{1.61}$$

and the equation expressing incompressibility as

$$\nabla \cdot \mathbf{u} = 0 \tag{1.62}$$

where $\mathbf{u}(\mathbf{x}, t)$, $T(\mathbf{x}, t)$ and $p(\mathbf{x}, t)$ are the velocity, temperature and pressure fields; ν_0 and κ_0 are the kinematic viscosity and molecular diffusivity respectively. We use Boussinesq approximation [87, 24], and we write $p = p_0 + p'$, $T = T_0 + T'$, and $\rho = \rho_0 + \rho'$, where p' is the small pressure fluctuation measured from p_0, ρ_0 is the constant mean density, T' is the small fluctuation of T with respect to the mean temperature T_0, and the corresponding density variation can be expressed in terms of T' as

$$\rho' = (\partial \rho_0 / \partial T)_p T' = -\rho_0 \beta T'$$

Here the thermal expansion coefficient $\beta = -(1/\rho)\partial\rho/\partial T$ is assumed to be positive ($\beta > 0$). The condition of equilibrium is

$$(\nabla p_0 / \rho_0) = \mathbf{g}$$

Substituting these expressions in the above equations, one can obtain the corresponding equations for the fluctuating part in the Boussinesq approximation as

$$\frac{\partial \mathbf{u}}{\partial t} + (\mathbf{u} \cdot \nabla)\mathbf{u} = -\frac{\nabla p'}{\rho_0} + \nu_0 \nabla^2 \mathbf{u} - \beta T' \mathbf{g} \tag{1.63}$$

$$\frac{\partial T'}{\partial t} + (\mathbf{u} \cdot \nabla) T_0 + (\mathbf{u}.\nabla) T' = \kappa_0 \nabla^2 T' \tag{1.64}$$

Now considering the vertical mean temperature gradient along $\hat{e}_3$ (anti-parallel to gravity), the above equations can be written as

$$\frac{\partial \mathbf{u}}{\partial t} + (\mathbf{u} \cdot \nabla)\,\mathbf{u} = -\frac{\nabla p'}{\rho} + \nu_0 \nabla^2 \mathbf{u} + N \psi \hat{e}_3 \tag{1.65}$$

$$\frac{\partial \psi}{\partial t} + (\mathbf{u} \cdot \nabla)\, \psi = -N u_3 + \kappa_0 \nabla^2 \psi \tag{1.66}$$

$$\nabla \cdot \mathbf{u} = 0 \tag{1.67}$$

Here the scalar field $\psi(\mathbf{x}, t)$ is related with the fluctuating temperature field T' as

$$\psi = (\beta g/N) T'$$

in which N is the Brunt-Väisälä frequency given by $N^2 = \beta g (dT_0/dz)$.

In Chapter 4, we perform a Leslie-type perturbative treatment [90] on stably stratified turbulence, where the terms $N\psi\hat{e}_3$ and $-Nu_3$ in the above dynamical equations are treated as perturbation against the isotropic background fields. We make perturbation expansion of the velocity and scalar fields and derive the analytical expression for various anisotropic correlation functions, namely, velocity-velocity, temperature-temperature, and velocity-temperature correlations, which are capable of producing k^{-3} spectrum as was proposed by Lumley [101] and Weinstock [176]. Our calculation also yields a $k^{-7/3}$ buoyancy spectrum which was put forward by Lumley [101].

In Chapter 5, we perform a perturbation expansion similar to Kraichnan's direct interaction approximation (DIA) [78] to study the above problem of stratified turbulence with a stable stratification. We once again assume that the anisotropic buoyancy terms act as perturbation on the isotropic turbulent background fields. This enables us to evaluate the corresponding corrections to various correlation functions up to leading order terms. Unlike the previous Leslie-type treatment, here we see that the correction to the velocity-velocity and temperature-temperature correlations involve two extra terms each, signifying an improvement over the previous treatment. However, the velocity-temperature correlation remains the same as our previous Leslie-type calculations. We calculate the prefactors arising in the resulting anisotropic part of the energy and mean-square temperature spectra.

1.7.4 Relation of Stratified Turbulence to Atmospheric Flows

On the more practical level, stably stratified turbulence was thought to serve as a model for important scales of atmospheric and oceanographic motion. In this connection, we can mention the observations of Nastrom and Gage [115, 116]. In fact, they obtained, from the atmospheric data (upper troposphere and lower stratosphere) collected by NASA instrumented commercial Boeing 747 airliners, that the atmospheric energy spectra follow the -3 power law in the range extending from 1000 to 3000 km (the "synoptic scales") and the $-5/3$ power law in the scales extending from 600 km down to a few kilometers (the "mesoscales") with a smooth transition in between.

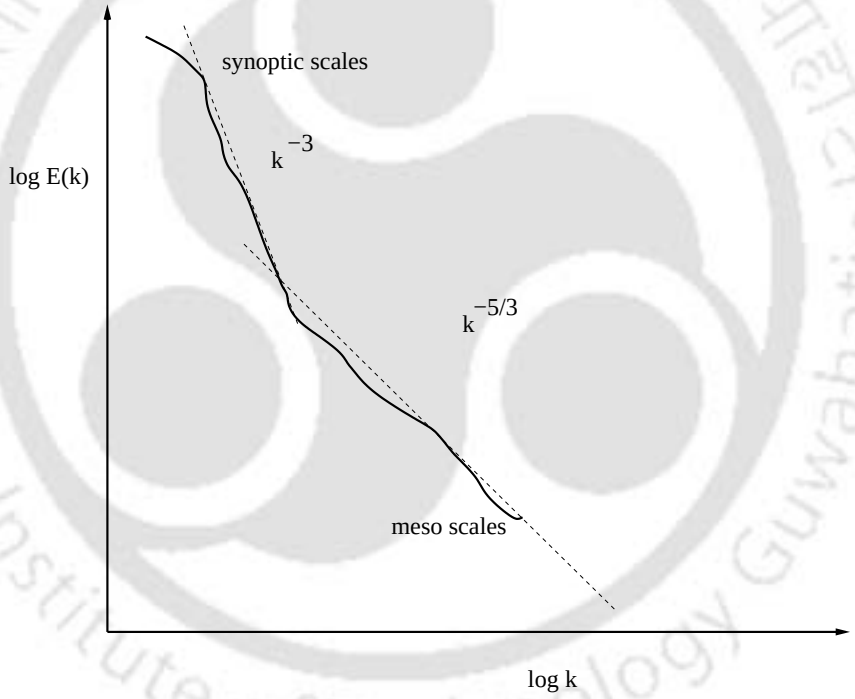

Figure 1.1: Schematic diagram of Nastrom-Gage spectrum.

They further argued that the underlying dynamics of the energy spectrum in this range was the inverse cascading of essentially two dimensional turbulence. More recently, Cho and Lindborg [29] examined aircraft data collected in the MOSAIC program [40, 119], for evidence of inverse cascade dynamics in the mesoscale range. Focusing on the third order structure function, rather

than the energy spectra, they found little evidence for inverse cascade dynamics. Their analysis, in fact, inferred a downscale cascade of energy ($k^{-5/3}$) in the mesoscale range of atmospheric motions with a transition scale around 10^3 km. They also suggested that the origin of large scale k^{-3} spectrum could be explained on the basis of the balance between Coriolis and pressure terms. In order to fully solve the problem of the origin of $k^{-5/3}$ mesoscale wavenumber energy spectra, Lindborg [98] carried out a set of numerical simulation of the full Boussinesq equations including system rotation, and thereby studied the effect of rotation on the energy spectra, and have shown that it can prevail when rotation is sufficiently weak. In a companion paper, Lindborg [96] also showed that such a mesoscale spectrum can arise as a result of forward energy cascade in the limit of strong stratification.

Kitamura and Matsuda [72], in order to investigate the energy cascade process due to synoptic scale forcing, performed numerical experiments with a three-dimensional nonhydrostatic model (within Boussinesq approximation) of stratified turbulence, and found a downscale energy cascade on the tails of a steep synoptic scale spectrum. Recent direct numerical simulations of homogeneous turbulence with a strong and uniform stratification [18] showed that stratification may enforce a three-dimensional dynamics and a forward $k^{-5/3}$ energy cascade. The basic ingredients in this DNS were three-dimensional Boussinesq equations and the transport equation for a passive gradient. They were solved employing pseudo-spectral code with periodic boundary condition in all three directions, and with forcing in rotational and divergent modes.

Tung and Orlando [167], from their two-level quasigeostrophic (QG) model, conjectured that the observed atmospheric energy spectra results from a downscale cascade of both enstrophy and energy, with the injection of energy taking place at the largest scales by baroclinic instability which finally is dissipated at the smallest length scales.

Understanding the source and structure of this spectrum has posed a great puzzle in atmospheric science for the past 25 years [29, 167]. Some of the earlier theoretical attempts to explain the energy cascade process in the atmospheric

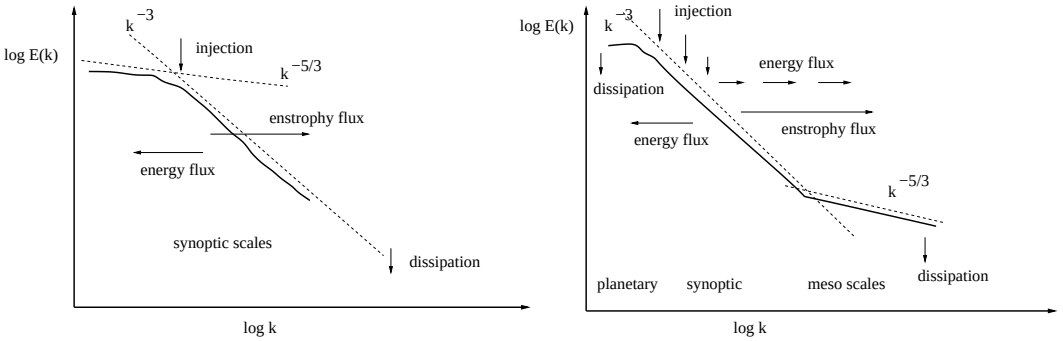

Figure 1.2: Schematic diagram of energy spectrum, injection, dissipation, and fluxes vs wavenumber: (a) traditional 2D turbulence thinking, (b)Tung and Orlando's QG model.

turbulence involved internal gravity waves (IGW) [35, 168]. Although different models of the IGW spectrum in the atmosphere have been proposed, the applicability of the approximations used in modelling of the IGW spectrum is still debated [97, 94]. Recently, Lindborg [94] investigated the effect of vertical vorticity on the mesoscale motions by constructing the two-point correlation of vertical and horizontal vorticities and their associated vorticity spectra from the second order structure functions [97]. He found that the mesoscale motions are not dominated by internal gravity waves. He further suggested that atmospheric spectra are generated by a strongly nonlinear dynamics, and stratified turbulence with a forward cascade of energy would possibly be able to explain the atmospheric observations.

1.8 Methods of Analysis

Here we present some sophisticated and powerful methods that have been extensively used in the analyses of turbulence dynamics. We shall be using these methods throughout the thesis.

1.8.1 Leslie's Perturbation Method

Leslie [90] suggested an appealing perturbation method for the case of homogeneous anisotropic turbulence. The basic idea was to treat the mean flow, which causes deviation from the isotropic state, as a weak perturbation to the isotropic state. For the homogeneous shear case, the mean velocity is $U_i = S_{ij}x_j$ with a uniform strain S_{ij}. Reynolds decomposition gives the Navier-Stokes equation as Eq. (1.38). The role of the shear is to strain the isotropic background field and induce anisotropy; the information about the anisotropy is conveyed by the anisotropic operator $\hat{N}_{ij}(\mathbf{k})$. Following Leslie, we consider this anisotropic term as a perturbation against the isotropic background state. We make perturbation expansion of the velocity correlation tensor and obtain, in the leading order approximation, the anisotropic part of the equal-time velocity correlation tensor. This is presented in Chapter 2.

In the case of stably stratified turbulence, the temperature field is coupled to the velocity field by the Boussinesq terms in Eqs. (1.65) and (1.66). In the absence of these terms the scenario reduces to the passive scalar case. Thus following Leslie [90], the extra terms, namely $N\psi\hat{e}_3$ and $-Nu_3$, can be treated as perturbation against the isotropic background fields. Accordingly we make perturbation expansion of the velocity and temperature fields. We carry out the analysis up to leading order term and obtain the anisotropic correction to the velocity-velocity and temperature-temperature correlation functions which scale as k^{-5} leading to the corresponding spectra as k^{-3}. Further, the velocity-temperature correlation turns out to be $k^{-13/3}$ leading to a buoyancy spectrum $k^{-7/3}$. The calculations are presented in detail in Chapter 4.

1.8.2 Direct Interaction Approximation (DIA)

Turbulence theory deals with the statistical solutions of the Navier-Stokes equation which are nonlinear and equivalent to an infinite hierarchy of equations coupling together all the moments of the random velocity field. Any finite subset of the infinite hierarchy of equations is not closed, and possesses

more unknowns than are determined by the subset. This is called the closure problem of turbulence theory. One has to make ad hoc assumptions to make the number of equations equal to the number of unknowns. The central problem of turbulence theory is to find proper approximate methods of converting the infinite hierarchy of equations into a closed subset.

To solve the closure problem, Kraichnan proposed the Direct interaction approximation (DIA) [78] and applied it to incompressible homogeneous isotropic turbulence, obtaining two integral equations for two unknown functions, namely, the energy equation and the response equation. In fact, the DIA takes into account integrals over triads of directly interacting wavevector and neglect higher order interactions. This is an approximation without neglecting the nonlinearity of the basic equation, and without introducing any ad hoc adjustable parameters. To bring into play the physics associated with the response of the turbulent system to small perturbations, the DIA makes essential and intimate use of the response function $G_{ij}(\mathbf{x}, \mathbf{x}', t, t') = \langle \delta u_i(\mathbf{x}, t)/\delta f_j(\mathbf{x}', t') \rangle$, where the deviation $\delta u_i(\mathbf{x}, t)$ in the velocity field is due to the infinitesimal disturbance $\delta f_j(\mathbf{x}', t')$ in the force field. Thus it captures the way in which the Navier-Stokes equation respond to perturbation. Finally a closed set of equations comprising the velocity covariance and mean infinitesimal response function is obtained. DIA is not restricted to either isotropy or homogeneity. However, the final closed equations are most easily written for homogeneous isotropic statistics.

In Fourier space, the Navier-Stokes equation looks like

$$\left(\frac{\partial}{\partial t} + \nu_0 k^2\right) u_i(\mathbf{k}, t) + \frac{i\lambda}{2} P_{ijl}(\mathbf{k}) \sum_{\mathbf{p}+\mathbf{q}=\mathbf{k}} u_j(\mathbf{p}, t) u_l(\mathbf{q}, t) = f_i(\mathbf{k}, t) \qquad (1.68)$$

Here $f_i(\mathbf{k}, t)$ is an external random force with Gaussian statistics, and $P_{ijl}(\mathbf{k}) = k_j P_{il}(\mathbf{k}) + k_l P_{ij}(\mathbf{k})$ with $P_{ij}(\mathbf{k}) = \delta_{ij} - k_i k_j/\mathbf{k}^2$; the summation sign represents integrations on $\mathbf{p}$ and $\mathbf{q}$ with triad relation $\mathbf{p} + \mathbf{q} = \mathbf{k}$.

Now, replacing u_i by $u_i + \delta u_i$, and f_i by $f_i + \delta f_i$ in the above equation, and subtracting the new equation from the original one, we get the equation

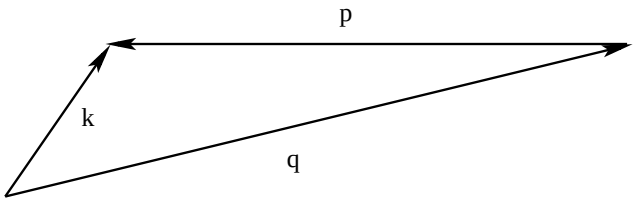

Figure 1.3: The triangle condition for triad interactions $\mathbf{p}+\mathbf{q}=\mathbf{k}$.

of motion for the perturbed fields as

$$\left(\frac{\partial}{\partial t}+\nu_0 k^2\right)\delta u_i(\mathbf{k},t)+i\lambda P_{ijl}(\mathbf{k})\sum_{\mathbf{p}+\mathbf{q}=\mathbf{k}}u_j(\mathbf{p},t)\delta u_l(\mathbf{q},t)=\delta f_i(\mathbf{k},t) \quad (1.69)$$

Solution of Eq.(1.69) is given by

$$\delta u_i(\mathbf{k},t)=\int_{-\infty}^{t} ds\; G_{ij}(\mathbf{k},t,s)\delta f_j(\mathbf{k},s) \quad (1.70)$$

where the Green function $G_{ij}(\mathbf{k},t,s)$ satisfies

$$\left(\frac{\partial}{\partial t}+\nu_0 k^2\right)G_{in}(\mathbf{k},t,s)+i\lambda P_{ijl}(\mathbf{k})\sum_{\mathbf{p}+\mathbf{q}=\mathbf{k}}u_j(\mathbf{p},t)G_{ln}(\mathbf{q},t,s)=P_{in}(\mathbf{k})\delta(t-s) \quad (1.71)$$

Now a perturbation theory is developed by making perturbation expansion of the velocity field and the response about the Gaussian state as

$$u_i(\mathbf{k},t)=u_i^{(0)}(\mathbf{k},t)+\lambda u_i^{(1)}(\mathbf{k},t)+\ldots$$

$$G_{ij}(\mathbf{k},t)=G_{ij}^{(0)}(\mathbf{k},t)+\lambda G_{ij}^{(1)}(\mathbf{k},t)+\ldots$$

These expansions are substituted in the above equations and perturbation series for the correlation and response functions are generated. The leading order terms in the perturbation series yield integral equations involving the zeroth order correlation and response functions. Replacing the zeroth order functions by the full functions, Kraichnan obtained the DIA equations. A similar procedure was applied for the case of passive scalar.

Kraichnan's DIA was the first "microscopic" theory of three dimensional turbulence [90] and it was the first complete field-theoretic approach to the theory of turbulence. This theory also resembles the Dyson-Schwinger formulation of quantum field theory [178, 64].

The DIA was formulated in the Eulerian framework and it was found to be inconsistent with the Kolmogorov $k^{-5/3}$ spectrum. Kraichnan identified this failure with the sweeping of smaller eddies by the larger ones. Edwards [38] pointed out that it is due to the divergence in the response integral coming from low wavenumbers. Eulerian framework fails to extract the small effect of Kolmogorov cascade among the small eddies from the large effect of their being swept around. As a result, it incorrectly yields a $k^{-3/2}$ spectrum instead of $k^{-5/3}$. To systematically eliminate this spurious effect of advection, Kraichnan reformulated the theory in a Lagrangian framework [81, 82]. Lagrangian version of DIA [82, 66, 71] gives excellent predictions for various statistical quantities such as the Kolmogorov universal form of the energy spectrum function and the skewness of the velocity gradient. The universal Kolmogorov constant C calculated within this framework was found to be $C = 1.43$ and 1.77 in two different schemes of calculations [82].

In this thesis, we are motivated to examine the scaling behaviour of stratified turbulence starting from the Navier-Stokes equation with Boussinesq approximation. We perform a perturbation expansion about the isotropic background state to obtain expansions resembling the DIA and Leslie's scheme. These expansions are found to be capable of yielding anisotropic corrections to the isotropic scaling laws. Such an approach is taken up in Chapter 5.

1.8.3 Heisenberg Approximation and Kraichnan's Distant Interaction Algorithm

In order to analyze the effect of nonlocal (distant) interactions, Kraichnan formulated the distant-interaction algorithm (DSTA) [76, 77], which involved approximations similar to Yakhot and Orszag's [184] calculation. The essence of the Kraichnan's DSTA is that the dynamics of modes in the inertial and dissipation ranges are assumed to be dominated by nonlocal interaction among the wavenumbers, that are modeled by white noise force acting against a dynamical viscosity, and this effective viscosity is estimated by extrapolation from the small contribution of interactions that are very nonlocal in wavenumber.

Kraichnan applied DSTA to the energy equation of DIA and obtained an asymptotic expression for the eddy-viscosity $\nu(k|p')$ in the Heisenberg approximation [57]. In this formalism, the basic assumption is that eddy viscosity felt at the wave number k, is assumed to represent interactions with wavenumbers $(p,q) > p'$, for $p' \gg k$. The dynamical interactions between wavevectors strictly follow the triangular condition $\mathbf{p}+\mathbf{q}=\mathbf{k}$, with $\mathbf{k}$ the external wave vector. p' is then extrapolated to a wavenumber λk where λ is an $O(1)$ numerical constant, characterizing the degree of nonlocality of the interaction. Thus

$$\nu(k|\lambda k) = \lim_{p' \to \lambda k} \nu(k|p')$$

which implies that dynamical damping arises solely from interaction of k with sufficiently higher wavenumbers. Finally, the eddy-viscosity at k is represented as

$$\nu(k) \equiv \nu(k|\lambda k)$$

In this formalism, the effect of (p,q)$\ll p'$ is entirely ignored. Thus, it restricts wave numbers on the UV side of the spectrum where the integrations are carried out by picking up only the UV pole, and thereby confining the dynamics to distant interaction eddy damping effects.

Following Kraichnan's [90, 78], the DIA energy transfer equation can be written as

$$\left(\frac{d}{dt} + 2\nu_0 k^2\right) E(k;t,t) = T(k;t,t)$$

The energy density $E(k,t,t)$ is related with the scalar correlation function $Q(k,t,t)$ as

$$E(k,t) = \frac{d-1}{2}\frac{S_d}{[2\pi]^d} k^{d-1} Q(k,t,t)$$

Thus, one can obtain the transfer $T(k,t,t)$ in d-dimensions as

$$T(k;t,t) = T(k) = \frac{8k^2}{(d-1)^2} k^{d-1} \int \frac{d^d p}{S_d} \theta_1(k,p,q) \times$$
$$\times \quad \left[a(k,p,q)\frac{E(p)}{p^{d-1}}\frac{E(q)}{q^{d-1}} - \frac{1}{2} b(k,q,p)\frac{E(p)}{p^{d-1}}\frac{E(k)}{k^{d-1}} - \frac{1}{2} b(k,p,q)\frac{E(q)}{q^{d-1}}\frac{E(k)}{k^{d-1}} \right] \tag{1.72}$$

Applying Heisenberg approximation, an asymptotic form of the eddy-viscosity can be derived from Eq. (1.72) as

$$T(k|p') = -2\nu(k|p')k^2E(k) \tag{1.73}$$

which is obtained from the transfer integral $T(k)$ by setting an IR cut-off at p'. The eddy viscosity can thus be calculated in the limit $p' \gg k$ (where $p \approx q$) using Eq. (1.72) as [113]

$$\nu(k|p') = \frac{2}{(d-1)^2}\int_{p'}^{\infty} dp \oint \frac{d\Omega}{S_d}\,\theta_1(k,p,q) \left[b(k,q,p)E(p) + b(k,p,q)\frac{E(q)}{q^{d-1}}p^{d-1}\right] \tag{1.74}$$

In this work, we apply Kraichnan's implementation of Heisenberg approximation to the problem of passive scalar turbulence. We derive analytical expressions for the eddy-viscosity and eddy-diffusivity from the transfer integrals of energy and mean-square scalar [90, 78]. We also evaluate the flux integrals for energy and mean-square scalar. We calculate the universal numbers, namely, Batchelor constant (Ba) and turbulent Prandtl number (σ). The details of calculation and result are presented in Chapter 3.

1.8.4 Dynamic Renormalization Group

The existence of universal scaling exponents and their calculation for various systems is a central problem of statistical mechanics. A main goal for many years has been to calculate the exponents for the Ising model, a simple spin model that captures the essential features of many magnetic systems. A major breakthrough occurred in 1971, when Wilson introduced the renormalization group (RG) method to permit a systematic calculation of the scaling exponents [177]. Since then RG has been applied successfully to a large number of interacting systems, by now becoming one of the standard tools of statistical mechanics and condensed matter physics. It has been successful in describing the physical phenomena in its own domain to an astonishing degree of accu-

racy. It can also be applied to stochastic equations in order to determine their scaling behavior in the large-distance long-time hydrodynamic limit.

The dynamic RG was used by Forster, Nelson and Stephen [43] for the case of Navier-stokes fluid along with the coupled problem of the advection of a passive scalar subjected to random driving forces. They adapted the procedure developed earlier by Ma and Mazenko [103]. It was observed by DeDominicis and Martin [34] that for a particular case of randomly stirred model, Kolmogorov scaling is realizable. Yakhot and Orszag [184] applied this model and performed an RG analysis to calculate various universal numbers. Their findings for various universal numbers were in good agreement with experiments. Afterwards, extensive theoretical research on turbulence has been carried out on the basis of RG approaches [187]. The hydrodynamical equations (Navier-Stokes and the evolution of a scalar field) for an anisotropically stirred fluid was studied through dynamic RG by Carati and Brenig [22] who evaluated the turbulent Prandtl number. Buša et al. [19], performed RG analysis of randomly stirred fluid with anisotropic distribution of random forces, and thereby evaluated the Kolmogorov constant and the amplitude of longitudinal and transverse projection operators with respect to the preferred direction in the energy spectrum. Applying recursive RG scheme together with the quasinormal approximation, Lin et al. [93] investigated the thermal turbulent transport properties and offered an estimation for the Prandtl number and Batchelor constant which was shown to depend on several characteristic wavenumbers of the particular flow under consideration.

The dynamic RG technique is concerned with applying mode-elimination ideas to evolution equations (such as Navier-Stokes equation) instead of the statistical-mechanical partition function employed in the study of critical phenomena [36]. It consists of a coarse-graining of the system followed by rescaling. Successive application of this transformation leads to what is called the RG flow of parameters appearing in the equations. The critical exponents, which characterize the scaling behavior of correlation function, are calculated at the fixed points of RG transformation. Thus, RG allows one to calculate the

scaling exponents in the combined presence of fluctuations and nonlinearities, and to calculate the exact asymptotic scaling of the correlation function in all the basins of attraction. In this section, we outline the basic steps of the method directly applied to the Navier-Stokes (NS) equation.

In order to apply the RG to the NS equation, we must put the NS equation in a suitable form. The idea is to try to solve perturbatively the NS equation, starting from the known solution of the linear problem. The RG can be done most conveniently using the Fourier components of the velocity field

$$\mathbf{u}_i(\mathbf{x},t) = \int_{k\leqslant k_d} \frac{d^d\mathbf{k}}{[2\pi]^d} \int_{-\infty}^{\infty} \frac{d\omega}{[2\pi]} \mathbf{u}_i(\mathbf{k},\omega) e^{i(\mathbf{k}\cdot\mathbf{x}-\omega t)} \tag{1.75}$$

in $(d+1)$ dimensions where the momentum integrals are subjected to the upper cutoff $k_d = (\nu^3/\bar{\varepsilon})^{1/4}$ related to the Kolmogorov microscale where dissipation occurs.

The space-time Fourier transformed Navier-Stokes equation becomes

$$(-i\omega + \nu_0 k^2)\, \mathbf{u}_i(\mathbf{k},\omega) = \mathbf{f}_i(\mathbf{k},\omega)$$
$$-\frac{i\lambda_o}{2} P_{ijl}(\mathbf{k}) \int_{q<\Lambda} \frac{d^d\mathbf{q}}{[2\pi]^d} \int_{-\infty}^{\infty} \frac{d\omega'}{[2\pi]} \mathbf{u}_j(\mathbf{q},\omega')\mathbf{u}_l(\mathbf{k}-\mathbf{q},\omega-\omega') \tag{1.76}$$

where $P_{ijl}(\mathbf{k}) = k_j P_{il}(\mathbf{k}) + k_l P_{ij}(\mathbf{k})$, and $\lambda_0(=1)$is the formal expansion parameter. The random stirring force field $f_i(\mathbf{k},\omega)$ is assumed to have Gaussian white-noise statistics with correlation given by Eq. (1.24).

Equation (1.76) can be rewritten as

$$\mathbf{u}_i(\mathbf{k},\omega) = G_0(\mathbf{k},\omega)\mathbf{f}_i(\mathbf{k},\omega)$$
$$-\frac{i\lambda_0}{2} G_0(\mathbf{k},\omega) P_{ijl}(\mathbf{k}) \int \frac{d^d\mathbf{q}d\omega'}{[2\pi]^{d+1}} \mathbf{u}_j(\mathbf{q},\omega')\mathbf{u}_l(\mathbf{k}-\mathbf{q},\omega-\omega') \tag{1.77}$$

where $G_0(\mathbf{k},\omega) = (-i\omega + \nu_0 k^2)^{-1}$ is the bare propagator. Equation (1.77) allows us to calculate $\mathbf{u}_i(\mathbf{k},\omega)$ perturbatively in powers of λ.

1.8.5 Renormalization Procedure

The important steps of the renormalization group procedure are as follows.

(1) The RG treatment begins with decomposition of the integral equation (1.76) into modes involving long wavelengths and short wavelengths and then

to systematically eliminate the fast modes $u^{>}$ from thin shells of momentum space (belonging to $\Lambda e^{-r} < k < \Lambda$) starting from the UV end.

Figure 1.4: Decomposition of the fast mode, $u^{>}(\mathbf{k},\omega)$, and slow mode, $u^{<}(\mathbf{k},\omega)$ lying in the bands $\Lambda e^{-r} < k < \Lambda$ and $0 < k < \Lambda e^{-r}$ respectively. Here Λ is the internal cutoff wave number.

Physically, this step serves to thin out the degrees of freedom (coarse graining), and reduces the spatial resolution of the system. The resulting equation for the slow modes is given by

$$(-i\omega + \nu_0 k^2)\mathbf{u}_i^{<}(\mathbf{k},\omega) = f_i^{<}(\mathbf{k},\omega)$$
$$-\frac{i\lambda_0}{2}P_{ijl}(\mathbf{k})\int\int \frac{d^d\mathbf{q}d\omega'}{[2\pi]^{d+1}}\mathbf{u}_j^{<}(\mathbf{q},\omega')\mathbf{u}_l^{<}(\mathbf{k}-\mathbf{q},\omega-\omega') + R_i(\mathbf{k},\omega) \quad (1.78)$$

with

$$R_i(\mathbf{k},\omega) = -\Sigma_{ij}(\mathbf{k},\omega)u_j(\mathbf{k},\omega) \quad (1.79)$$

The term $R_i(\mathbf{k},\omega)$, when transferred to the left-hand side of Eq. (1.78), gives correction to the bare quantity $\nu_0 k^2$, given by the self-energy

$$-\Sigma_{in}(\mathbf{k},\omega) = 4\left(\frac{-i\lambda_0}{2}\right)^2 P_{ijl}(\mathbf{k})$$
$$\times\int \frac{d^d q d\omega'}{[2\pi]^{d+1}}Q_{jm}^{>}(\mathbf{q},\omega')G_{lk}^{>}(\mathbf{k}-\mathbf{q},\omega-\omega')P_{kmn}(\mathbf{k}-\mathbf{q}) \quad (1.80)$$

Here, $G_{ij}(\mathbf{k},\omega) = (-i\omega + \nu_0 k^2)^{-1} P_{ij}(\mathbf{k})$ is the propagator and $Q_{in} = G_{ij}F_{jl}G_{ln}^{*}$ is the velocity correlation. The coupling constant λ_0, however, does not undergo any relevant correction due to Galilean invariance. This elimination process is repeated in recursive steps with infinitesimal r. The recursion relations can be obtained easily from the diagrammatic perturbation expansions explained in Section 1.8.6.

(2) After elimination of scales, the resulting equation has a smaller cut-off, namely Λe^{-r}. This difference from the original equation is removed by rescaling procedure. After this rescaling we must get the dynamical equation in the same form as the original ones. Applying these steps to the one-loop expressions, we obtain a set of differential renormalization group flow equations for the coupling constants (dimensionless parameters) that depend on r.

(3) Finally, the exponents are calculated by looking for a relevant fixed point of the flow equations. Thus, RG fixed point analysis can be used for predicting the asymptotic large-scale, long-time behavior of the correlation functions.

1.8.6 Diagrammatic Approach

The diagrammatic perturbation theory suggested by Wyld [178] is a regular procedure for investigating hydrodynamic turbulence. Analogous to Feynman diagrams, which are useful in studying the renormalization problem in quantum field theory [63, 64], these diagrams are constructed following a simple set of rules in such a way that there is a one-to-one correspondence between the diagrams and the terms in the perturbation series. This device is useful because it is much easier to draw the diagrams and examine their topological structure than it is to study the properties of the integrals to which they correspond. This technique was later generalized by Martin, Siggia and Rose [106], who demonstrated that it may be used to investigate the fluctuation effects in the low-frequency dynamics of any condensed-matter system. In fact this technique is also a classical limit of the Keldysh diagrammatic technique [69] which is applicable to any physical system described by interacting Fermi and Bose fields. Zakharov and L'vov [186] extended the Wyld technique to the statistical description of Hamiltonian nonlinear-wave fields including hydrodynamic turbulence in the Clebsch variables [182, 102].

Diagrammatic expansion is an efficient method to simplify the calculations. To escape from manipulating long and complicated expressions through boring calculations, it is convenient to use the diagrammatic representation of Eq.

(1.77) as indicated in Fig. 1.5. We replace every term in the equation with a symbol and establish the rules for handling the symbols. With properly defined rules, the perturbation expansion can be carried out merely by combining the diagrams. In the final step, the diagrams are translated back into formulas.

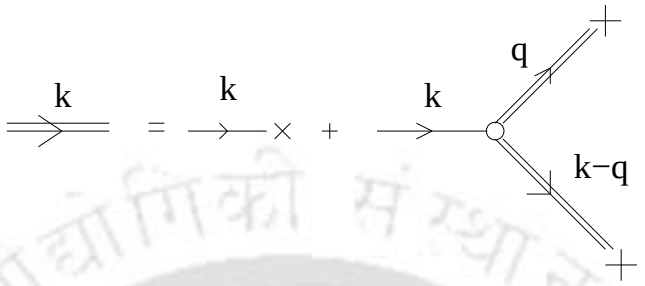

Figure 1.5: Diagrammatic representation of Eq. (1.77). Single arrow represents the bare propagator $G_0(\mathbf{k},\omega)$, cross the forcing $f_i(\mathbf{k},\omega)$, and the open circle represents the vertex $(-i\lambda_0/2)P_{ijl}(\mathbf{k})\int d^dq/[2\pi]^d$.

Fig. 1.5 illustrates a method of replacing the starting equation (1.77) of the perturbation expansion with symbols. We have for $\lambda = 0$

$$u_i(\mathbf{k},\omega) = G_0(\mathbf{k},\omega)f_i(\mathbf{k},\omega) \tag{1.81}$$

The expansion is done in powers of λ around this zeroth order solution for u_i. In general we define

$$u_i(\mathbf{k},\omega) \equiv G(\mathbf{k},\omega)f_i(\mathbf{k},\omega) \tag{1.82}$$

In Fig. 1.5, $G_0(\mathbf{k},\omega)$ is replaced with a simple arrow, carrying a momentum $(\mathbf{k},\omega)$; $G(\mathbf{k},\omega)$ is replaced with a double arrow; the integral over $\mathbf{q}$ and ω is represented by the vertex, ◯. There is wave number conservation at each vertex. It is a property of the Fourier transform that the arguments of the $\mathbf{u}$'s under the integral in (1.77) sum up to $(\mathbf{k},\omega)$. This leads to a conservation rule: The momenta $(\mathbf{k},\omega)$ going into the vertex are equal to the sum of the momenta coming out from the vertex.

To perform a perturbation expansion in powers of λ, we must replace the u_i terms under the integral in (1.77) with the full form of $u_i(\mathbf{k},\omega)$ given by (1.77). The newly-appearing u_i terms can again be replaced by (1.77). Using

the diagrams we replace the double line corresponding to $u_i(\mathbf{k}, \omega)$ in the rhs of Fig. 1.5. Fig. 1.6 shows the expansion up to second order in λ.

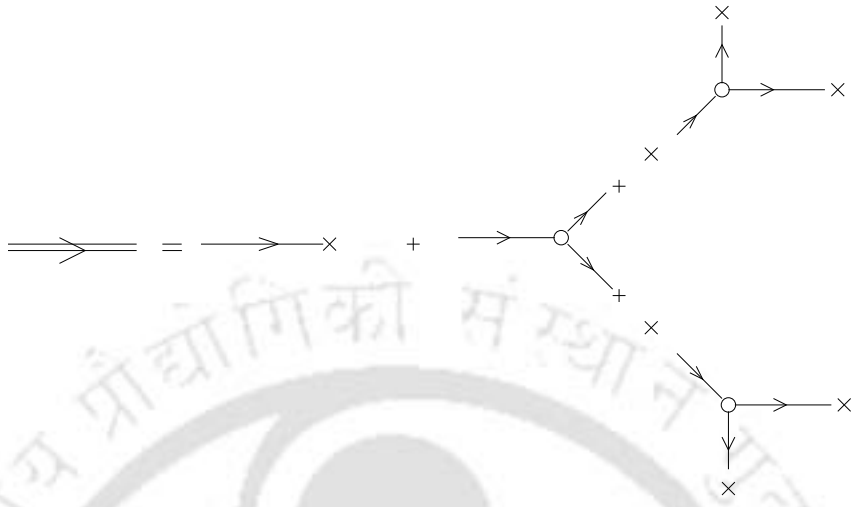

Figure 1.6: Perturbation expansion for the propagator $G(\mathbf{k}, \omega)$.

To obtain the effective propagator, we must average over the stochastic noise i.e., we must perform the $\langle \ldots \rangle$ average for every diagram. If there is only one noise term in the diagram, that diagram vanishes, since the noise has zero average. If there are two noise terms (which within a single diagram multiply each other), according to Eq. 1.24, the average over the product of the two noise terms generates a delta function. Thus two noise terms in the same diagram can be paired up and replaced with a delta function. The delta function leads to an another useful property of the average over the noise: denoting by a bubble, $\otimes$, the contraction of the two noise terms, the sum of the momenta going into the bubble must be zero. In general, if there is an even number of noise terms in a diagram, they can be paired up, and the diagram may be nonzero. However, if there is an odd number of noise terms, there is always one unpaired noise, whose average is zero, so the whole diagram gives zero contribution. The final diagrams, the one-loop correction to G_0, are shown in Fig. 1.7. Concerning the momenta on the legs of the diagrams, we note that following three simple rules, one can find all the variables on the legs. We summarize the rules bellow:

(i) The incoming and outgoing variables are $(\mathbf{k}, \omega)$, set by the variables of the expansion $u_i(\mathbf{k}, \omega)$.

(ii) The sum of the momenta going into a vertex equals the sum of the momenta going out from the vertex.

(iii) The noise term has two identical momenta both going into the bubble.

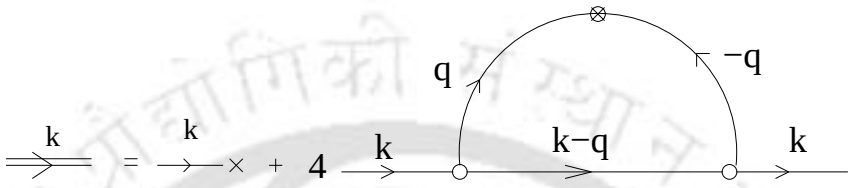

Figure 1.7: The effective propagator obtained by averaging over the noise.

Using these rules systematically, we can derive all the variables on the legs of the diagrams. Having the diagrams, we can go back to the formulas and identify every element of the diagram with the corresponding term. In particular, every simple arrow corresponding to G_0, the bubble $\otimes$ to a noise term, and the vertex $\bigcirc$ to an integral. We integrate over the internal coordinates $(\mathbf{q}, \omega')$. The variables can be read off from the legs of the diagrams of Fig. 1.7.

Finally we obtain $G(\mathbf{k}, \omega)$ as a perturbation expansion in λ

$$G(\mathbf{k},\omega) = G_0(\mathbf{k},\omega) + 4\left(\frac{-i\lambda_0}{2}\right)^2 F(k) G_0^2(\mathbf{k},\omega) P_{ijl}(\mathbf{k}) \int \frac{d^dq}{[2\pi]^d} \int_{-\infty}^{+\infty} \frac{d\omega}{[2\pi]}$$

$$\times P_{lmn}(\mathbf{k}-\mathbf{q}) G_0(\mathbf{k}-\mathbf{q}, \omega-\omega') G_0(\mathbf{q},\omega) G_0(-\mathbf{q},-\omega) P_{jm}(\mathbf{q}) + O(\lambda^4) \quad (1.83)$$

This result could have been obtained by following the same program without diagrams, doing the integrals and averaging over the noise directly. However, the diagrammatic expansion is much faster and simpler.

Thus, we have seen that, the one-loop correction to the bare propagator in turn gives correction to the bare viscosity, $\nu_0 k^2$, due to the one-loop Feynman diagrams for self-energy as shown in Fig. 1.7. In order to evaluate the corresponding integral expression, we perform proper symmetrization with respect to wavevectors of the self-energy integral as shown in Fig. 1.8, which allow us

to easily evaluate the integral in the large-scale, long-time limit ($k \to 0, \omega \to 0$) by picking up the leading contribution form the regions $q \gg k$ and $p \gg k$ [114].

Vertex Renormalization

In order to calculate perturbatively the mode-interaction vertex shown in Fig. 1.5, the two legs of the vertex are replaced with the expression for $u_i(\mathbf{k}, \omega)$ as shown in Fig. 1.9, and the perturbation expansion is iterated twice in order to obtain all one-loop diagrams. We simplify the diagrams with two noise terms, and average over all remaining noise terms. As a result, contribution may arise from diagrams A, D and E since B and C vanish, having only one noise term remaining. There are three possible noise contractions that can be carried out on the diagrams D and E, giving the perturbation expansion shown in Fig. 1.9(c). They give zero contribution as a consequence of Galilean invariance.

Noise Renormalization

The above iterative procedure is capable of generating corrections to the noise amplitude D_0 defined by

$$\langle u_i(\mathbf{k}, \omega) u_j(\mathbf{k}', \omega') \rangle = 2\tilde{D} k^{-y} P_{ij}(\mathbf{k}) G(k, \omega) G(-k, -\omega) \times [2\pi]^d \delta^d(\mathbf{k} + \mathbf{k}') [2\pi] \delta(\omega + \omega') \quad (1.84)$$

which can be obtained using Eq. (1.24). The diagrammatic representation of the perturbation series is given in Fig. 1.10. After averaging over the noise, the diagrams C and D vanish. Nonzero contributions arising from A and B are shown in Fig. 1.10(c). The resulting expression is

$$\tilde{D} = D_0 + 2D_0^2 \left(-\frac{i\lambda_0}{2} \right)^2 P_{ijl}(\mathbf{k}) \int \frac{d^d q d\omega'}{[2\pi]^{d+1}} |G_0(q, \omega)|^2 \times |G_0(k - q, \omega - \omega')|^2 P_{jm}(\mathbf{q}) P_{lmn}(\mathbf{k} - \mathbf{q}) \quad (1.85)$$

In Chapter 5, we use the dynamic RG scheme to achieve a coarse-grained description of turbulent flow field with density stratification via successive

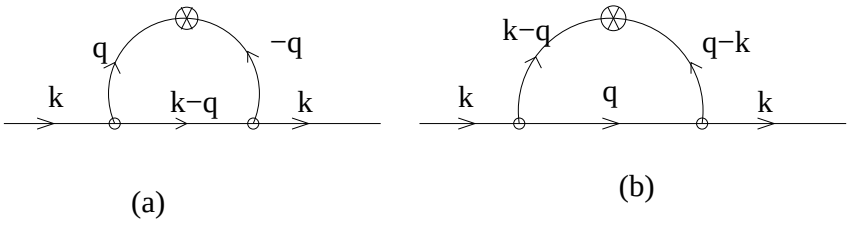

Figure 1.8: Symmetrization of the one-loop Feynman diagram for self-energy correction to the bare viscosity.

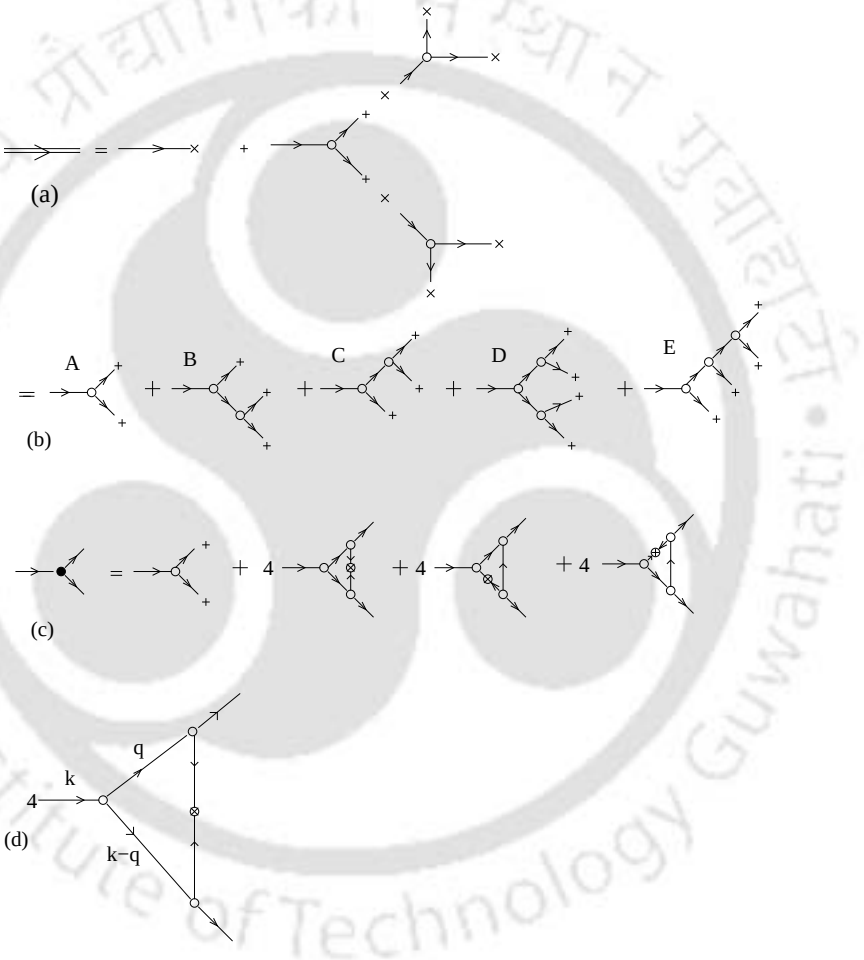

Figure 1.9: Perturbation expansion for the vertex λ. In (a), the leg of the vertex are replaced with the full expansion shown in Fig. 1.6. Iterating the perturbation expansion twice (by replacing the leg again with the full expansion), we obtain the five terms as shown in (b). The effective vertex function, obtained after averaging over the noise, is shown in (c). The variable used for the calculation is shown in (d).

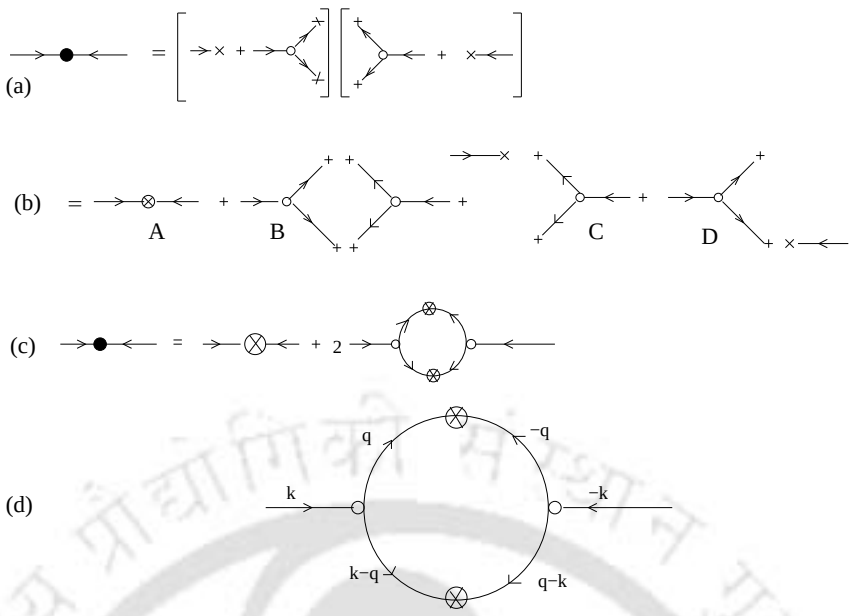

Figure 1.10: Perturbation expansion for the noise correlation term. (a) The noise term can be expanded in series using Eq. (1.77). The term in (b) must be averaged over the noise, resulting in the nonzero diagrams shown in (c). The essential variables used for calculations of the one-loop Feynman diagrams are given in (d).

elimination of small scale modes. This yields the effective viscosity and diffusivity as a result of corrections coming from the self energy diagrams. This leads to the emergence of vertical and horizontal eddy viscosities and diffusivities as a result of anisotropy. We further investigate the realizability of the Kolmogorov fixed point in the limit of weak stratification.

1.9 Layout of the Thesis

The thesis is organized as follows:

In **Chapter 2**, we investigate the homogeneous shear flow turbulence by Leslie's perturbation method and thereby extract the information of anisotropy. Considering only the lowest order of our perturbative evaluation, we derive the anisotropic correction to the equal-time velocity correlation tensor. We calculate the universal numbers associated with these corrections using inputs from renormalization group results.

In **Chapter 3**, we investigate the passive scalar convection problem implementing Kraichnan's method [90, 78] and Heisenbergs approximation [57]. We derive analytic expressions for eddy-viscosity and eddy-diffusivity from the transfer integrals of energy and mean-square scalar. We also evaluate the flux integrals for energy and mean-square scalar. These procedures allow us to evaluate relevant amplitude ratios, from which we calculate the universal numbers.

In **Chapter 4**, we present a Leslie-type perturbative treatment on stably stratified turbulence with Boussinesq approximation, where the buoyancy terms in the corresponding dynamical equations are treated as perturbations against the isotropic background fields. The corresponding corrections to various correlation functions, namely, velocity-velocity, temperature-temperature, and velocity-temperature correlations are evaluated up to the leading order terms. We find that the prefactors associated with the anisotropic corrections to the velocity-velocity, temperature-temperature and velocity-temperature correlation functions depend on the Kolmogorov constant C, Batchelor (or Obukhov-Corrsin) constant Ba, and turbulent Prandtl number σ. We calculate the universal numbers occurring as prefactors in the various anisotropic correlation functions. Our calculations yield the anisotropic part of energy and mean-square scalar spectra as k^{-3} and the anisotropic buoyancy spectrum as $k^{-7/3}$.

In **Chapter 5**, we present our calculations on stably stratified turbulence with the help of perturbation expansion motivated by Kraichnan's direct interaction approximation (DIA). Unlike the Leslie-type treatment, here we find that the correction to the velocity-velocity and temperature-temperature correlation functions acquire new terms, whereas velocity-temperature correlation remains the same as the previous Leslie-type treatment. The anisotropic spectra corresponding to various correlations are found to remain the same as in the previous calculations. However, the prefactors depend on the isotropic universal numbers in a more complicated fashion than before.

In **Chapter 6**, we use the dynamic RG scheme up to one-loop order to

achieve a coarse-grained description of turbulent flow field with a stable temperature stratification via successive elimination of small shells of modes from the ultraviolet (UV) end of wavenumbers. The scale elimination procedure is found to generate corrections to the viscosity and diffusivity in an anisotropic fashion. Due to the presence of anisotropy, the perturbative RG treatment of this problem involves many extra Feynman diagrams along with those of Yakhot and Orszag's [183]. We find that, apart from the usual isotropic viscosity and diffusivity terms ($\nu_0 k^2$ and $\kappa_0 k^2$), there appear different terms ($\nu_3 k_3^2$ and $\kappa_3 k_3^2$) corresponding to the vertical motion. This gives rise to a very complicated RG analysis. However, in the limit of weak stratification, the stability analysis of the flow equations can be performed with less difficulty. It is found that the Kolmogorov scaling regime exists and thus we expect that the energy cascade would follow the Kolmogorov type scaling.

Finally, we present the summary and conclusion in **Chapter 7**.

Chapter 2

Leslie-type Treatment of Homogeneous Shear Turbulence

2.1 Introduction

As noted earlier, the statistical properties of velocity fluctuations in turbulent flows is characterized by remarkable power laws, describing the scale dependence of the correlation functions. The most famous example is the Kolmogorov's universal inertial range energy spectrum [74, 121]

$$E(k) = C\bar{\varepsilon}^{2/3}k^{-5/3} \tag{2.1}$$

where C is the universal Kolmogorov constant, $\bar{\varepsilon}$ is the energy dissipation rate, and k is the wavenumber. This universal scaling law has been derived originally assuming that the flow properties become statistically homogeneous and isotropic [45] at small scales in the process of energy cascade from large to small scales (without dissipation); the anisotropy introduced at large scales by forcing (boundary conditions, geometry of an obstacle, etc.) is assumed to be diminished rapidly when the energy is transferred down to the smaller scales owing to the cascade mechanism [111, 45]. This highly idealized case turns out to provide a very deep insight into the structure of turbulent flows. Nevertheless, deviation from this idealized case is expected when the flow is inherently anisotropic, as in essentially any flow of natural and engineering

relevance.

A number of recent work confirms this picture for the even correlation function, thus giving some quantitative support to the aforementioned hypothesis on the restored local isotropy on the inertial range turbulence for the velocity and passive scalar fields [4, 5, 137, 7]. Nevertheless, the anisotropy survives in the inertial range and reveals itself in odd correlation functions, in disagreement with what was expected on the basis of the cascade ideas. The so-called skewness factor decreases down the scales much slower than expected [146, 131], while the higher-order dimensionless ratios (hyperskewness, etc.) increase, thus signaling of persistent small-scale anisotropy as suggested in [5].

To investigate the persistence of anisotropy, considerable attention has been made during the last few decades in experimental anisotropic turbulence [47, 141], and numerical homogeneous shear flows [130, 129]. This flow contains the complicated coupling of turbulent and mean velocity fields which is characteristic of most natural and engineering turbulent flows, but it has statistical homogeneity as a simplification. In fact, most turbulent flows that are generated by a large scale forcing or in the presence of geometrical boundaries or obstacles, usually breaks the isotropy and homogeneity symmetries at the largest scales. Simple theoretical reasoning, as well as decades of careful experimental work has suggested that anisotropy most probably remains even at the smallest scales of the motion [137, 138]. A number of numerical and experimental investigations in shear flow turbulence have shown that the anisotropy appears not only at higher order moments, but also at second order moments. Measurement of structure functions in shear turbulence [153] indicated that the large scale shear persists down to smallest scales. This observed anisotropic effects in small scale turbulence are both theoretical and practical challenge.

It may also be noted that, under the influence of strong uniform magnetic filed, turbulence becomes anisotropic. Ishida and Kaneda [60] performed theoretical and numerical investigation on magnetohydrodynamic turbulence under

an externally applied strong stationary uniform magnetic field and, thereby obtained the scale and angular dependence of the anisotropic velocity correlation spectrum at small scales.

From a fundamental view point, it is interesting to understand how the externally imposed large scale anisotropy to an incompressible fluid produces a disturbance which set the fluid into a macroscopic motions that obey the linear relation between the rate of strain tensor S_{ij} and the stress tensor τ_{ij} given by

$$\tau_{ij} = C_{ijab} S_{ab} \tag{2.2}$$

where C_{ijab}, is a tensor of rank four. In the presence of mean flow, which causes deviation from the isotropy, it was found that [61] the deviation of the velocity correlation tensor from the equilibrium state at small scales due to the mean shear can be given by

$$\Delta Q_{ij}(\mathbf{k}) = C_{ijab}(\mathbf{k}) S_{ab} \tag{2.3}$$

where unlike Eq. (2.2), C_{ijab} now depend on wave vector k and its property of isotropy has been lost, thereby reflecting the effect of anisotropy on the velocity correlation tensor.

We note that, using Lagrangian renormalized approximation (LRA) scheme [66], Ishihara and Yoshida [185] carried out an analysis on the anisotropic property of the velocity correlation tensor and obtained the universal numbers, namely, A and B, associated with the spectrum (defined in Eq. (2.29) below) where the value of B was found to be significantly higher than the experimental [164] as well as their direct numerical simulation (DNS) values [61]. They attributed this underestimate to the nature of LRA– they proposed that it's results are applicable only in the inviscid limit (infinitely large Reynolds number), whereas DNS and experiment are performed at modest Reynolds numbers [185].

It was long ago that Kraichnan had formulated the Lagrangian closure schemes, namely, abridged Lagrangian history direct interaction approxima-

tion (ALHDIA) [81], the strain based abridged Lagrangian history DIA (SBALHDIA) [83]. The main reason that such approaches were taken was that the Kraichnan's (Eulerian) direct interaction approximation (DIA) suffers from the well-known infrared (IR) divergence problem due to advection of the small eddies by the larger ones. In the ALHDIA and SBLHDIA formulations the IR problem was removed. These formulations, being more detailed than LRA, we expect that they would produce better results than LRA. However, for the isotropic case itself, these formulations are mathematically too cumbersome. In order to overcome the mathematical difficulties, Kraichnan himself considered the problem in Eulerian framework using the Eulerian DIA closure based test-field model (TFM) [79]. All these developments were made for the case of homogeneous isotropic turbulence. Leslie [90], however, offered a perturbative model to incorporate the anisotropic effects by means of perturbation analysis within the DIA framework of Kraichnan. However, Leslie's treatment did not restore the properties of symmetry in tensor indices and solenoidality of the correlation tensor. A modified theoretical investigation [112] on Leslie's model could restore both the properties. Using Kraichnan's TFM coupled with Leslie's model, it was shown that the results corresponding to the anisotropic correlation tensor were in somewhat good agreement with experiment [164] for the case of three-dimensional anisotropic homogeneous turbulence.

It has also been found that, the cases of anisotropic turbulence have been mostly dealt with $SO(3)$ decomposition [7, 6, 102], where one can assess the anisotropic effects by systematically finding the projections of measured structure functions on the irreducible representations of the $SO(3)$ group of all rotations. The idea is to decompose any correlation function in a complete basis of eigenfunctions with well defined properties under rotations. Each eigenfunction identifies a specific anisotropic sector with angular momentum, l, and its projection, m, on a given axis. The scaling exponents were extracted from theoretical [102], experimental [153, 152, 86, 143] as well as numerical [16, 15, 23] data. For $l = 0$, and $l = 2$ the corresponding scaling exponents for the second-order velocity structure tensor were found in various experiments

as 0.69 and 0.67 [143], 0.708 and 1.22 [85], 0.68 ± 0.01 and 1.38 ± 0.1 [86], and 0.7 and 1.5 [153], whereas in LES it was 0.69 and 0.72 [23], in DNS 0.70 ± 0.21 and 1.15 ± 0.5 [16, 15], and in theory 2/3 and 1.252 [102] respectively.

Quite recently [14], a finite-dimensional inertial range approximation of the anisotropic two-point, second-order velocity correlation tensor, $R_{ij}(\mathbf{x}, \mathbf{r}) = \langle u_i(\mathbf{x}) u_j(\mathbf{x}+\mathbf{r}) \rangle$, was constructed in real space in terms of three linearly independent structure tensors proposed by Kassinos et al. [68], which contains the information about the structure of the anisotropy. They noted that unlike the $SO(3)$ representation, the linear representation in terms of structure tensors is not a complete basis for $R_{ij}(\mathbf{r})$. The number of degrees of freedom in this model is reduced by imposing continuity and self-consistency constraints, and the inertial-range assumption led to a power law dependence in r.

Here we take an alternative route to the problem of homogeneous anisotropic turbulence and hence we are interested to tackle directly the anisotropic terms appearing in the dynamical equations by means of "standard" perturbative method. We employ Leslie's perturbative method and take inputs from the renormalization group calculation of Yakhot and Orszag [184]. This amounts to making a perturbative expansion of the velocity correlation tensor, which has contributions due to isotropy as well as due to imposed anisotropy. Through direct calculations, we derive the form of anisotropic equal-time velocity correlation tensor. It may particularly be noted that we do not make any conjecture about the form of the correlation tensor. Nor do we make any hypothesis about the form of the anisotropic parts of the correlation tensor. The form of the correlation tensor is automatically obtained through derivations in the perturbative scheme. Further, the anisotropic part of the correlation tensor is found to be of the form

$$Q_{ij}^{(1)}(\mathbf{k}; 0)$$

$$= S_{ab} \left[P_{ia}(\mathbf{k}) P_{jb}(\mathbf{k}) + P_{ja}(\mathbf{k}) P_{ib}(\mathbf{k}) \right] R^{(1,1)}(k) + S_{lm} \frac{k_l k_m}{\mathbf{k}^2} P_{ij}(\mathbf{k})\, R^{(1,3)}(k) \quad (2.4)$$

In this expression for anisotropic correlation tensor, the scaling factors, namely $R^{(1,1)}(k)$ and $R^{(1,3)}(k)$, are determined by isotropic correlation and response

functions, and they are found to be of the form $R^{(1,1)}(k) = A\ \varepsilon^{1/3}k^{-13/3}$ and $R^{(1,3)}(k) = B\ \varepsilon^{1/3}k^{-13/3}$, where A and B are two non-dimensional universal numbers. We calculate A and B using inputs from renormalization group calculations. Our calculated values of A and B are $A = -0.13$ and $B = -0.48$. These values are found to be very close to the experimental values $A \approx -0.17$ and $B \approx -0.45$ [164]. Thus, this method enables us to calculate fully the leading order correction due to the homogeneous shear.

2.2 Mathematical Formulations

We start from the full Navier-Stokes equation for an incompressible fluid given by

$$\frac{\partial v_i}{\partial t} + v_j\frac{\partial v_i}{\partial x_j} = -\frac{\partial p}{\partial x_i} + \nu_0\frac{\partial^2 v_i}{\partial x_j \partial x_j}$$

where $v_i(\mathbf{x}, t)$ is the velocity field, $p(\mathbf{x}, t)$ is the pressure field divided by density, and ν_0 the kinematic viscosity of the fluid. The pressure field can be expressed in terms of the velocity field using incompressibility condition, $\nabla \cdot \mathbf{u} = 0$, coming from the equation of continuity.

As discussed earlier, after Reynolds decomposition[160, 58] of the full velocity field, $v_i = U_i + u_i$, the randomly forced Navier-Stokes equation for the fluctuating part is obtained as

$$\frac{\partial u_i}{\partial t} + U_j\frac{\partial u_i}{\partial x_j} + u_j\frac{\partial U_i}{\partial x_j} + u_j\frac{\partial u_i}{\partial x_j} = f_i - \frac{1}{\rho}\frac{\partial p}{\partial x_i} + \frac{\partial \overline{u_i u_j}}{\partial x_j} + \nu\frac{\partial^2 u_i}{\partial x_j \partial x_j} \tag{2.5}$$

where $\overline{u_i u_j}$ represents Reynolds stress. Here, we consider a general form of mean velocity

$$U_i = S_{ij}x_j \tag{2.6}$$

where the strain S_{ij} is assumed to be uniform in space and constant in time, and $S_{ii} = 0$ due to incompressibility.

In Eq. (2.5), the terms $U_j\dfrac{\partial u_i}{\partial x_j}$ and $u_j\dfrac{\partial U_i}{\partial x_j}$ represent direct coupling of mean and fluctuating velocity fields, while the terms $u_j\dfrac{\partial u_i}{\partial x_j}$ and $\dfrac{\partial \overline{u_i u_j}}{\partial x_j}$ represent the

nonlinear coupling within the fluctuating fields. If v_l be the characteristic velocity of eddies of size l, then from dimensional considerations, the order of magnitudes of the terms associated with the motion of these eddies are found as follows:

Direct coupling terms:

$$U_j\frac{\partial u_i}{\partial x_j},\quad u_j\frac{\partial U_i}{\partial x_j}\ \sim Sv_l$$

Nonlinear convective terms:

$$u_j\frac{\partial u_i}{\partial x_j},\quad \frac{\partial\overline{u_iu_j}}{\partial x_j}\ \sim v_l^2/l$$

and viscous dissipation term:

$$\nu\frac{\partial^2 u_i}{\partial x_j\partial x_j}\ \sim \nu v_l/l^2,$$

where $S=\max|S_{ij}|$

Thus,

$$\frac{\text{Direct coupling}}{\text{Nonlinear convection}}\sim\frac{Sl}{v_l}\equiv\delta_l$$

From Kolmogorov theory, $v_l\sim(\varepsilon l)^{1/3}$, giving $\delta_l\sim Sl^{2/3}\varepsilon^{-1/3}$. This indicates that, for $l\ll\varepsilon^{1/2}S^{-3/2}$, magnitude of direct coupling term is negligible compared to the nonlinear convective term. The nonlinear term affects the large scales given by $l\gg\varepsilon^{1/2}S^{-3/2}$.

In terms of characteristic time scales τ_S and τ_l associated with the direct coupling terms and nonlinear convective terms respectively, we get

$$\tau_S\sim\frac{1}{S},\qquad \tau_l\sim\frac{l}{v_l}=\frac{l}{(\varepsilon l)^{1/3}}=\left(\frac{1}{\varepsilon k^2}\right)^{1/3},$$

which gives

$$\frac{\tau_l}{\tau_S}=\delta(k)=\frac{S}{(\varepsilon k^2)^{1/3}}$$

τ_S does not depend on k whereas τ_l depends on k and, in the inertial range, where $k\gg k_0$ ($k_0\sim 1/L$), the nonlinear coupling between the eddies is more dominant than direct interaction with the mean flow. Hence it follows that

the statistics of turbulence at sufficiently small scales, i.e., high wavenumbers, is dominated by Navier Stokes dynamics with small effects from the direct coupling terms, so that the direct coupling terms may be treated as small perturbation to the dynamics against the isotropic background state.

Performing Fourier transformation on Eq. (2.5), we obtain

$$\begin{aligned}\left(-i\omega+\nu_0 k^2\right) u_i(\mathbf{k},\omega) \quad &+ \quad \frac{i}{2}P_{ijl}(\mathbf{k})\int\frac{d^3p}{(2\pi)^3}\int_{-\infty}^{\infty}\frac{d\omega_1}{(2\pi)}u_j(\mathbf{p},\omega_1)u_l(\mathbf{q},\omega_2)\\ &= \quad f_i(\mathbf{k},\omega)+\lambda\hat{N}_{ij}(\mathbf{k})u_j(\mathbf{k},\omega) \qquad (2.7)\end{aligned}$$

Here $\mathbf{p}+\mathbf{q}=\mathbf{k}$, and $\omega_1+\omega_2=\omega$,

$$P_{ijl}(\mathbf{k}) = k_j P_{il}(\mathbf{k}) + k_l P_{ij}(\mathbf{k}) \qquad (2.8)$$

$$P_{ij}(\mathbf{k}) = \delta_{ij} - k_i k_j/\mathbf{k}^2 \qquad (2.9)$$

The anisotropic operator

$$\hat{N}_{ij}(\mathbf{k}) = -S_{ij} + 2\frac{k_i k_l}{\mathbf{k}^2}S_{lj} + \delta_{ij}k_l S_{lm}\frac{\partial}{\partial k_m} \qquad (2.10)$$

consists of pure strain (the first term), rapid pressure (second term) and wave vector space deformation (last term). Since the dynamics is assumed to be disturbed by the uniform shear, an expansion parameter λ (= 1) is inserted in the last term of Eq. (2.7) in order to make a perturbation expansion about the isotropic background field [90], whereas the forcing term $f_i(\mathbf{k},\omega)$ is introduced in order to maintain a steady state for the isotropic background field, $u_i^{(0)}(\mathbf{k},\omega)$.

The objective of this study is to examine the effect of the anisotropic term (involving λ) on the isotropic Navier-Stokes dynamics. Thus, the homogeneous isotropic turbulence is going to be affected by the imposed mean shear. We are interested to tackle directly the anisotropic term by treating it as a perturbation as suggested by Leslie [90]. Starting from Eq. (2.7) and by making a perturbation expansion of the velocity field we readily obtain the equation for the zeroth order velocity field representing the isotropic background state in addition to the first order perturbation to the velocity field which arises due to the imposed anisotropy. The detailed derivation is presented in a systematic fashion in the following sections.

2.3 Leslie-type Perturbative Treatment of Homogeneous Shear

In order to evaluate the spectral amplitudes associated with the anisotropic correlation function, here we carry out the calculation based on renormalization group (RG) [184] estimates. Starting with Eq. (2.7), and treating $(-i\omega + \nu_0 k^2)$ as the inverse of bare propagator $G_0(k,\omega)$, one can obtain the expression for renormalized viscosity by performing a systematic dynamic RG analysis, similar to Yakhot and Orszag's [184]. The corresponding renormalized propagator will have contributions due to the random stirring as well as the anisotropy term on the right-hand side of Eq. (2.7). Now we make a perturbative expansion of this renormalized propagator,

$$G_{ij}(\mathbf{k},\omega) = G_{ij}^{(0)}(\mathbf{k},\omega) + \lambda G_{ij}^{(1)}(\mathbf{k},\omega) + \ldots \tag{2.11}$$

where the zeroth order term is identical with the renormalized propagator of Yakhot and Orszag, whereas the higher order terms arise due to the anisotropy. Carrying out the RG analysis up to one loop order, the renormalized propagator $G_{ij}^{(0)}(\mathbf{k},\omega)$ is obtained as

$$G_{ij}^{(0)}(\mathbf{k},\omega) = \left[-i\omega + \Sigma(k)\right]^{-1} P_{ij}(\mathbf{k}) \tag{2.12}$$

where $\Sigma(k)$ is the self-energy correction to the bare viscosity ν_0. Now, following Leslie's original suggestion [90], we take the lowest order renormalized propagator and neglect the next higher order term in our calculation of the correlation function.

Using a perturbation expansion of the velocity field about the isotropic background field as

$$u_i(\mathbf{k},\omega) = u_i^{(0)}(\mathbf{k},\omega) + \lambda u_i^{(1)}(\mathbf{k},\omega) + \ldots \tag{2.13}$$

and equating equal powers of λ, we obtain the first order correction to the velocity field as

$$u_i^{(1)}(\mathbf{k},\omega) = G_{ij}^{(0)}(\mathbf{k},\omega)\hat{N}_{jm}(\mathbf{k})\, u_m^{(0)}(\mathbf{k},\omega) \tag{2.14}$$

Here we define the velocity correlation tensor $Q_{ij}(\mathbf{k},\omega)$ as

$$\langle u_i(\mathbf{k},\omega)u_j(\mathbf{k}',\omega')\rangle = Q_{ij}(\mathbf{k},\omega)(2\pi)^4\delta^3(\mathbf{k}+\mathbf{k}')\delta(\omega+\omega') \tag{2.15}$$

where the angular brackets denote an ensemble average and $\delta^3(\mathbf{k}+\mathbf{k}')$ and $\delta(\omega+\omega')$ are Dirac delta functions. Now, using the perturbation expansion as defined in Eq. (2.13), we expand the correlation tensor perturbatively about the isotropic background as

$$Q_{ij} = Q_{ij}^{(0)} + \lambda Q_{ij}^{(1)} + \dots \tag{2.16}$$

Here, $Q_{ij}^{(0)}(\mathbf{k},\omega)$ denotes the isotropic part defined as

$$\left\langle u_i^{(0)}(\mathbf{k},\omega)u_j^{(0)}(\mathbf{k}',\omega)\right\rangle = Q_{ij}^{(0)}(\mathbf{k},\omega)(2\pi)^4\delta^3(\mathbf{k}+\mathbf{k}')\delta(\omega+\omega') \tag{2.17}$$

and, $Q_{ij}^{(1)}(\mathbf{k};\omega)$ denotes the corresponding first order correction to the anisotropic part given by

$$\begin{aligned}\left\langle u_i^{(1)}(\mathbf{k},\omega)u_j^{(0)}(\mathbf{k}',\omega')\right\rangle + \left\langle u_i^{(0)}(\mathbf{k},\omega)u_j^{(1)}(\mathbf{k}',\omega')\right\rangle \\ = Q_{ij}^{(1)}(\mathbf{k};\omega)(2\pi)^4\delta^3(\mathbf{k}+\mathbf{k}')\delta(\omega+\omega')\end{aligned} \tag{2.18}$$

Now using Eq. (2.14), the first term in the above equation can be expressed as

$$\left\langle u_i^{(1)}(\mathbf{k},\omega)u_j^{(0)}(\mathbf{k}',\omega')\right\rangle = G_{ia}^{(0)}(\mathbf{k},\omega)\left\langle u_j^{(0)}(\mathbf{k}',\omega')\hat{N}_{ab}(\mathbf{k})\,u_b^{(0)}(\mathbf{k},\omega)\right\rangle \tag{2.19}$$

Similarly the second term of Eq. (2.18) is obtained as

$$\left\langle u_i^{(0)}(\mathbf{k},\omega)u_j^{(1)}(\mathbf{k}',\omega')\right\rangle = G_{ja}^{(0)}(\mathbf{k}',\omega')\left\langle u_i^{(0)}(\mathbf{k},\omega)\hat{N}_{ab}(\mathbf{k}')\,u_b^{(0)}(\mathbf{k}',\omega')\right\rangle \tag{2.20}$$

Thus, it is obvious that the anisotropic operator, $\hat{N}_{ij}$, operating on a velocity field, solely contribute to the anisotropic part of the correlation tensor. As given by Eq. (2.10), the operator $\hat{N}_{ij}$ involves three terms. Eventually, the right hand side of Eq. (2.18) also comprises of three corresponding parts, which we will denote below by $Q_{ij}^{(1,1)}$, $Q_{ij}^{(1,2)}$, and $Q_{ijm}^{(1,3)}$ (excluding the Dirac delta functions) respectively. The first term of Eq. (2.10), namely the pure shear term gives rise to

$$Q_{ij}^{(1,1)}(\mathbf{k},\mathbf{k}';\omega,\omega') = -S_{ab}\left[G_{ia}^{(0)}(\mathbf{k},\omega)Q_{jb}^{(0)}(\mathbf{k}',\omega') + G_{ja}^{(0)}(\mathbf{k}',\omega')Q_{ib}^{(0)}(\mathbf{k},\omega)\right] \tag{2.21}$$

The rapid pressure term of Eq. (2.10) yields no contribution due to the property of the isotropic parts. The response and correlation tensors associated with the background field satisfy the relation $G_{ij}^{(0)}(\mathbf{k},\omega) = G^{(0)}(k,\omega)P_{ij}(\mathbf{k})$ and $Q_{ij}^{(0)}(\mathbf{k},\omega) = Q^{(0)}(k,\omega)P_{ij}(\mathbf{k})$ due to the property of isotropy. Thus, we obtain $Q_{ij}^{(1,2)} = 0$.

The third term of Eq. (2.10), which indicates the wave vector space deformation due to imposed mean strain, involves the derivative with respect to wave vector components. We derive the corresponding contribution to Eq. (2.18), namely, $Q_{ijm}^{(1,3)}$, by means of inverse Fourier transformation, yielding

$$\left\langle u_i^{(0)}(\mathbf{k}',\omega')\frac{\partial u_j^{(0)}(\mathbf{k},\omega)}{\partial k_m}\right\rangle = Q_{ij}^{(0)}(\mathbf{k}',\omega')(2\pi)^4\frac{\partial\delta^3(\mathbf{k}+\mathbf{k}')}{\partial(k_m+k'_m)}\delta(\omega+\omega') \tag{2.22}$$

Combining the above two expressions, we get

$$\begin{aligned} Q_{ij}^{(1)}(\mathbf{k},\omega)\delta^3(\mathbf{k}+\mathbf{k}')\delta(\omega+\omega') &= Q_{ij}^{(1,1)}(\mathbf{k},\mathbf{k}';\omega,\omega')\delta^3(\mathbf{k}+\mathbf{k}')\delta(\omega+\omega') \\ &+Q_{ijm}^{(1,3)}(\mathbf{k},\mathbf{k}';\omega,\omega')\frac{\partial\delta^3(\mathbf{k}+\mathbf{k}')}{\partial(k_m+k'_m)}\delta(\omega+\omega') \end{aligned} \tag{2.23}$$

with

$$Q_{ijm}^{(1,3)}(\mathbf{k},\mathbf{k}';\omega,\omega') = \delta_{ab}S_{lm}\left[k_l G_{ia}^{(0)}(\mathbf{k},\omega)Q_{jb}^{(0)}(\mathbf{k}',\omega') + k'_l G_{ja}^{(0)}(\mathbf{k}',\omega')Q_{ib}^{(0)}(\mathbf{k},\omega)\right] \tag{2.24}$$

Now, by keeping $\mathbf{k}$ and ω fixed, we integrate both sides of Eq. (2.23) over $\mathbf{k}'$ and ω'. This gives

$$Q_{ij}^{(1)}(\mathbf{k},\omega) = Q_{ij}^{(1,1)}(\mathbf{k},-\mathbf{k};\omega,-\omega) - \left[\frac{\partial}{\partial k'_m}Q_{ijm}^{(1,3)}(\mathbf{k},\mathbf{k}';\omega,\omega')\right]_{\mathbf{k}'=-\mathbf{k},\omega'=-\omega} \tag{2.25}$$

Here the last term arises from integration of the last term of Eq. (2.23) by parts, the surface term yields no contribution. The right-hand terms of Eq. (2.25) can be readily evaluated using the expression of Eqs. (2.21) and (2.24) and the property of isotropy of the response and correlation tensors associated with the background field. Now, since we are interested in equal-time correlation resulting from

$$Q_{ij}^{(1)}(\mathbf{k};t-t') = \int_{-\infty}^{+\infty} Q_{ij}^{(1)}(\mathbf{k},\omega)e^{-i\omega(t-t')}\frac{d\omega}{2\pi}, \tag{2.26}$$

we carry out the contour integration on the complex ω plane by choosing a proper contour for $(t-t') \to 0^+$ as shown in Fig. 2.1. This yields

$$Q_{ij}^{(1)}(\mathbf{k};0) = S_{ab}\left[P_{ia}(\mathbf{k})P_{jb}(\mathbf{k}) + P_{ja}(\mathbf{k})P_{ib}(\mathbf{k})\right] R^{(1,1)}(k) + S_{lm}\frac{k_l k_m}{\mathbf{k}^2} P_{ij}(\mathbf{k})\, R^{(1,3)}(k) \tag{2.27}$$

Here the first and second term arises from the $Q_{ij}^{(1,1)}$ and $Q_{ijm}^{(1,3)}$ of Eq. (2.25), respectively, with

$$R^{(1,1)}(k) = -\frac{q^{(0)}(k)}{2\Sigma(k)} \quad \text{and} \quad R^{(1,3)}(k) = \frac{k}{2\Sigma(k)}\frac{\partial q^{(0)}(k)}{\partial k} \tag{2.28}$$

where $q^{(0)}(k) = Q^{(0)}(k;0)$, and $\Sigma(k)$ is the self-energy obtained via the Yakhot Orszag renormalization group calculations.

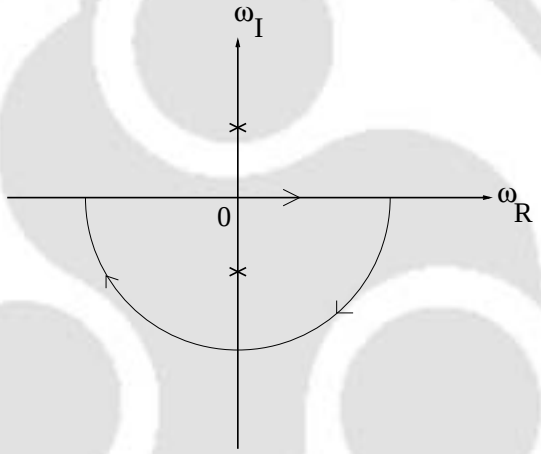

Figure 2.1: The integration contour in the complex ω plane for Eq. (2.26). Here, ω_R and ω_I denote the real and imaginary axes respectively. The crosses indicate the poles.

Thus, we see that the tensorial form of the anisotropic velocity-velocity correlation tensor, given by Eq. (2.27), that account for the effect of anisotropy present in the flow, automatically emerges from the governing dynamical equation (Eq. 2.5). We see that this tensor form is symmetric with respect to the interchange of tensorial indices, namely

$$Q_{ij}^{(1)}(\mathbf{k};t,t) = Q_{ji}^{(1)}(\mathbf{k};t,t)$$

and it also satisfies the condition of solenoidality, namely

$$k_i Q_{ij}^{(1)}(\mathbf{k}; t, t) = 0$$

These conditions must be maintained by the correlation tensor because of the nature of definition given by Eq. (2.15).

In the following section, we shall use the renormalization group results in addition to Kraichnan's results to calculate universal numbers associated with this correlation tensor.

2.4 Calculation of Universal Numbers

Here we would like to calculate the universal numbers associate with the scaling functions $R^{(1,1)}(k)$ and $R^{(1,3)}(k)$, using RG results together with Kraichnan's numerical results.

We know that, according to the Kolmogorov theory, the scalar quantity $q^{(0)}(k)$ in the inertial range is of the form

$$q^{(0)}(k) = \frac{C}{4\pi}\bar{\varepsilon}^{2/3}k^{-11/3}$$

where C is the Kolmogorov constant and $\bar{\varepsilon}$ is the energy dissipation rate appearing in the energy spectrum given by Eq. (2.1). Further, a scaling law for the self energy $\Sigma(k)$, defined by Kraichnan [79], is expressed as

$$\Sigma(k) = \mu\sqrt{C}\bar{\varepsilon}^{1/3}k^{2/3}$$

where μ is another constant. Using these scaling laws in Eq. (2.28), we obtain

$$R^{(1,1)}(k) = A\,\bar{\varepsilon}^{1/3}k^{-13/3} \quad \text{and} \quad R^{(1,3)}(k) = B\,\bar{\varepsilon}^{1/3}k^{-13/3} \tag{2.29}$$

with

$$A = -\frac{1}{8\pi}\frac{\sqrt{C}}{\mu} \quad \text{and} \quad B = -\frac{11}{24\pi}\frac{\sqrt{C}}{\mu}. \tag{2.30}$$

Kraichnan [79], further obtain a relation between the universal numbers C and μ by numerically solving the energy transport equation of the DIA, leading to

$$C = 3.022\mu^{2/3}$$

This enables us to estimate the non-dimensional numbers A and B as

$$A = -\frac{1}{8\pi}\frac{(3.022)^{3/2}}{C} \quad \text{and} \quad B = -\frac{11}{24\pi}\frac{(3.022)^{3/2}}{C} \tag{2.31}$$

Table 2.1: Experimental, theoretical, and DNS values of A and B.

Method	A	B	*References*
DNS	-0.16 ± 0.03	-0.40 ± 0.06	Ishihara et al. [61]
DNS	-0.15 ± 0.01	-0.48 ± 0.02	Yoshida et al. [185]
Experiment	≈ -0.17	≈ -0.45	Tsuji [164]
Theory (LRA)	-0.12 ± 0.002	0.009 ± 0.014	Yoshida et al. [185]
Theory (TFM)	-0.10	-0.37	Previous theory [112]
Leslie+RG	-0.13	-0.48	Present Chapter

Now, renormalization group calculation gives us the value of the universal Kolmogorov constant as $C = 1.6057$ [184]. When we substitute this value we get

$$A = -0.13 \quad \text{and} \quad B = -0.48$$

These values are comparable with the experimental, DNS, and other theoretical values as shown in Table 2.1.

2.5 Discussion and Conclusion

Considering the simplest anisotropic case for homogeneous shear flow, Leslie [90] constructed an anisotropic model on the basis of Kraichnan's closure formulation [78, 79]. Treating the uniform shear in the mean flow as a perturbation to the isotropic background, a $k^{-7/3}$ spectrum was obtained in the leading order. However, Leslie's treatment for the perturbation method did not maintain the realizability conditions of solenoidality and symmetry in tensor indices of the correlation tensor.

Ishihara, Yoshida and Kaneda [61, 185], on the other hand, conjectured a suitable form of the correlation tensor with the above properties of solenoidality and symmetry. With these assumptions, they performed an analytical (LRA) as well as numerical (DNS) calculations of the two universal numbers

A and B. Their DNS results were in good agreement with the experimental values [164]. However, their LRA values were not in good agreement with the experimental values.

To maintain the realizability conditions, a modification of Leslie's treatment was necessary. Such a treatment was attempted and the TFM of Kraichnan was applied [112]. The calculations, although crude, produced better agreement with experimental values.

Motivated by this partial success, it was realized that something better than TFM coupled with Leslie-type calculations would give still better results.

Thus, as we have seen in this chapter, when the RG results are combined with Leslie-type calculations, we get very good agreements with the experimental values. This also indicates that Leslie's suggestion of using the anisotropic term as perturbation is indeed a deep intuition close to reality.

This further motivates us to apply similar procedure in other problems. We shall be using this method in Chapter 4 for the case of stably stratified turbulence.

Chapter 3

Heisenberg Approximation in Passive Scalar Turbulence

3.1 Introduction

Considerable attention has been focused in the last few decades on the mixing of a passive scalar field in turbulent flows [175, 145]. It possesses an interest of its own and has been used to describe a variety of phenomena like pollutant or tracer transport and is clearly related to models describing forced diffusion through porous media [51]. The well-known universal Kolmogorov energy spectrum [74, 121]

$$E(k) = C\varepsilon^{2/3}k^{-5/3} \tag{3.1}$$

where C is the Kolmogorov constant, ε is the energy flux, and k is the wave number, has been assumed in situations where the flow properties are statistically homogeneous and isotropic [45]. For passive scalar convection, a scaling law, similar to the Kolmogorov's, holds for three-dimensional mean-square scalar given by [121, 12, 33]

$$\mathcal{E}(k) = \text{ Ba } \chi\ \varepsilon^{-1/3}\ k^{-5/3} \tag{3.2}$$

where χ is the scalar flux, and Ba, the well-known Batchelor (or Obukhov-Corrsin) constant, have been measured in several studies [90, 111]. Various attempts have been made to calculate the universal numbers associated with

the above mentioned universal scaling laws (Eqs. (3.1) and (3.2)), starting from the stochastic versions of the Navier-Stokes and passive scalar dynamics. Motivated by the earlier pioneering works [34, 43], Yakhot and Orszag [184, 183] carried out a rigorous dynamic-renormalization group (RG) calculations (together with ϵ expansion) on homogeneous isotropic turbulence to calculate the Kolmogorov constant and thereby evaluated the Batchelor constant by considering Pao's formulation [123, 124].

Using an RG procedure essentially different from Yakhot and Orszag, Elperin and Kleeorin [39] studied the problem of passive scalar convection in turbulent fluid flow in the presence of an external gradient of passive scalar concentration. Indeed, in their method, the spectrum and statistical properties of the background hydrodynamic turbulence were assumed to be known, and thereby studied the problem of weak response of homogeneous and isotropic turbulence to a weak external gradient of the mean passive scalar field. Moreover, in contrast to the Corrsin-Obukhov theory, they considered a completely different mechanism of excitation of passive scalar fluctuations, namely, passive scalar fluctuations are generated by tangling of an external gradient of mean passive scalar field by a turbulent velocity field. In this analysis, the turbulent Prandtl number, σ, for large Reynolds number was estimated to be $\sigma \approx 0.792$.

Lin et al. [93], assuming quasinormal approximation for the statistical correlation between the velocity and temperature fields, performed a renormalization group (RG) analysis to investigate thermal turbulent transport properties, and obtained a functional relationship between turbulent Prandtl number and Peclet number. To investigate the Batchelor constant, they further carried out their calculations with a modification in original Batchelor spectrum (Eq. (3.2)) by introducing two connecting functions so that scaling laws fit better the measured spectra. Employing their solution of the effective thermal eddy diffusivity, they found that the Batchelor constant depends on Prandtl number and several characteristic wavenumbers of the particular flow under consideration.

Extending the field theoretic RG calculations of Zhou and Vahala [188] to higher dimensions, Verma [171] calculated the passive scalar cascade rate in the inertial-convective range from the flux integrals and the renormalized parameters (calculated within the same framework). The final integral expressions are then computed using Gaussian quadrature, and it has been found that the integrals converge for all dimension $d \geqslant 2$. The computed values of the Batchelor constant (Ba), Kolmogorov constant (C), and turbulent Prandtl number (σ) in 3D were Ba $= 1.25$, $C = 1.53$, and $\sigma = 0.42$ respectively. In the same work, it was also speculated that $\sigma \approx 1$ and Ba $\approx d^{1/3}$ for large space dimensions (d). Considering a simple hypothesis that large scale eddies are statistically independent from the smaller eddies [107], Chang et.al. [25] performed an RG analysis on Navier-Stokes equation and obtained an inhomogeneous ordinary differential equation for the invariant effective eddy-viscosity, the closed form solution of which yields an expression of the Kolmogorov constant, which is found to be in the range $C \approx 1.35 - 2.06$.

Adzhemyan et al. [2] calculated the turbulent Prandtl number (σ) in the field theoretic renormalization group framework up to two-loop order coupled with ε expansion, and obtained $\sigma \approx 0.7179$ and $\sigma \approx 0.7693$ in one-loop and two-loop approximation, respectively. The difference in the two results was strikingly small when compared to the similar two-loop calculations of the Kolmogorov constant and skewness factor [1]. They further pointed out that, in the two-loop approximation, the main contribution is due to graphs having a singularity at $d = 2$ and it is necessary to sum such graphs. Since in the calculation of σ this singularity is absent, the two-loop contribution is relatively small and the results of the usual ε expansion appear fairly reliable at the level of accuracy suggested by the two-loop corrections.

Recently, Brethouwer and Lindborg [18] investigated statistics of a passive scalar in randomly forced and strongly stratified turbulence with a constant horizontal mean gradient, and observed the isotropic $k^{-5/3}$ passive scalar spectrum in the inertial range with Batchelor constant in one dimension as Ba$' \approx 0.5$.

Our main motivation in the problem of passive scalar turbulence originates from the fact that we shall ultimately be interested in the problem of turbulence with stable temperature stratification where the temperature or density field acts as an active scalar. In our analysis of this problem, it was found that inputs regarding the universal numbers associated with the passive scalar dynamics were necessary. As a result, we are motivated to make a theoretical investigation on passive scalar turbulence. In order to calculate the passive scalar universal numbers, we shall be using the Heisenberg approximation [57]. Within this scheme, we derive analytic expressions for eddy-viscosity and eddy-diffusivity from Kraichnan's transfer integrals of energy and mean-square scalar [90, 78]. In the same scheme, we evaluate the flux integrals for energy and mean-square scalar. These procedures allow for the evaluation of relevant amplitude ratios, from which we calculate the universal numbers, namely, Batchelor constant (Ba), and turbulent Prandtl number (σ) under two different schemes (with ϵ expansion and without ϵ expansion). Our calculations yield $\sigma = 0.7179$ and $\mathrm{Ba} = 1.0311$ (with ϵ expansion). These results are comparable with other theoretical calculations, namely, Yakhot-Orszag's renormalization group calculation ($\mathrm{Ba} = 1.16$ and $\sigma = 0.7179$) [183] and experimental investigations ($\mathrm{Ba} \approx 0.67 - 1.35$ and $\sigma \approx 0.7 - 0.9$) [90, 111]. As a byproduct, we obtain a relation between Kolmogorov constant (C), Batchelor constant (Ba) and turbulent Prandtl number (σ), namely, $\mathrm{Ba} = \sigma\, C$, which is consistent with that of Yakhot and Orszag's result (derived from Pao's formulations) [183]. To compare our results with various experimental results, we also calculate the corresponding one-dimensional Batchelor constant (Ba').

3.2 Heisenberg Approximation

The randomly stirred incompressible Navier-Stokes equations in presence of passive scalar can be written as

$$\frac{\partial u_i}{\partial t} + u_j \frac{\partial u_i}{\partial x_j} = -\frac{\partial p}{\partial x_i} + \nu_0 \frac{\partial^2 u_i}{\partial x_j \partial x_j} + f_i \tag{3.3}$$

$$\frac{\partial \psi}{\partial t} + u_j \frac{\partial \psi}{\partial x_j} = \kappa_0 \frac{\partial^2 \psi}{\partial x_j \partial x_j} + \theta \tag{3.4}$$

with the incompressibility condition

$$\frac{\partial u_i}{\partial x_i} = 0 \tag{3.5}$$

where $\mathbf{u}(\mathbf{x}, t)$, $\psi(\mathbf{x}, t)$ and $p(\mathbf{x}, t)$ are the fluctuating velocity, density and pressure fields with zero mean, respectively; ν_0 and κ_0 are the kinematic viscosity and molecular diffusivity respectively. $f_i(\mathbf{x}, t)$ and $\theta(\mathbf{x}, t)$ are the Gaussian random forces. We write Eqs. (3.3)-(3.5) in d-dimensional Fourier space as

$$\left(\frac{\partial}{\partial t} + \nu_0 k^2\right) u_i(\mathbf{k}, t) = f_i(\mathbf{k}, t) - \frac{i}{2} P_{ijl}(\mathbf{k}) \sum_{\mathbf{p}+\mathbf{q}=\mathbf{k}} u_j(\mathbf{p}, t) u_l(\mathbf{q}, t) \tag{3.6}$$

and

$$\left(\frac{\partial}{\partial t} + \kappa_0 k^2\right) \psi(\mathbf{k}, t) = \theta(\mathbf{k}, t) - i k_j \sum_{\mathbf{p}+\mathbf{q}=\mathbf{k}} u_j(\mathbf{p}, t) \psi(\mathbf{q}, t) \tag{3.7}$$

$$k_i u_i(\mathbf{k}, t) = 0 \tag{3.8}$$

Here, the random external stirring force fields $f_i(\mathbf{k}, t)$ and $\theta(\mathbf{k}, t)$ are assumed to have Gaussian statistics with correlation

$$\langle f_i(\mathbf{k}, t) f_j(\mathbf{k}', t') \rangle = F(k) P_{ij}(\mathbf{k}) [2\pi]^d \delta^d(\mathbf{k} + \mathbf{k}') \delta(t - t') \tag{3.9}$$

$$\langle \theta(\mathbf{k}, t) \theta(\mathbf{k}', t') \rangle = \Theta(k) [2\pi]^d \delta^d(\mathbf{k} + \mathbf{k}') \delta(t - t') \tag{3.10}$$

in which F(k) and $\Theta(k)$ are modeled as

$$F(k) = \frac{2D_0}{k^{d-4+\epsilon}} \quad \text{and} \quad \Theta(k) = \frac{2\mathcal{D}_0}{k^{d-4+\epsilon'}} \tag{3.11}$$

where d is the space dimension. The noise added in the concentration field equation of motion is meant to facilitate the calculation of correlation functions. This forms have been assumed in order to ensure the fact that the Kolmogorov spectrum for the velocity field and the Batchelor spectrum for the passive scalar field will be obtained for conserved transport of energy and mean-square scalar. It will turn out that these conservation laws are obeyed only for the values $\epsilon = 4$ and $\epsilon' = 4$. These values automatically lead to the Kolmogorov and Batchelor spectra (Eqs. (3.1) and (3.2)).

The spatial Fourier transformed velocity correlation tensor $Q_{ij}(\mathbf{k},t,t')$, and scalar correlation $\Psi(\mathbf{k},t,t')$ are defined as

$$\langle\psi(\mathbf{k},t)\psi(\mathbf{k}',t')\rangle = \Psi(\mathbf{k},t,t')[2\pi]^d\delta^d(\mathbf{k}+\mathbf{k}') \tag{3.12}$$

$$\langle u_i(\mathbf{k},t)u_j(\mathbf{k}',t')\rangle = Q_{ij}(\mathbf{k},t,t')[2\pi]^d\delta^d(\mathbf{k}+\mathbf{k}') \tag{3.13}$$

Now, as noted earlier, following Kraichnan [90, 78], we write the energy transfer equation as

$$\left(\frac{d}{dt}+2\nu_0 k^2\right)E(k;t,t) = T(k;t,t) \tag{3.14}$$

and, similarly the transfer equation for mean square scalar correlation as

$$\left(\frac{d}{dt}+2\kappa_0 k^2\right)\mathcal{E}(k;t,t) = \mathcal{T}(k;t,t) \tag{3.15}$$

Here $T(k,t,t)$ and $\mathcal{T}(k;t,t)$ represent the energy transfer function and mean-square scalar transfer function respectively. We write $T(k,t,t)$ and $\mathcal{T}(k;t,t)$ in d-dimensional Fourier space and obtain

$$T(k;t,t) = T(k) = \frac{8k^2}{(d-1)^2}k^{d-1}\int\frac{d^dp}{S_d}\theta_1(k,p,q)$$
$$\times\left[a(k,p,q)\frac{E(p)}{p^{d-1}}\frac{E(q)}{q^{d-1}} - \frac{1}{2}b(k,q,p)\frac{E(p)}{p^{d-1}}\frac{E(k)}{k^{d-1}} - \frac{1}{2}b(k,p,q)\frac{E(q)}{q^{d-1}}\frac{E(k)}{k^{d-1}}\right] \tag{3.16}$$

$$\mathcal{T}(k;t,t) = \mathcal{T}(k) = \frac{4k^2}{d-1}k^{d-1}\int\frac{d^dp}{S_d}\theta_2(k,p,q)$$
$$k_ik_jP_{ij}(\mathbf{p})\frac{E(p)}{p^{d-1}}\left[\frac{\mathcal{E}(q)}{q^{d-1}} - \frac{\mathcal{E}(k)}{k^{d-1}}\right] \tag{3.17}$$

Here $\theta_1(k,p,q)$ and $\theta_2(k,p,q)$ are the triad relaxation times. In the Edwards' simplified assumption of exponential decay of the response and correlation functions [38], we obtain these triad relaxation times as

$$\theta_1(k,p,q) = \frac{1}{\nu(k)k^2+\nu(p)p^2+\nu(q)q^2}$$

$$\theta_2(k,p,q) = \frac{1}{\kappa(k)k^2+\kappa(q)q^2+\nu(p)p^2}$$

In Eqs. (3.16) and (3.17), $b(k,p,q)$, $b(k,q,p)$, and $a(k,p,q)$ are the geometrical coefficients given by

$$b(k,p,q) = \frac{p}{k}(z^3 + xy) + \frac{d-3}{2}(1-y^2)$$

$$b(k,q,p) = \frac{q}{k}(y^3 + xz) + \frac{d-3}{2}(1-z^2)$$

$$2a(k,p,q) == b(k,p,q) + b(k,q,p)$$

where

$$x = -\frac{\mathbf{p}\cdot\mathbf{q}}{pq}, \qquad y = \frac{\mathbf{k}\cdot\mathbf{q}}{kq} \quad \text{and} \quad z = \frac{\mathbf{k}\cdot\mathbf{p}}{kp} \tag{3.18}$$

The energy spectrum $E(k,t)$ and mean square scalar spectrum $\mathcal{E}(k,t)$ are related to the spatial Fourier transform correlations by

$$E(k,t) = \frac{d-1}{2}\frac{S_d}{[2\pi]^d}k^{d-1}Q(k,t,t) \tag{3.19}$$

and

$$\mathcal{E}(k,t) = \frac{S_d}{[2\pi]^d}k^{d-1}\Psi(k,t,t) \tag{3.20}$$

where $S_d = 2\pi^{d/2}/\Gamma(d/2)$ is the surface area of a unit sphere embedded in the d-dimensional space.

Here we will derive an asymptotic form of the eddy viscosity and eddy diffusivity from the energy and mean-square scalar transfer Eqs. (3.14) and (3.15), and describe our results with and without ϵ expansion. As noted earlier, in Heisenberg's approximation [57], the eddy-viscosity $\nu(k|p')$ and eddy-diffusivity $\kappa(k|p')$ can be obtained from the transfer integrals as the effect on the wave number k due only to wavenumbers $(p,q) > p'$ and thereby neglecting the effect of the region $(p,q) < p'$. Following Kraichnan, we define the eddy-viscosity and eddy-diffusivity in the Heisenberg's approximation as

$$T(k|p') = -2\nu(k|p')k^2E(k) \tag{3.21}$$

and

$$\mathcal{T}(k|p') = -2\kappa(k|p')k^2\mathcal{E}(k) \tag{3.22}$$

which are obtained from the transfer integrals $T(k)$ and $\mathcal{T}(k)$ by setting an IR cut-off at p'.

In the limit $p' \gg k$ we have $p \approx q$, the eddy viscosity can thus be calculated using Eq. (3.21) as [113]

$$\nu(k|p') = \frac{2}{(d-1)^2}\int_{p'}^{\infty} dp \oint \frac{d\Omega}{S_d}\,\theta_1(k,p,q) \left[b(k,q,p)E(p) + b(k,p,q)\frac{E(q)}{q^{d-1}}p^{d-1}\right] \tag{3.23}$$

Using the same procedure as above we calculate the eddy-diffusivity from the transfer integral $\mathcal{T}(k)$ in the $p' \gg k$ limit as

$$\kappa(k|p') = \frac{2}{d-1}\int_{p'}^{\infty} dp \oint \frac{d\Omega}{S_d}\,\theta_2(k,p,q)\left[1 - \frac{(\mathbf{k}.\mathbf{p})^2}{k^2p^2}\right]E(p) \tag{3.24}$$

Now, we know that

$$\mathcal{E}(k) \sim k^{d-1}\int_{-\infty}^{+\infty}\frac{d\omega}{[2\pi]}|\mathcal{G}(k,\omega)|^2\Theta(k) \tag{3.25}$$

$$E(k) \sim k^{d-1}\int_{-\infty}^{+\infty}\frac{d\omega}{[2\pi]}|G(k,\omega)|^2F(k) \tag{3.26}$$

with the renormalized propagator

$$\mathcal{G}(k,\omega) = \left[-i\omega + \kappa(k)k^2\right]^{-1}$$

and

$$G(k,\omega) = \left[-i\omega + \nu(k)k^2\right]^{-1}$$

This yields the scaling

$$\mathcal{E}(k) \sim \frac{k^{1-\epsilon'}}{\kappa(k)}, \quad \text{and} \quad E(k) \sim \frac{k^{1-\epsilon}}{\nu(k)} \tag{3.27}$$

respectively. Further, when scaling arguments are applied to Eqs. (3.23) and (3.24), we get

$$\kappa(k) \sim E(k)/k\kappa(k) \quad \text{and} \quad \nu(k) \sim E(k)/k\nu(k) \tag{3.28}$$

Thus, Eqs. (3.27) and (3.28) yields the following scaling relations:

$$\mathcal{E}(k) \sim k^{1-\epsilon'+\epsilon/3} \quad \text{and} \quad \kappa(k) \sim k^{-\epsilon/3} \tag{3.29}$$

$$E(k) \sim k^{1-2\epsilon/3} \quad \text{and} \quad \nu(k) \sim k^{-\epsilon/3} \tag{3.30}$$

To find the ultraviolet behavior ($p \to \infty$) of this integrals, we expand the integrand in the limit $p \gg k$, and then pick up the lowest-order contribution in k/p. In this limit, we have $q \approx p$. Thus, we obtain

$$\nu(k|p') = \frac{1}{d-1}\left[A_d(\epsilon) f(\epsilon) + B_d\right] \frac{E(p')}{p'\nu(p')} \tag{3.31}$$

and

$$\kappa(k|p') \;=\; \frac{2}{d} f(\epsilon) \frac{E(p')}{p'[\nu(p') + \kappa(p')]} \tag{3.32}$$

where

$$A_d(\epsilon) = \frac{d^2 - d - 2\epsilon/3}{d(d+2)}, \quad B_d = \frac{1}{d(d+2)} \quad \text{and} \quad f(\epsilon) = \frac{3}{\epsilon} \tag{3.33}$$

Now, we identify the eddy-viscosity and eddy diffusivity at k as $\nu(k) \equiv \nu(k|\lambda k)$ and $\kappa(k) \equiv \kappa(k|\lambda k)$ where $\nu(k|\lambda k)$ and $\kappa(k|\lambda k)$ are obtained by extrapolating p' to a wave number λk, i.e., $\nu(k|\lambda k) = \lim_{p' \to \lambda k} \nu(k|p')$, where $\lambda \geqslant 1$ an $O(1)$ numerical constant. In the resulting expressions, we use the scaling relations

$$\begin{aligned} E(q) &= C\, \varepsilon^{2/3} q^{1-2\epsilon/3} \quad \text{and} \quad \nu(q) = \alpha\, \varepsilon^{1/3} q^{-\epsilon/3} \\ \mathcal{E}(q) &= \text{Ba}\, \chi\, \varepsilon^{-1/3}\, q^{1-\epsilon'+\epsilon/3} \quad \text{and} \quad \kappa(q) = \beta\, \varepsilon^{1/3} q^{-\epsilon/3} \end{aligned} \tag{3.34}$$

This yields

$$\frac{\alpha^2}{C} = \frac{1}{d-1}\left[A_d(\epsilon) f(\epsilon) + B_d\right] \lambda^{-\epsilon/3} \tag{3.35}$$

and

$$\frac{\beta(\alpha+\beta)}{C} = \frac{2}{d} f(\epsilon) \lambda^{-\epsilon/3} \tag{3.36}$$

The UV pole in the expressions (3.35) and (3.36) can be extracted by a Laurent expansion about $\epsilon = 0$.

3.3 Conserved Transfer

The fluxes of energy and mean-square scalar through a wave number j are defined as [78]

$$\Pi(j) = \int_j^\infty T_{(p,q)<j}(k)dk - \int_0^j T_{(p,q)>j}(k)dk \tag{3.37}$$

and

$$\Xi(j) = \int_j^\infty \mathcal{T}_{(p,q)<j}(k)dk - \int_0^j \mathcal{T}_{(p,q)>j}(k)dk \tag{3.38}$$

where the inequalities expressed as subscripts refer to the region of the (p, q) integration in Eqs. (3.16) and (3.17), with the triangle condition $\mathbf{p} + \mathbf{q} = \mathbf{k}$. Using the scaling relation given by Eq. (3.34) in Eqs. (3.16) and (3.17), the dimension of the flux integrals are found to be

$$\Pi(j) \sim j^{4-\epsilon} \quad \text{and} \quad \Xi(j) \sim j^{4-\epsilon'}$$

Thus we see that Π and Ξ are wavenumber independent only when $\epsilon = \epsilon' = 4$. Thus, the conditions of conserved transport of energy and mean-square scalar are obtained only when $\epsilon = \epsilon' = 4$.

Now we implement Heisenberg approximation for the evaluation from the flux integrals. The energy and mean-square scalar transfer rate to all wavenumbers $(p, q) > p'$ from distant wavenumber $k < k'$ is obtained from Eqs. (3.37) and (3.38) as

$$\Pi(k'|p') = -\int_0^{k'} T(k|p')dk, \quad p' \gg k' \tag{3.39}$$

and

$$\Xi(k'|p') = -\int_0^{k'} \mathcal{T}(k|p')dk, \quad p' \gg k' \tag{3.40}$$

We note that the first integral terms in Eqs. (3.37) and (3.38) are negligible because it involves the region $k > p'$ and $(p, q) < k'$, where the triangle condition can hardly be satisfied in the limit $p' \gg k'$. Thus, using Eqs. (3.21) and (3.23) in Eq. (3.39), and similarly, using Eqs. (3.22) and (3.24) in Eq. (3.40), we get

$$\Pi(k'|p') = \frac{2}{d-1}\left[A_d(\epsilon)f(\epsilon) + B_d\right]\frac{E(p')}{p'\nu(p')}g_1(\epsilon)k'^3E(k') \tag{3.41}$$

$$\Xi(k'|p') = \frac{4}{d} f(\epsilon) \frac{E(p')}{p'[\nu(p') + \kappa(p')]} g_2(\epsilon)(k')^3 \mathcal{E}(k') \tag{3.42}$$

where

$$g_1(\epsilon) = \frac{1}{4 - 2\epsilon/3} \quad \text{and} \quad g_2(\epsilon) = \frac{1}{4 - \epsilon' + \epsilon/3}$$

Now, extrapolating p' to a wave number $\lambda k'$ and then identifying the flux at wave number k' as $\Pi(k') \equiv \Pi(k'|\lambda k')$ on Eq. (3.41), we obtain

$$\Pi(k') \equiv \Pi(k'|\lambda k') = \frac{2}{d-1} \left[A_d(\epsilon) f(\epsilon) + B_d\right] \frac{E(\lambda k')}{\lambda k' \nu(\lambda k')} g_1(\epsilon) k'^3 E(k') \tag{3.43}$$

Using the same procedure for the flux integral of mean-square scalar transfer rate given by Eq. (3.42), we obtain

$$\Xi(k') \equiv \Xi(k'|\lambda k') = \frac{4}{d} f(\epsilon) \frac{E(\lambda k')}{\lambda k'[\nu(\lambda k') + \kappa(\lambda k')]} g_2(\epsilon)(k')^3 \mathcal{E}(k') \tag{3.44}$$

Now, applying the scaling relations from Eq. (3.34) together with $\Pi(q) = \varepsilon\, q^{4-\epsilon}$, $\Xi(q) = \chi\, q^{4-\epsilon'}$, we get two algebraic expressions as

$$\frac{\alpha}{C^2} = \frac{2}{d-1} \left[A_d(\epsilon) f(\epsilon) + B_d\right] g_1(\epsilon) \lambda^{-\epsilon/3} \tag{3.45}$$

$$\frac{\alpha + \beta}{C\ \mathrm{Ba}} = \frac{4}{d} f(\epsilon) g_2(\epsilon) \lambda^{-\epsilon/3} \tag{3.46}$$

3.4 Calculations

Here we calculate the Kolmogorov constant (C), Prandtl number(σ) and Batchelor constant (Ba) from the algebraic expressions arising from the eddy-viscosity, eddy-diffusivity and the flux integral equations derived in the previous sections. Eqs. (3.35) and (3.36) gives

$$\frac{\alpha^2}{C} = \frac{1}{d+2} \left[\frac{3}{\epsilon} + O(\epsilon^0)\right] \quad \text{and} \quad \frac{\beta(\alpha+\beta)}{C} = \frac{2}{d} \left[\frac{3}{\epsilon} + O(\epsilon^0)\right] \tag{3.47}$$

which are obtained by performing Laurent expansion about the UV pole at $\epsilon = 0$, the leading order being $O(1/\epsilon)$. Again, Eqs. (3.45) and (3.46) yields

$$\frac{\alpha}{C^2} = \frac{2}{d+2} \left[\frac{3}{\epsilon} + O(\epsilon^0)\right] g_1(\epsilon) \quad \text{and} \quad \frac{\alpha+\beta}{C\ \mathrm{Ba}} = \frac{4}{d} \left[\frac{3}{\epsilon} + O(\epsilon^0)\right] g_2(\epsilon) \tag{3.48}$$

where $g_1(\epsilon)$ and $g_2(\epsilon)$ are the IR poles coming from the flux integrals. Thus, for the Kolmogorov value $\epsilon = 4$, and $d = 3$, we obtain,

$$\frac{\alpha^2}{C} = \frac{3}{20} \quad \text{and} \quad \frac{\alpha}{C^2} = \frac{9}{40}$$

$$\frac{\beta(\alpha+\beta)}{C} = \frac{1}{2} \quad \text{and} \quad \frac{(\alpha+\beta)}{C\ \mathrm{Ba}} = \frac{3}{4}$$

which yields

$$C = 1.4363$$

$$\sigma = \alpha/\beta = 0.7179$$

$$\mathrm{Ba} = 1.031$$

Further, by making no ϵ expansion, and setting $\lambda = 1$ we obtain for $\epsilon = 4$ and $d = 3$

$$\frac{\alpha^2}{C} = \frac{7}{60} \quad \text{and} \quad \frac{\alpha}{C^2} = \frac{7}{40}$$

$$\frac{\beta(\alpha+\beta)}{C} = \frac{1}{2} \quad \text{and} \quad \frac{(\alpha+\beta)}{C\ \mathrm{Ba}} = \frac{3}{4}$$

giving

$$C = 1.5618$$

$$\sigma = 0.61351$$

$$\mathrm{Ba} = 0.9583$$

We note that the value of Kolmogorov constant $C = 1.5618$, obtained by making no ϵ expansion, is in exact agreement with Kraichnan's [76] result. Our calculated value of Batchelor constant Ba = 1.03 and Prandtl number

$\sigma = 0.7179$, both are obtained by doing ϵ expansion, are in close agreements with Yakhot and Orszag's [184, 183] RG calculations, namely Ba = 1.16 and $\sigma = 0.7179$, and with experimental results [111].

We further note that Yakhot and Orszag calculated the Batchelor constant by using Pao's formulation [123, 124] which is quite different from our formulation. However, our analysis also yield a relation between Kolmogorov constant, Batchelor constant and Prandtl number, namely, Ba $= \sigma\ C$. This relation is independent of ϵ expansion.

3.5 Relation between 1D and 3D Batchelor Constant

It is worthwhile to point out that different authors use different definitions for scalar dissipation rate as well as for Batchelor constant. For example, some authors define the scalar dissipation rate by half of that used in Eq. (3.2) while others use a different "Batchelor constant" coming from the one dimensional spectrum. In order to avoid confusion, here we find out a relation between three-dimensional Batchelor spectrum (Eq. (3.2)) and the corresponding one-dimensional spectrum given by

$$\mathcal{E}(k_1) = \ \mathrm{Ba}'\ \chi\ \varepsilon^{-1/3}\ k_1^{-5/3} \tag{3.49}$$

We know that

$$\int_0^\infty \mathcal{E}(k)dk = \int \frac{d^3\mathbf{k}}{[2\pi]^3}\Psi(k,0) = \int_0^\infty dk \frac{4\pi k^2}{[2\pi]^3}\Psi(k,0)$$

Thus

$$\Psi(k,0) = \frac{[2\pi]^3}{4\pi}\mathrm{Ba}\ \chi\ \varepsilon^{-1/3}k^{-11/3}$$

Therefore

$$\int_0^\infty \mathcal{E}(k_1)dk_1 = \int \frac{d^3\mathbf{k}}{[2\pi]^3}\Psi(k,0)$$

$$= \frac{\mathrm{Ba}}{4\pi}\ \chi\ \varepsilon^{-1/3}\int_{-\infty}^{\infty}\int_{-\infty}^{\infty}\int_{-\infty}^{\infty}\frac{dk_1dk_2dk_3}{(k_1^2+k_2^2+k_3^2)^{11/6}} \tag{3.50}$$

In order to evaluate this integral we use the definition of Gamma (Γ) function:

$$\frac{\Gamma(\alpha)}{(k^2+m^2)^\alpha} = \int_0^\infty x^{\alpha-1} e^{-(k^2+m^2)x} dx$$

which yields

$$\int_{-\infty}^{\infty} \frac{dk}{(k^2+m^2)^\alpha} = \frac{\sqrt{\pi}}{\Gamma(\alpha)} \int_0^\infty dx\ x^{\alpha-3/2}\ e^{-m^2 x} = \frac{\sqrt{\pi}\ \Gamma(\alpha-1/2)}{\Gamma(\alpha)(m^2)^{\alpha-1/2}}$$

Using this definition, we integrate the right hand side of Eq. (3.50) over the components k_2 and k_3, and obtain

$$\int_0^\infty \mathcal{E}(k_1) dk_1 = \frac{\mathrm{Ba}}{4\pi}\ \chi\ \varepsilon^{-1/3} \frac{2\pi\Gamma(5/6)}{\Gamma(11/6)} \int_0^\infty dk_1 k_1^{-5/3}$$

Thus

$$\mathcal{E}(k_1) = \frac{3}{5}\ \mathrm{Ba}\ \chi\ \varepsilon^{-1/3}\ k_1^{-5/3} \tag{3.51}$$

Thus, from Eqs. (3.49) and (3.51) we obtain a relation between one-dimensional Batchelor constant, Ba$'$, and three-dimensional Batchelor constant, Ba, as

$$\mathrm{Ba}' = \frac{3}{5}\ \mathrm{Ba}$$

In Table 3.1, we summarize the values of these constants obtained for various flows with their sources.

Table 3.1: Values of Ba$'$ and Ba in various flows.

Method	*Source*	Ba$'$	Ba
Expt. Atmospheric	Boston and Berling [17]	0.81 ± 0.09	1.35 ± 0.15
Tidal Channel	Wyngaard and Cote [179]	0.40 ± 0.05	0.67 ± 0.08
Grid turbulence	K. R. Sreenivasan [151]	0.40	0.67
RG	Yakhot and Orszag [184]	0.70	1.16
Field theoretic RG	M. K. Verma [171]	0.75	1.25
DNS	R. M. Kerr [70]	0.6	1.0
DNS	Lindborg and Cho [99]	1.2	2.0
DNS	Brethouwer [18]	0.5	0.83
Heisenberg Approximation	Our results	0.62	1.03

3.6 Calculations in Higher Dimensions

Here we would like to calculate the behavior of the universal numbers at large space dimensions. From the amplitude ratios, namely Eqs. (3.35) and (3.36) it can be shown that, for the physical values of $\epsilon = \epsilon' = 4$

$$\frac{\alpha^2}{C} = \frac{3}{4}\frac{1}{d+2} \tag{3.52}$$

and

$$\frac{\beta(\alpha+\beta)}{C} = \frac{3}{2d} \tag{3.53}$$

Similarly, from Eqs. (3.45) and (3.46), we get

$$\frac{\alpha}{C^2} = \frac{9}{8(d+2)} \tag{3.54}$$

and

$$\frac{\alpha+\beta}{C\ \mathrm{Ba}} = \frac{9}{4d} \tag{3.55}$$

Solving the above equations for any space dimension d, we obtain the following results for the Kolmogorov constant C, Batchelor constant Ba, and the turbulent Prandtl number σ.

$$C = \left(\frac{16(d+2)}{27}\right)^{1/3} \tag{3.56}$$

$$\frac{1}{\sigma} = \frac{\beta}{\alpha} = \frac{1}{2}\left(-1 \pm \sqrt{9+\frac{16}{d}}\right) \tag{3.57}$$

and

$$\mathrm{Ba} = \sigma\ C \tag{3.58}$$

We show in Table 3.2 the numerical values of the above universal numbers for various space dimensions d up to 200.

We see that with increasing values of space dimensions, Prandtl number σ increases and approaches unity, while the Kolmogorov constant C and Batchelor constant Ba approach very close to each other. In the field theoretic RG calculations of these universal numbers in Ref. [171], a similar trend was observed.

Table 3.2: Values of σ, C and Ba in various space dimensions.

Dimension (d)	$\sigma = \alpha/\beta$	C	Ba
3	0.7179	1.4363	1.0311
4	0.7676	1.5262	1.1715
5	0.8023	1.6067	1.2891
7	0.8476	1.7471	1.4808
10	0.8866	1.9229	1.7049
15	0.9204	2.1597	1.9879
20	0.9387	2.3535	2.2093
30	0.9580	2.6667	2.5546
40	0.9680	2.9197	2.8262
50	0.9742	3.1351	3.0542
70	0.9814	3.4943	3.4293
100	0.9869	3.9245	3.8731
150	0.9912	4.4826	4.4432
200	0.9934	4.9284	4.8958

In order to investigate the dependence of these universal numbers at very large space dimensions, we perform an expansion in powers of $1/d$, yielding

$$\frac{\alpha^2}{C} = \frac{3}{4}\frac{1}{d+2} = \frac{3}{4d} + O\left(\frac{1}{d^2}\right) \tag{3.59}$$

$$\frac{\alpha}{C^2} = \frac{9}{8(d+2)} = \frac{9}{8d} + O\left(\frac{1}{d^2}\right) \tag{3.60}$$

so that

$$C = \frac{(\alpha^2/C)^{1/3}}{(\alpha/C^2)^{2/3}} = \left(\frac{16}{27}\right)^{1/3} d^{1/3} + O\left(\frac{1}{d^{2/3}}\right) \tag{3.61}$$

$$\frac{\alpha}{\beta} = 1 + O\left(\frac{1}{d}\right) \tag{3.62}$$

Thus, we find that, at very high space dimensions, Kolmogorov constant C, Batchelor constant Ba, and Prandtl number σ are obtained as

$$C = C_0\ d^{1/3} \tag{3.63}$$

$$\mathrm{Ba} = \mathrm{Ba}_0\ d^{1/3} \tag{3.64}$$

and

$$\sigma = \frac{\alpha}{\beta} = 1 \tag{3.65}$$

where

$$C_0 = \mathrm{Ba}_0 = \left(\frac{16}{27}\right)^{1/3} \approx 0.83995 \tag{3.66}$$

3.7 Discussion and Conclusion

In this chapter, we calculated the universal constants namely, Kolmogorov constant, C, Prandtl number, σ, and Batchelor constant, Ba, from the energy and mean-square scalar transfer integrals arising from the passive scalar dynamics. The calculation of our results was based on Heisenberg's approximation together with a procedure of ϵ expansion. In the UV limit, $p' \gg k$, we calculated the eddy-viscosity $\nu(k|p')$ and eddy-diffusivity $\kappa(k|p')$ as the effect on the wave number k due to wave numbers $(p, q) > p'$ as a result of the Heisenberg approximation on the transfer integrals. The integrations were carried out by picking up the UV pole. Our calculated values namely, $\sigma = 0.7179$ and $\mathrm{Ba} = 1.0311$, are comparable with other theoretical calculations, namely Yakhot-Orszag's renormalization group calculation ($\mathrm{Ba} = 1.16$ and $\sigma = 0.7179$) [184, 183] and experimental investigations ($\mathrm{Ba} \approx 0.67 - 1.35$ and $\sigma \approx 0.7 - 0.9$) [90, 111]. The agreement with the experiments for the Batchelor constant can also be seen in Table 1. We also obtain a relation between Kolmogorov constant (C), Batchelor constant (Ba), and turbulent Prandtl number (σ), namely, $\mathrm{Ba} = \sigma\, C$, which was obtained by Yakhot and Orszag [183] using Pao's formulation.

As we have noted earlier, Adzhemyan et al. [2] obtained $\sigma = 0.7179$ in one-loop approximation and $\sigma = 0.7693$ in two-loop approximation in their field theoretic RG calculations.

We would like to point out that Verma [171] used field-theoretic perturbation technique to calculate the universal numbers associated with the passive scalar dynamics from the corresponding flux integrals and the renormalized

transport constants in the inertial-convective range. Using Gaussian quadrature, he obtained Ba = 1.25, $C = 1.53$, and $\sigma = 0.42$ in three dimensions. Within the framework of his calculations, these numbers in higher dimensions could also be calculated. He obtained that the Batchelor constant goes like $d^{1/3}$ and the Prandtl number approaches unity in the limit of large space dimensions. This is qualitatively similar to our results presented in our previous section.

As we have already noted, our basic purpose of calculations for the passive scalar dynamics is to attack the problem of active scalar turbulence with stable temperature stratification. These universal numbers calculated in this chapter are useful in the statistical description of such active scalar problem. We note that, using the atmospheric data collected in the MOZAIC program [40, 119], Cho and Lindborg [99], from their data analysis, investigated the second-order structure function of temperature in the lower stratosphere which appeared to have the same functional form as that of the Batchelor (or Obukhov-Corrsin) scaling with the universal number Ba = 2.0. In a recent numerical simulations on strongly stratified turbulence by Brethouwer and Lindborg [18], the one-dimensional passive scalar spectrum was investigated and it was found to be consistent with atmospheric observations. Their estimated value of one-dimensional Batchelor constant, $\mathrm{Ba}' \approx 0.5$, is comparable to our theoretical value, namely, $\mathrm{Ba}' = 0.62$.

To carry out the problem further, detailed theoretical analyses of stably stratified turbulence are performed in the following chapters.

However, before we end this chapter, it seems worthwhile to note about another approach called the eddy-damped quasinormal Markovian (EDQNM) closure [30, 89, 122, 159]. In this closure, the equations for energy transfer and scalar transfer remain similar to the ones in the present calculations. However, in EDQNM, a phenomenological relationship for eddy-viscosity and eddy-diffusivity is assumed. For example, the eddy-viscosity is modeled as $\eta(k) = \nu(k)k^2 = K\sqrt{(\int_0^k q^2 E(q)dq)}$ and a similar model for the eddy-diffusivity. The prefactor K is a free parameter not determined by the theory and it is chosen

to fit experiments. In contrast, the advantage of our approach is that the eddy-viscosity and eddy-diffusivity are derived from transfer integrals of energy and mean-square scalar (invoking the Heisenberg approximation) coming from the Navier-Stokes dynamics and passive scalar dynamics. We do not have any free parameters in our calculations.

Chapter 4

Leslie-type Treatment of Stably Stratified Turbulence

4.1 Introduction

As discussed earlier, stably stratified turbulent flow, in which the scalar (temperature or density) is coupled to the turbulent dynamics by buoyant forces, has long been treated as a challenging problem in geophysical or astrophysical applications [126, 21, 136]. Stable and strong stratification is a common phenomena in the atmospheres of planets [65], oceans and lakes [8, 50]. Due to their importance for the understanding of geophysical flows, and because of their relevance to engineering problems [110], stratified flows have been extensively investigated in many theoretical, experimental and numerical studies. Density stratification in atmospheric boundary layers [147, 162] and salt stratification in oceanic mixed layers [54] due to gravity force, are found to be almost stable which tends to reduce the vertical mixing leading to the development of spatial anisotropy. The equilibrium state is modified due to the existence of external disturbances namely, buoyant forces. The deviation from the universal isotropic energy as well as mean square scalar spectrum [74, 121, 12], namely

$$E(k) = C\varepsilon^{2/3}k^{-5/3} \tag{4.1}$$

and

$$\mathcal{E}(k) = \text{ Ba } \chi \, \varepsilon^{-1/3} \, k^{-5/3} \tag{4.2}$$

where C is the Kolmogorov constant, Ba, the Batchelor (or Obukhov-Corrsin) constant, χ the scalar flux,, ε the energy flux, and k is the wave number, are expected when the flow is inherently anisotropic, as in the case of stratified flow.

4.1.1 Phenomenological Models

The statistics of energy as well as temperature fluctuations in the presence of buoyant forces, and how the presence of these forces affect the scaling properties of turbulence, is a topic of much interest. Lumley [101] conjectured that local inertial scaling like Kolmogorov [74] might be supposed even though ε depends upon k where the buoyancy flux $\zeta(k)$ affects the rate of kinetic energy transfer $\varepsilon(k)$ from wavenumbers less than k to wavenumbers greater than k as $\partial\varepsilon/\partial k + \zeta(k) = 0$. With further supposition Lumley argued that

$$\zeta(k) = -C_1 N^2 \left[\varepsilon(k)\right]^{1/3} k^{-7/3} \tag{4.3}$$

where

$$\varepsilon(k) = \varepsilon_0 \left[1 + \left(\frac{k_B}{k}\right)^{4/3}\right]^{3/2} \tag{4.4}$$

so that

$$E(k) = C\varepsilon_0^{2/3} \left[1 + \left(\frac{k_B}{k}\right)^{4/3}\right] k^{-5/3} \tag{4.5}$$

Here C and C_1 are empirical constants (C is the universal Kolmogorov constant), N is the Brunt-Väisälä frequency, ε_0 is the dissipation rate for kinetic energy, $k_B = \left(N^3/\varepsilon_0\right)^{1/2}$ is the buoyancy wavenumber, and $E(k)$ is energy density. Lumley assumed that the dynamics of stratified turbulence are nearly inertial as in the usual Kolmogorov cascade, its statistical properties depend only upon the net flux of energy across a given wavenumber. However, this

flux is assumed to be k dependent owing to the leakage of kinetic energy by conversion into potential energy via the buoyancy flux. Applying the condition that, for large scales ($k_B/k \gg 1$), it is obvious from Lumley's analysis that $E(k) \sim N^2 k^{-3}$. Further, he makes a rough estimate for the constant C_1 in terms of Prandtl number, σ, and found $C_1 = 2\sigma^{-1}$. The associated potential energy spectrum was proposed by Phillips [127], who derived a theoretical density spectra in the buoyancy subrange as

$$B(k) \sim \phi(k)\varepsilon_0^{-1/3} \left[1 + (k_B/k)^{4/3}\right]^{-1/2} k^{-5/3} \tag{4.6}$$

where the scale dependent mean square density flux, $\phi(k)$, is defined in terms of buoyancy spectra, $\zeta(k)$, as

$$\phi(k) = \phi_0 + N^2 \int_k^\infty dq\zeta(q) \tag{4.7}$$

with ϕ_0 is the value of $\phi(k)$ in the inertial subrange. This in turn produces the well-known Batchelor-Obukhov scaling law [121], $B(k) \sim \phi_0\ \varepsilon^{-1/3}k^{-5/3}$ in the inertial subrange. By introducing a conditional speculation that in the buoyancy subrange ($k_B/k \gg 1$), $\phi(k) \sim \phi_0$, Phillips obtained the density spectra as $B(k) \sim \phi_0 N^{-1}k^{-1}$, which was not consistent with observations. Following carefully Phillips' derivation, Weinstock [176] derived the temperature spectrum as

$$B(k) \sim N^2\varepsilon_0^{2/3} \left[1 + (k_B/k)^{4/3}\right] k^{-5/3} \tag{4.8}$$

In the Boussinesq approximation, temperature fluctuation could be regarded as proportional to the density fluctuation [87]. Thus, in the $k_B/k \gg 1$ limit, he obtained $B(k) \sim N^4 k^{-3}$. Though using quite different hypotheses, Holloway [59] obtained kinetic energy and potential energy spectra showing the same functional form as Lumley's kinetic energy spectrum, with a radically distinct physical interpretation. Ramsden and Holloway [132] investigated the nonlinear interactions among internal gravity waves by direct numerical experiments in 2D and 3D Navier-Stokes turbulence and found that the transfer of kinetic energy (KE) from large to small scales is less efficient than the transfer

of potential energy (PE). The imbalance between these transfers leads to a characteristic buoyancy flux spectrum which is negative (KE to PE) at large scales and positive (PE to KE) at small scales.

Most of the above mentioned phenomenological models, akin to the well-known Kolmogorov-Obukhov theories [74, 120], visualize a fundamental picture of the scaling and universality of stratified turbulence. A detailed theoretical analysis is a necessity in order to assess the information about the influence of anisotropy induced by stable temperature (or density) stratification on Navier-Stokes dynamics.

4.1.2 Observations and Attempts

The remarkable universality possessed by the atmospheric kinetic energy spectra in the upper troposphere and lower stratosphere remains a topic of much interest among researchers for a long time. From observational analysis using the Global Atmospheric Sampling Program (GASP) data set, Nastrom and Gage [115, 116] obtained a synoptic scale k^{-3} dependence of the atmospheric kinetic energy spectrum, along with a transition to a $k^{-5/3}$ dependence in the mesoscale. Although some scenarios have been proposed, the origin of such spectra remains unknown. Understanding the source and structure of this spectrum has posed a great puzzle in atmospheric science for the past 25 years.

Some of the earlier theoretical attempts for the explanation of the energy cascade process in the atmospheric turbulence involved internal gravity waves (IGW) [35, 168]. IGW are observed in the atmosphere, at scales ranging from meters to kilometers, and dominate fluctuations in the stratosphere. Simulations of internal wave breaking have had greater success in reproducing the observed N^2k^{-3} spectrum [154]. Chunchuzov [32] proposed a model of IGW spectrum, which takes into account the effects of strong nonlinear wave-wave interactions on the formation of the Eulerian spectrum of atmospheric internal wave, and has shown that strongly anisotropic 3D temperature and wind speed irregularities can occur in non-linear field of random IGW's in stably

stratified atmosphere. The approximate expressions for regularized 3D spectrum of temperature fluctuations is derived from the 3D spectrum of vertical displacements induced by a random IGW field, and the obtained spectrum was in good agreement with its observed form in the middle atmosphere. Recently, Gurvich and Chunchuzov [55] proposed a phenomenological model for the three-dimensional spectrum of temperature irregularities by introducing a variable anisotropy hypothesis into the earlier theory of Chunchuzov [32]. They derive asymptotic expressions for the 3D vertical and horizontal temperature spectra, which produced the observed $k^{-5/3}$ and k^{-3} spectra. They further suggested that internal wave-wave interactions may contribute to the large scale k^{-3} spectra. All these theories of IGWs conjectured a direct energy cascade as in 3D turbulence. Although different models of the IGW spectrum in the atmosphere have been proposed, the applicability of the approximations used in modeling of the IGW spectrum is still debated [97, 94].

Attempts have been made using Kraichnan's two-dimensional turbulence [92] and Charney's [26] quasigeostrophic (QG) turbulence model to explain the observed atmospheric spectra. Based on Charney's QG model with a modification, Tung and Orlando [167] proposed a two-level QG model and conjectured that the observed atmospheric energy spectrum results from the downscale cascade of enstrophy and energy injected at the large scales by baroclinic instability which finally dissipated at the smallest length scales. Tulloch and Smith [165, 150] demonstrated that by limiting surface quasigeostrophic (SQG) flow to a finite depth (hence called finite-depth SQG (fSQG) model) one can obtain a natural transition scale, and when the flow is forced at large scales, the kinetic energy spectrum is k^{-3} at scales above the transition scale and $k^{-5/3}$ below it with a transition scale $k_t \sim NH/f$, where N is the buoyancy frequency, f the Coriolis parameter, and H the depth of the fluid. In order to accurately represent surface advection at the boundaries, and in order to remove the deficiencies of fSQG model, they further proposed a two-mode two-surface (TMTS) model (mainly, by including interior potential vorticity anomalies in the flow) [166] which captures all major types of baroclinic insta-

bility (generated from barotropic-baroclinic interactions, surface-surface interactions, and from interactions between either surface and the interior), and demonstrated that the surface dynamics at the tropopause can explain the transition to a shallow k^{-3} energy spectrum at sub-synoptic scales, consistent with the observed atmospheric kinetic energy spectrum.

Observations, in fact, play an important role in evaluating proposed explanations of the mesoscale spectrum. In order to confirm whether $k^{-5/3}$ power law arises either due to inverse energy cascade of 2D turbulence, or due to the direct cascade in 3D, a third-order velocity structure function was computed by Cho et al. [29], based on MOSAIC program [40, 119] database which accumulated wind velocities measured on 7630 aircraft flights. The structure functions at length scales between 10 and 100 km was found to be negative, which led to suggest them a downscale energy transfer in the mesoscale, thereby casting doubt on the inverse cascade idea. They further suggested that the origin of large scale k^{-3} spectrum could be explained on the basis of the balance between Coriolis and pressure terms. Tung and Orlando [167] claimed, in contradiction to basic quasigeostrophic turbulence phenomenology, that in the sub-synoptic scales enstrophy flux is important, which determines the k^{-3} spectrum. At a transition scale determined by $\varepsilon\ k_t^2 = \eta$, where ε is the downscale energy flux and η is the downscale enstrophy flux, the spectrum undergoes a transition to the $k^{-5/3}$ form determined by an energy flux in the mesoscale wavenumbers.

Numerical simulations of stratified turbulence have had mixed success in reproducing the observed spectra. In flows dominated by vortical motion, spectra have been found to be steeper than $k^{-5/3}$ in the horizontal direction, and shallower than k^{-3} in the vertical. Laval et al. [88], found steep horizontal spectra (with slopes near -5) and very shallow vertical spectra when large-scale vortical motion was forced. Waite and Bartello [172] performed numerical simulations of stably stratified, vortically forced turbulence for various values of stratification, and obtained approximately a $k^{-5/3}$ spectrum of vortical energy. Further simulations of randomly forced internal gravity waves, in a uniformly stratified Boussinesq fluid [173], yield a saturation spectrum close to k^{-3}. Re-

cently Waite and Snyder [174], through numerical simulations, examined the mesoscale spectrum and spectral energy budget of an idealized baroclinic life cycle. This simulation is a natural extension of rotating stratified turbulence to a more realistic atmosphere with a troposphere and lower stratosphere. It is found that upper tropospheric kinetic energy spectrum is dominated by rotational motion through the mesoscale, as seen in the previous data analysis [29, 94] and GCM experiment [158, 56]. Falkovich [42], however, have suggested that the large scale k^{-3} spectrum can result from an inverse cascade of inertia gravity waves. Kitamura and Matsuda [72], in order to investigate the energy cascade process due to synoptic scale forcing, performed numerical experiments with a three-dimensional non-hydrostatic model (within Boussinesq approximation) of stratified turbulence, and found a downscale energy cascade on the tails of a steep synoptic scale spectrum. Recent direct numerical simulations of homogeneous turbulence with a strong and uniform stratification [18], in which three-dimensional Boussinesq equations and the transport equation for a passive gradient are solved employing pseudo-spectral code with periodic boundary conditions in all three directions, and with forcing in rotational and divergent modes, show that stratification may enforce a three-dimensional dynamics and the forward $k^{-5/3}$ energy cascade. In order to fully solve the problem of the origin of $k^{-5/3}$ mesoscale wavenumber energy spectra, Lindborg [98] carried out a set of numerical simulations of the full Boussinesq equations including system rotations, and thereby studied the effect of rotation on such an energy cascade, and has shown that this spectrum prevails when rotation is sufficiently weak. In a companion paper, Lindborg [96] also showed that such a mesoscale spectrum can arise as a result of forward energy cascade in the limit of strong stratification.

In a series of recent experiments in two-dimensional turbulence by Xia et al. [140, 180], it has been suggested that the main energy at large scales is actually not in turbulent fluctuations but in a long-correlated flow (condensate), which can be either generated by external forces or appear in the process of spectral condensation. The k^{-3} spectrum arises due to the condensation of inverse

energy cascade in two dimensions. Quite recently, in Ref. [181], they reviewed their previous experiments and presented a new experiment on quasi 2D flow, in which they investigated the effect of large scale uniform dissipation (bottom friction) and spectral condensation on the turbulence statistics. They found that, in addition to the Kraichnan's [75] $k^{-5/3}$ inertial inverse energy cascade range and k^{-3} direct enstrophy cascade range, there is a large-scale condensate range where the spectrum is very close to k^{-3}. Further, the value of the Kolmogorov constant was found to be $C \approx 1.8$ in the strongest condensate regime and $C \approx 1.2-1.8$ in the energy cascade range. As these values are very close to that of the 3D turbulence [113], they suggested that the presence of the strong condensate substantially reduces the efficiency of the spectral energy transfer via the inverse cascade process. However, the two dimensionality of such experiments have been regarded with doubts [95], and it appears that this problem still poses the same old challenge of explaining the origin of the spectra.

4.1.3 Present Motivation

The main theoretical challenge arises from the presence of the terms due to the buoyant forces in the governing dynamical equations. These terms are anisotropic in nature and the difficulty of the original isotropic problem enhances to a great extent. However, Leslie showed a way to deal with such terms in a perturbative manner in the case of homogeneous shear turbulence. An improved version of Leslie's perturbative procedure was adapted in this thesis in Chapter 2. It was found that such treatment could reproduce the experimental results satisfactorily for the case of homogeneous shear turbulence.

In this chapter, motivated by the above calculation, we perform a Leslie-type perturbative treatment [90] on stably stratified turbulence, where the buoyancy terms in the corresponding dynamical equations are treated as perturbations against the isotropic background fields. Subsequently, we make perturbation expansions of the velocity and temperature fields. This enables us to evaluate the corresponding corrections to various correlation functions,

namely, velocity-velocity, temperature-temperature, and velocity-temperature correlations. It is found that the prefactors in the resulting anisotropic corrections to the correlation functions depend on Kolmogorov constant C, Batchelor constant Ba, and the turbulent Prandtl number σ. As presented in Chapter 3, we calculated these universal numbers by deriving analytic expressions for eddy-viscosity and eddy-diffusivity from the transfer integrals of energy and mean-square scalar applying Heisenberg approximation [57]. Thus, using these values of the universal numbers, in this chapter, we are able to calculate the relevant numbers associated with the anisotropic spectra of stably stratified turbulence. Our calculations yield the anisotropic part of energy and mean-square scalar spectra as k^{-3} and the anisotropic buoyancy spectrum as $k^{-7/3}$. We note that, at sufficiently large scales, the anisotropic k^{-3} spectrum would dominate over the isotropic $k^{-5/3}$ spectrum. Thus we expect a k^{-3} power law behavior of energy spectrum at sufficiently large scales. It may be noted that this scenario is similar to the analysis of experimental investigations by Nastrom and Gage [115, 116] as mentioned earlier.

4.2 Stratified Dynamics

To begin with, we take the full Navier-Stokes equations in the presence of a gravitational field, $\mathbf{g}$, which takes the form [126, 87]

$$\frac{\partial \mathbf{u}}{\partial t} + (\mathbf{u}\cdot\nabla)\,\mathbf{u} = -\frac{\nabla p}{\rho} + \nu_0\nabla^2\mathbf{u} + \mathbf{g} \tag{4.9}$$

The thermal convection equation can be written as

$$\frac{\partial T}{\partial t} + (\mathbf{u}\cdot\nabla)\,T = \kappa_0\nabla^2 T \tag{4.10}$$

and the equation expressing incompressibility as

$$\nabla\cdot\mathbf{u} = 0 \tag{4.11}$$

where $\mathbf{u}(\mathbf{x},t)$, $T(\mathbf{x},t)$ and $p(\mathbf{x},t)$ are the velocity, temperature and pressure fields; ν_0 and κ_0 are the kinematic viscosity and molecular diffusivity respectively. We use Boussinesq approximation [87, 24], and we write, $p = p_0 + p'$,

$T = T_0 + T'$, and $\rho = \rho_0 + \rho'$, where p' is the small pressure fluctuation measured from p_0, ρ_0 is the constant mean density, T' is the small fluctuation of T with respect to the mean temperature T_0, and the corresponding density variation can be expressed in terms of T' as $\rho' = (\partial\rho_0/\partial T)_p T' = -\rho_0\beta T'$. Here the thermal expansion coefficient $\beta = -(1/\rho)\partial\rho/\partial T$ is assumed to be positive ($\beta > 0$). The condition of equilibrium is $(\nabla p_0/\rho_0) = \mathbf{g}$. Substituting these expressions in the above equations, we readily get the corresponding equations for the fluctuating part in the Boussinesq approximation as

$$\frac{\partial \mathbf{u}}{\partial t} + (\mathbf{u}\cdot\nabla)\mathbf{u} = -\frac{\nabla p'}{\rho_0} + \nu_0\nabla^2\mathbf{u} - \beta T'\mathbf{g}$$

$$\frac{\partial T'}{\partial t} + (\mathbf{u}\cdot\nabla)T_0 + (\mathbf{u}.\nabla)T' = \kappa_0\nabla^2 T'$$

Now considering the vertical mean temperature gradient along $\hat{e}_3$ (anti-parallel to gravity), we write

$$\frac{\partial \mathbf{u}}{\partial t} + (\mathbf{u}\cdot\nabla)\,\mathbf{u} = \mathbf{f} - \frac{\nabla p'}{\rho} + \nu_0\nabla^2\mathbf{u} + N\psi\hat{e}_3 \tag{4.12}$$

$$\frac{\partial \psi}{\partial t} + (\mathbf{u}\cdot\nabla)\,\psi = \theta - Nu_3 + \kappa_0\nabla^2\psi, \tag{4.13}$$

$$\nabla\cdot\mathbf{u} = 0 \tag{4.14}$$

Here the scalar field, $\psi(\mathbf{x},t)$, is related with the fluctuating temperature field, T', as $\psi = (\beta g/N)T'$, in which N is the Brunt-Väisälä frequency given by $N^2 = \beta g(dT_0/dz)$; the Gaussian random forces, $\mathbf{f}(\mathbf{x},t)$ and $\theta(\mathbf{x},t)$, are introduced in order to maintain turbulence in a statistically steady state.

Similar to the previous analysis for homogeneous shear turbulence given in Section 2.2, we can perform an order of magnitude estimate for the present case of stably stratified turbulence. Here the scalar field is coupled to the momentum equation by an imposed buoyancy force ($N\psi\hat{e}_3$ term in the momentum equation). In addition, an extra term (namely, $-Nu_3$) appears in the advection equation for the scalar field. In terms of characteristic time scales τ_s and τ_l associated with the direct coupling terms and nonlinear convective term respectively, we get

$$\tau_s \sim \frac{1}{N}, \qquad \tau_l \sim \frac{l}{v_l} = \frac{l}{(\varepsilon l)^{1/3}} = \left(\frac{1}{\varepsilon k^2}\right)^{1/3}$$

Therefore,

$$\frac{\tau_l}{\tau_s} \equiv \delta_l \sim \frac{Nl}{v_l} = Nl^{2/3}\varepsilon^{-1/3} = \frac{N}{(\varepsilon k^2)^{1/3}}$$

This suggests that for small length scales the extra coupling terms are not important as compared to the nonlinear convective term whereas for large length scales the extra coupling terms become significant.

4.3 Leslie-type Treatment

In Eqs. (4.12) and (4.13), the extra terms involving N represent the coupling of scalar field $\psi(\mathbf{x},t)$ with the velocity field $\mathbf{u}(\mathbf{x},t)$. Following Leslie [90], these extra terms can be treated as perturbations to the original dynamics. We write Eqs. (4.12), (4.13) and (4.14) in Fourier space as

$$\left(\frac{\partial}{\partial t} + \nu_0 k^2\right) u_i(\mathbf{k},t) + \frac{i}{2} P_{ijl}(\mathbf{k}) \sum_{\mathbf{p}+\mathbf{q}=\mathbf{k}} u_j(\mathbf{p},t) u_l(\mathbf{q},t)$$
$$= f_i(\mathbf{k},t) + \lambda N P_{i3}(\mathbf{k}) \psi(\mathbf{k},t) \qquad (4.15)$$

$$\left(\frac{\partial}{\partial t} + \kappa_0 k^2\right) \psi(\mathbf{k},t) + ik_j \sum_{\mathbf{p}+\mathbf{q}=\mathbf{k}} u_j(\mathbf{p},t) \psi(\mathbf{q},t)$$
$$= \theta(\mathbf{k},t) - \lambda N u_3(\mathbf{k},t) \qquad (4.16)$$

and

$$k_i u_i(\mathbf{k},t) = 0 \qquad (4.17)$$

Here $P_{ijl}(\mathbf{k}) = k_j P_{il}(\mathbf{k}) + k_l P_{ij}(\mathbf{k})$, with $P_{ij}(\mathbf{k}) = \delta_{ij} - k_i k_j/\mathbf{k}^2$, the summation sign represents integrations on $\mathbf{p}$ and $\mathbf{q}$ with triad relation $\mathbf{p}+\mathbf{q}=\mathbf{k}$; $\lambda(=1)$ is introduced as an expansion parameter. Now, making perturbation expansion about the isotropic turbulent states as

$$u_i(\mathbf{k},t) = u_i^{(0)}(\mathbf{k},t) + \lambda u_i^{(1)}(\mathbf{k},t) + \ldots$$

$$\psi(\mathbf{k},t) = \psi^{(0)}(\mathbf{k},t) + \lambda \psi^{(1)}(\mathbf{k},t) + \ldots$$

and equating equal powers of λ we obtain

$$u_i^{(0)}(\mathbf{k},t) = \int_{-\infty}^{t} ds G_{ij}^{(0)}(\mathbf{k};t,s) f_j(\mathbf{k},s)$$
$$\psi^{(0)}(\mathbf{k},t) = \int_{-\infty}^{t} ds \mathcal{G}^{(0)}(\mathbf{k};t,s) \theta(\mathbf{k},s)$$
$$u_i^{(1)}(\mathbf{k},t) = \int_{-\infty}^{t} ds G_{ij}^{(0)}(\mathbf{k};t,s) \left[N P_{j3}(\mathbf{k}) \psi^{(0)}(\mathbf{k},s)\right]$$
$$\psi^{(1)}(\mathbf{k},t) = \int_{-\infty}^{t} ds \mathcal{G}^{(0)}(\mathbf{k};t,s) \left[-N u_3^{(0)}(\mathbf{k},s)\right]$$

in which the statistical quantities $G_{ij}^{(0)}(k;t,s)$ and $\mathcal{G}^{(0)}(k;t,s)$ are the infinitesimal response functions. The three-dimensional spatial Fourier transformed correlation functions, namely, velocity correlation tensor, $Q_{ij}(\mathbf{k},t,t')$, scalar correlation, $\Psi(\mathbf{k},t,t')$ and current, $J_i(\mathbf{k};t,t')$, are defined as

$$\langle u_i(\mathbf{k},t) u_j(\mathbf{k}',t')\rangle = Q_{ij}(\mathbf{k};t,t')[2\pi]^3\delta^3(\mathbf{k}+\mathbf{k}')$$
$$\langle \psi(\mathbf{k},t) \psi(\mathbf{k}',t')\rangle = \Psi(\mathbf{k};t,t')[2\pi]^3\delta^3(\mathbf{k}+\mathbf{k}')$$
$$\langle \psi(\mathbf{k},t) u_i(\mathbf{k}',t')\rangle = J_i(\mathbf{k};t,t')[2\pi]^3\delta^3(\mathbf{k}+\mathbf{k}') \tag{4.18}$$

Using a similar perturbation expansion as above, these correlation functions can be expanded perturbatively about the isotropic background as

$$Q_{ij} = Q_{ij}^{(0)} + \lambda Q_{ij}^{(1)} + \lambda^2 Q_{ij}^{(2)} + \cdots$$
$$\Psi = \Psi^{(0)} + \lambda \Psi^{(1)} + \lambda^2 \Psi^{(2)} + \cdots$$
$$J_i = J_i^{(0)} + \lambda J_i^{(1)} + \lambda^2 J_i^{(2)} + \cdots$$

with

$$[2\pi]^3\delta^3(\mathbf{k}+\mathbf{k}')Q_{ij}^{(0)}(\mathbf{k};t,t') = \langle u_i^{(0)}(\mathbf{k},t) u_j^{(0)}(\mathbf{k}',t')\rangle \tag{4.19}$$
$$[2\pi]^3\delta^3(\mathbf{k}+\mathbf{k}')\Psi^{(0)}(\mathbf{k};t,t') = \langle \psi^{(0)}(\mathbf{k},t) \psi^{(0)}(\mathbf{k}',t')\rangle \tag{4.20}$$
$$J_i^{(0)}(\mathbf{k};t,t') = 0 \tag{4.21}$$

The isotropic part of the velocity correlation and response tensor satisfy the relations

$$Q_{ij}^{(0)}(\mathbf{k};t;t') = Q^{(0)}(k;t,t') P_{ij}(\mathbf{k})$$

$$G_{ij}^{(0)}(\mathbf{k};t;t') = G^{(0)}(k;t,t')P_{ij}(\mathbf{k})$$

Using these properties, it is possible to show that

$$Q_{ij}^{(1)}(\mathbf{k};t,t') = 0$$

$$\Psi^{(1)}(k;t,t') = 0$$

The corresponding corrections to the correlation functions up to the leading order term are obtained as

$$Q_{ij}^{(2)}(\mathbf{k};t,t') = N^2 P_{i3}(\mathbf{k})P_{j3}(\mathbf{k}) \times \int_{-\infty}^{t} ds \int_{-\infty}^{t'} ds' G^{(0)}(k;t,s)G^{(0)}(k;t',s')\Psi^{(0)}(k;s,s') \quad (4.22)$$

$$\Psi^{(2)}(k;t,t') = N^2 P_{33}(\mathbf{k}) \times \int_{-\infty}^{t} ds \int_{-\infty}^{t'} ds' \mathcal{G}^{(0)}(k;t,s)\mathcal{G}^{(0)}(k;t',s')Q^{(0)}(k;s,s') \quad (4.23)$$

and

$$J_i^{(1)}(k;t,t') = NP_{i3}(\mathbf{k}) \int_{-\infty}^{t'} ds G^{(0)}(k;t',s)\Psi^{(0)}(k;t,s) - NP_{i3}(\mathbf{k}) \int_{-\infty}^{t} ds \mathcal{G}^{(0)}(k;t,s)Q^{(0)}(k;t',s) \quad (4.24)$$

Thus we see that the corrections due to anisotropy are expressed in terms of the isotropic response and correlation functions. Now, as suggested by Edwards [38], we assume exponential decay of the response and correlation functions, namely

$$G^{(0)}(k;t,t') = \theta(t-t')e^{-\eta(k)(t-t')}, \qquad Q^{(0)}(k;t,t') = Q^{(0)}(k)e^{-\eta(k)|t-t'|}$$
$$\mathcal{G}^{(0)}(k;t,t') = \theta(t-t')e^{-\zeta(k)(t-t')}, \qquad \Psi^{(0)}(k;t,t') = \Psi^{(0)}(k)e^{-\zeta(k)|t-t'|}$$

where $\theta(t-t')$ is the Heaviside step-function, $\eta(k)$ and $\zeta(k)$ are the damping factors.

As we are interested in the calculation of equal time correlations, we set $t = t'$ in Eqs. (4.22), (4.23) and (4.24). The integrations are performed by choosing the proper region in the s-s' space as shown in Fig. 4.1. In Fig.

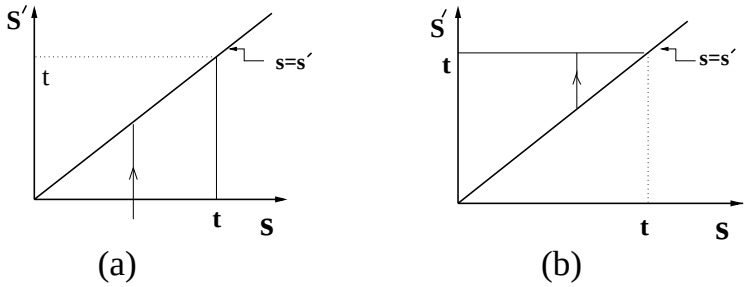

Figure 4.1: The region of integration for the time-integral expressions (4.22) and (4.23). The integration is performed (a) in the region $s > s'$ (the lower triangular region), ans (b) in the region $s < s'$ (the upper triangular region).

4.1(a), the region of integration is $s > s'$, in which s' varies from $-\infty$ to s and s varies from $-\infty$ to t. Similarly, in Fig. 4.1(b), the region of integration is $s < s'$, in which s' varies from s to t and s varies from $-\infty$ to t.

Thus, the leading order anisotropic corrections to the equal-time correlations are obtained from Eq. (4.22) to Eq. (4.24) as

$$Q_{ij}^{(2)}(k;t,t) = N^2 P_{i3}(\mathbf{k}) P_{j3}(\mathbf{k}) [2\pi]^3 a(k) \tag{4.25}$$

$$\Psi^{(2)}(k;t,t) = N^2 P_{33}(\mathbf{k}) [2\pi]^3 b(k) \tag{4.26}$$

$$J_i^{(1)}(k;t,t) = N P_{i3}(\mathbf{k}) [2\pi]^3 c(k) \tag{4.27}$$

with the scaling factors

$$a(k) = \frac{\Psi^{(0)}(k)}{\eta(k)\left[\eta(k)+\zeta(k)\right]} \tag{4.28}$$

$$b(k) = \frac{Q^{(0)}(k)}{\zeta(k)\left[\zeta(k)+\eta(k)\right]} \tag{4.29}$$

$$c(k) = \frac{\Psi^{(0)}(k) - Q^{(0)}(k)}{\left[\eta(k)+\zeta(k)\right]} \tag{4.30}$$

Thus, we see that the above anisotropic corrections are obtained in terms of isotropic correlations, which, in turn, are related to the expressions for three-dimensional spectra

$$E(k) = \frac{1}{[2\pi]^3} 4\pi k^2 Q^{(0)}(k) = C\varepsilon^{2/3} k^{-5/3} \tag{4.31}$$

$$\mathcal{E}(k) = \frac{1}{[2\pi]^3} 4\pi k^2 \Psi^{(0)}(k) = \text{Ba}\ \chi\ \varepsilon^{-1/3} k^{-5/3} \tag{4.32}$$

and the eddy damping rates

$$\eta(k) = \alpha\ \varepsilon^{1/3} k^{2/3} \tag{4.33}$$

$$\zeta(k) = \beta\ \varepsilon^{1/3} k^{2/3} \tag{4.34}$$

Employing these known relations for the isotropic spectra, we obtain

$$a(k) = \frac{1}{4\pi} \frac{\text{Ba}}{\alpha(\alpha+\beta)} \varepsilon^{-1} \chi k^{-5} \tag{4.35}$$

$$b(k) = \frac{1}{4\pi} \frac{C}{\beta(\beta+\alpha)} k^{-5} \tag{4.36}$$

$$c(k) = \frac{1}{4\pi} \frac{\text{Ba}\varepsilon^{-2/3}\chi - C\varepsilon^{1/3}}{\beta+\alpha} k^{-13/3} \tag{4.37}$$

We see that the scaling factors $a(k)$, $b(k)$ and $c(k)$, which occur in the anisotropic part of the velocity-velocity, temperature-temperature, and velocity-temperature correlations, depend on ε, χ, and on the universal numbers C, Ba, α and β. As mentioned earlier, we calculated these universal numbers using the Heisenberg approximation [57] on the transfer integrals arising from the passive scalar dynamics (Chapter 3). We calculated these numbers under two different schemes, namely with ϵ expansion and without ϵ expansion. With ϵ expansion, we obtained $C = 1.4363$, $\sigma = \alpha/\beta = 0.7179$, and Ba $= 1.031$, and without ϵ expansion we obtained $C = 1.5618$, $\sigma = 0.61351$, and Ba $= 0.9583$. Based on these calculations, we carry out two sets of calculations, with and without ϵ expansion, and present them in the following section.

4.4 Calculation of Spectral Amplitudes

Taking ϵ expansion values for α, β, Ba, and C, we get

$$\frac{\text{Ba}}{\alpha(\alpha+\beta)} = 1.9997$$

$$\frac{C}{\beta(\beta+\alpha)} = 1.9997$$

$$\frac{C}{\alpha+\beta} = 1.2930$$

$$\frac{\mathrm{Ba}}{\alpha+\beta} = 0.9282$$

When we substitute these values in Eqs. (4.35), (4.36) and (4.37) we get

$$a(k) = 0.15906\ \varepsilon^{-1}\chi k^{-5}$$

$$b(k) = 0.15906\ k^{-5}$$

$$c(k) = \left(0.07383\ \varepsilon^{-2/3}\ \chi - 0.10285\ \varepsilon^{1/3}\right) k^{-13/3}$$

For no ϵ expansion, we obtain

$$\frac{\mathrm{Ba}}{\alpha(\alpha+\beta)} = 2.0001$$

$$\frac{C}{\beta(\beta+\alpha)} = 2.0001$$

$$\frac{C}{\alpha+\beta} = 1.3914$$

$$\frac{\mathrm{Ba}}{\alpha+\beta} = 0.8537$$

which give

$$a(k) = 0.15908\ \varepsilon^{-1}\chi k^{-5}$$

$$b(k) = 0.15908\ k^{-5}$$

$$c(k) = \left(0.06790\ \varepsilon^{-2/3}\ \chi - 0.11067\ \varepsilon^{1/3}\right) k^{-13/3}$$

Thus, from our above analysis, it is obvious that the anisotropic parts of the velocity-velocity and temperature-temperature correlation are

$$Q_{ij}^{(2)}(k;t,t) = C_1 N^2 P_{i3}(\mathbf{k}) P_{j3}(\mathbf{k}) k^{-5} \tag{4.38}$$

$$\Psi^{(2)}(k;t,t) = C_2 N^2 P_{33}(\mathbf{k}) k^{-5} \tag{4.39}$$

and velocity-temperature correlation is

$$J_i^{(1)}(k;t,t) = C_3 N P_{i3}(\mathbf{k}) k^{-13/3} \tag{4.40}$$

We see from Eqs. (4.38) and (4.39) that the corresponding anisotropic spectra for energy and mean-square scalar go like k^{-3}. Eq. (4.40), on the other hand, tells us that the anisotropic buoyancy spectrum goes like $k^{-7/3}$.

4.5 Conclusion

In this chapter, we investigated the anisotropic scaling laws, associated with stably stratified turbulence, by performing a perturbative treatment suggested by Leslie [90] for homogeneous shear turbulence. Here we treat the extra terms $N\psi P_{i3}(\mathbf{k})$ and $-Nu_3$ in the stratified dynamics as perturbations against the isotropic background fields. Making perturbation expansions of the velocity and temperature fields, we evaluated the corresponding leading order corrections to various correlation functions, namely velocity-velocity, temperature-temperature, and velocity-temperature correlations, as given by Eqs. (4.22), (4.23), and (4.24). We evaluated these time integrals by choosing a proper region in s-s' space, yielding the anisotropic corrections to the equal-time velocity-velocity, temperature-temperature, and the velocity-temperature correlation as given by Eqs. (4.25), (4.26), and (4.27). We find that the anisotropic corrections to the relevant correlation functions are determined by the well-known isotropic correlation functions. Thus, using the universal isotropic Kolmogorov-Obukhov scaling laws, given by Eqs.(4.31) to (4.34), we calculated the scaling factors, namely $a(k)$, $b(k)$ and $c(k)$, associated with the anisotropic

spectra. These scale factors were found to depend on energy flux ε, scalar flux χ, Kolmogorov constant C, Prandtl number σ, and Batchelor constant Ba. Putting the values of C, Ba, and σ , which were already evaluated in Chapter 3, we calculated the universal numbers occurring as prefactors in $a(k)$, $b(k)$ and $c(k)$. Based on our previously calculated values of C, Ba, and σ, here, we presented two different schemes of calculations, namely with ϵ expansion and without ϵ expansion.

We further obtained, from Eqs.(4.38) and (4.39), that the leading order anisotropic corrections to the velocity-velocity and temperature-temperature correlation functions give rise to the corresponding anisotropic spectra for energy and mean-square scalar as k^{-3}. The anisotropic corrections at orders higher than k^{-3} are expected to show effects at extremely large scales which may not be realized in practice. Thus, the two spectra, namely, the isotropic Kolmogorov part $k^{-5/3}$ and the anisotropic k^{-3} part, form an additive spectrum. Additive spectrum had earlier been conjectured by Lumley [101] and Weinstock [176] for the case of stratified turbulence. As mentioned earlier, Weinstock [176] derived the temperature spectrum $B(k)$ from the correlation of fluctuating temperature field $\langle T'(\mathbf{k},t)T'(\mathbf{k}',t')\rangle$ (multiplied by a factor $(g/T_0)^2$ as mentioned in [176]), and obtained $B(k) \sim N^4k^{-3}$. In our derivation of the temperature spectrum, we get the correlation $\langle\psi(\mathbf{k},t)\psi(\mathbf{k}',t')\rangle \sim N^2k^{-5}$, so that we get $B(k) \sim N^2k^{-3}$. The apparent difference in the powers of N is due to the fact that our scalar field is related to the temperature fluctuation T' as $\psi(\mathbf{x},t) = (\beta g/N)T'(\mathbf{x},t)$.

Further, from Eq. (4.40), one can easily obtain that the anisotropic buoyancy spectrum goes like $k^{-7/3}$. Lumley [101] defined his buoyancy spectrum, $\zeta(k)$, as $\zeta(k) = g/T_0\langle u_3T'\rangle$, thereby obtained $\zeta(k) \sim N^2k^{-7/3}$ whereas, we calculated it from the $\langle u_3\psi\rangle$ correlation, yielding $k^{-7/3}$ spectrum multiplied by N. Thus, we see the usefulness of Leslie's suggestion of tackling such problems treating the anisotropy as a perturbation acting on the isotropic background field. This method is capable of producing not only the scaling relations but also the universal constants associated with such scaling laws.

It can be pointed out that, at sufficiently large scales, the anisotropic k^{-3} spectrum would dominate over the isotropic $k^{-5/3}$ spectrum. Thus we expect a k^{-3} power law behavior of energy spectrum at sufficiently large scales. It may be noted that this scenario is similar to the analysis of experimental investigations by Nastrom and Gage [115, 116], which shows approximately a k^{-3} power-law over the synoptic scales and a clear $k^{-5/3}$ power-law behaviour for the mesoscale. This observation triggered numerous hypothesis on the origin of these spectra, such as 2D turbulence with two sources of energy in which the inverse energy cascade from the small-scale forcing arises from a strong convection [92], or a breakup of internal gravity waves [35, 55], or it can result from an inverse cascade of inertia gravity waves [42]. Calculation of third order structure function [29], however, suggested a forward cascade of $k^{-5/3}$ spectrum in the mesoscale range. This also led to hypothesize about a direct energy cascade in a two-layer QG model [167], surface QG models [165, 150], and stratified turbulence simulations [18]. Further, it was also found, in experiments, that the presence of the strong condensate substantially reduces the efficiency of the spectral energy transfer via the inverse cascade process [180, 181]. However, there has been little theoretical development about this condensation phenomenon giving rise to the observed k^{-3} spectrum. As a future work, it would be worthwhile to carry out a detailed theoretical analysis on the basis of Bose-Einstein condensate to confirm the origin and nature of k^{-3} atmospheric spectrum.

We would also like to point out that, in a recent investigation by Lindborg [94], it is suggested that the mesoscale motions are not dominated by internal gravity waves, rather the observed atmospheric spectra are generated by a strongly nonlinear dynamics, and therefore, stratified turbulence with a forward cascade of energy would possibly be able to explain the atmospheric dynamics. From our above results, we may as well suggest that the synoptic scale k^{-3} energy spectrum arises due to anisotropic corrections in three-dimensional stratified turbulence. However, a far stronger theoretical effort will be required to obtain a more confident prediction, especially anisotropy

will need to be treated explicitly. We hope our present study shed some light to carry out further work along this line.

To carry out the problem further, a detailed theoretical investigations on this problem is performed employing Kraichnan's direct interaction approximation (DIA), and we present it in the following chapter.

However, before we conclude this section, it would be interesting to point out some marked similarities as well as differences of stably stratified turbulence with Rayleigh-Bénard convective (RBC) turbulence [3]. The equations governing RBC are identical to those governing stably stratified turbulence as given by Equations (4.12) to (4.14), the only difference being that the Rayleigh number (R) takes the place of Brunt-Väisälä frequency (N). However, in RBC, the energy spectrum goes like $k^{-11/5}$ instead of the k^{-3} of stratified turbulence for low wave numbers. In both cases there is a transition to the Kolmogorov spectrum ($k^{-5/3}$) at small scales. The differences in spectra in the low wave number regime can possibly be explained by the fact that the k^{-3} spectrum is produced when we treat the N dependent term as a perturbation. This means that the k^{-3} spectrum is obtained when the extra term is small. On the other hand, in the case of RBC, the $k^{-11/5}$ spectrum has been observed in a numerical simulation [109] for large Rayleigh numbers ($\sim 10^6$). This suggests that the dominance of the extra term in the dynamics gives rise to $k^{-11/5}$ spectrum. A perturbative treatment of the extra (large) term cannot be expected to yield the $k^{-11/5}$ spectrum which occurs for large Rayleigh numbers as suggested by the numerical simulation [109].

Chapter 5

Improved Treatment of Stably Stratified Turbulence

5.1 Introduction

As already discussed, stable stratification, arising from variation of temperature, salinity, or suspended particles, is common in the ocean and atmosphere [126, 136]. In the atmosphere and ocean, stratification and rotation are both important at large scales. As one moves downscale into the atmospheric mesoscale and oceanic sub-mesoscale, Coriolis effects weaken and stratification dominates [98, 96]. Owing to this, stably stratified turbulence was thought to serve as a model for important scales of atmospheric and oceanographic motion. The deviation from the celebrated Kolmogorov's universal $k^{-5/3}$ inertial-range energy (as well as temperature) spectrum [74] due to anisotropy of fluctuating motion in stratified turbulence is of much interest among researchers in the last few decades. It remains a major task to assess the effect of anisotropy and to seek its corrections.

Three-dimensional stratified turbulence seems to serve as a model for atmospheric and oceanic turbulence. From the atmospheric data (upper troposphere and lower stratosphere) collected by NASA instrumented commercial Boeing 747 airliners, Nastrom and Gage [115, 116] found that the atmospheric energy spectra follow the -3 power law in the range extending from 1000 to

3000 km (the "synoptic scales") and the $-5/3$ power law in the scales extending from 600 km down to a few kilometers (the "mesoscales") with a smooth transition in between. This spectrum was confirmed by MOSAIC program [40, 119], and high-resolution general circulation model (GCM) [158, 56] as well as mesoscale numerical weather prediction (NWP) models [148, 149].

Several hypothesis has been put forward to explain the observed atmospheric energy spectra. Attempts have been made using Kraichnan's two-dimensional turbulence [92] and Charney's [26] quasigeostrophic (QG) turbulence model. In order to confirm whether $k^{-5/3}$ power law arises either due to inverse energy cascade of 2D turbulence, or due to the direct cascade in 3D, a third-order velocity structure function was computed by Lindborg and Cho [29], based on MOSAIC program database. Their calculation suggested a downscale $k^{-5/3}$ energy cascade in the mesoscale, thereby casting doubt on the inverse cascade idea [92]. This led to hypothesize about a direct energy cascade in a two-layer QG model [167] and surface QG models [165, 150]. Tung and Orlando [167] proposed a two-level QG model and conjectured that the observed atmospheric energy spectrum results from the downscale cascade of enstrophy and energy injected at the large scales by baroclinic instability and dissipated at the smallest length scales. Tulloch and Smith [165, 150] demonstrated that, by limiting surface quasigeostrophic (SQG) flow to a finite depth (hence called finite-depth SQG (fSQG) model), one can obtain a natural transition scale, and when the flow is forced at large scale, the kinetic energy spectrum is -3 at larger scales and $-5/3$ at smaller scales with a transition scale $k_t \sim NH/f$, where N is the buoyancy frequency, f the Coriolis parameter, and H the depth of the fluid. Recently [166], they also proposed a two-mode two-surface (TMTS) model which captures all major types of baroclinic instabilities. They demonstrated that the surface dynamics at the tropopause can explain the transition to a shallow k^{-3} energy spectrum at sub-synoptic scales, consistent with the observed atmospheric kinetic energy spectrum.

Some of the earlier theoretical attempts for the explanation of the en-

ergy cascade process in the atmospheric turbulence involved internal gravity waves (IGW) [35, 168]. Recently, Gurvich and Chunchuzov [55] proposed a phenomenological model for the three-dimensional spectrum of temperature irregularities by introducing a variable anisotropy hypothesis into the earlier IGW theory of Chunchuzov [32]. They derived asymptotic expressions for the 3D vertical and horizontal temperature spectra, which produced the observed $k^{-5/3}$ and k^{-3} spectra. They further suggested that internal wave-wave interactions may contribute to the large scale k^{-3} spectra. All these theories of IGWs conjectured a direct energy cascade as in 3D turbulence. Although different models of the IGW spectrum in the atmosphere have been proposed, the applicability of the approximations used in modeling of the IGW spectrum is still debated [94].

Recently, various high-resolution numerical efforts have been carried out to investigate the atmospheric power spectra and its inherent relations with atmospheric instability and turbulence. Kitamura and Matsuda [72], in order to investigate the energy cascade process due to synoptic scale forcing, performed numerical experiments with a three-dimensional non-hydrostatic model (within Boussinesq approximation) of stratified turbulence, and found a downscale energy cascade on the tails of a steep synoptic scale spectrum. Recent direct numerical simulations of homogeneous turbulence with a strong and uniform stratification [18], in which three-dimensional Boussinesq equations and the transport equation for a passive gradient are solved employing pseudo-spectral code with periodic boundary conditions in all three directions, and with forcing in rotational and divergent modes, show that stratification may enforce a three-dimensional dynamics and the forward $k^{-5/3}$ energy cascade. In order to fully solve the problem of the origin of $k^{-5/3}$ mesoscale wavenumber energy spectra, Lindborg [98] carried out a set of numerical simulations of the full Boussinesq equations including system rotations, and thereby studied the effect of rotation on such an energy cascade, and have shown that it can prevail when rotation is sufficiently weak. In a companion paper by Lindborg [96], it is also shown that such a mesoscale spectrum can arise as

a result of forward energy cascade in the limit of strong stratification. The above evidences overwhelmingly points to the downscale transfer of mesoscale kinetic energy. Other investigations, endeavored to simulate strongly stratified vortical motions, also suggested the similar picture. Waite and Bartello [172] performed numerical simulations of stably stratified, vortically forced turbulence at various magnitudes of stratification, and obtained approximately a $k^{-5/3}$ spectrum of vortical energy. Further simulations of randomly forced internal gravity waves in a uniformly stratified Boussinesq fluid [173], yields a saturation spectrum close to k^{-3}.

Recent interest in the condensate state was motivated by experimental [139] and numerical [27] observations of large scale coherent vortices associated with energy condensation in forced, two dimensional bounded flow. It was suggested that the main energy at large scales is actually not in turbulent fluctuations but in a long-correlated flow (condensate), which can be either generated by external forces or appear in the process of spectral condensation in which the k^{-3} spectra arises due to the spectral condensation of inverse cascade and not as an enstrophy cascade [180, 181].

Recently, Lindborg [94] investigated the effect of vertical vorticity on the mesoscale motions, by constructing the two-point correlation of vertical and horizontal vorticities and their associated vorticity spectra from the second order structure functions calculated in Ref. [97], and found that the mesoscale motions are not dominated by internal gravity waves. He further suggested that atmospheric spectra are generated by a strongly nonlinear dynamics, and stratified turbulence with a forward cascade of energy would possibly be able to explain the atmospheric observations.

Although various theoretical, experimental, and numerical investigations have been made in the last few decades, understanding the source and structure of this atmospheric spectrum has posed a great puzzle in atmospheric science. The present study is motivated by the ambiguous connection between the stratified turbulence and atmospheric observations. Here, we will study the effect of anisotropy on turbulence statistics due to the presence of stable

temperature stratification with the help of a perturbation treatment akin to Kraichnan's [78] direct interaction approximation.

The (Eulerian) Direct interaction approximation (DIA), originally introduced and applied to incompressible homogeneous isotropic turbulence by Kraichnan [78], was the first "microscopic" theory of (three dimensional) turbulence [90] that resembles the Dyson-Schwinger formulation of quantum field theory [178, 64]. In fact, it was the first detailed field-theoretic approach to the theory of turbulence based on the underlying Navier-Stokes dynamics of fluid motion. However, the DIA in Eulerian framework was found to be inconsistent with the Kolmogorov $k^{-5/3}$ spectrum due to its failure to capture the correct time scales associated with the cascade from the time scales of sweeping of smaller eddies by the larger ones. Edwards [38] identified this failure due to the divergence in the response integral coming from the large scales of motion (low wavenumbers). Eulerian framework is unable to represent this effect of sweeping properly, and thereby fails to extract the small effect of Kolmogorov cascade among the small eddies from the large effect of their being swept around. As a result, it incorrectly yields a $k^{-3/2}$ spectrum instead of $k^{-5/3}$. To systematically eliminate this spurious effect of sweeping, Kraichnan reformulated the theory in a Lagrangian framework [81, 82]. Lagrangian version of DIA [82, 66, 71] give excellent predictions for various statistical quantities such as the Kolmogorov universal form of the energy spectrum function and the skewness of the velocity gradient. The universal Kolmogorov constant, C, calculated within this framework, was found to be $C = 1.43$ and 1.77 under two different schemes of calculations [82].

In Chapter 4, we treated the case of stably stratified turbulence by Leslie's perturbation procedure. This led to the anisotropic scaling laws appearing as additive corrections to the isotropic scaling laws. In this chapter, we would like to explore whether any improvement over such perturbation treatment is possible.

Thus we once again assume that the anisotropic buoyancy terms act as perturbations on the isotropic turbulent background fields. However, an im-

provement over Leslie's treatment is found to be possible when we treat the perturbation procedure similar to the direct interaction approximation (DIA) which was originally introduced and applied to homogeneous isotropic turbulence by Kraichnan [78]. This enables us to evaluate the corresponding corrections to various correlation functions up to leading order terms. Unlike the previous Leslie-type treatment, here we will see that the correction to the velocity-velocity and temperature-temperature correlations involve two extra terms each, signifying an improvement over the previous treatment. However, the velocity-temperature correlation remains the same as our previous Leslie-type calculations. We calculate the prefactors arising in the resulting anisotropic part of the energy and mean-square temperature spectra.

5.2 Mathematical Treatment

As introduced in Chapter 4, we start with the incompressible Navier-Stokes equation with Boussinesq approximation [87, 24]

$$\frac{\partial \mathbf{u}}{\partial t} + (\mathbf{u}\cdot\nabla)\,\mathbf{u} = \mathbf{f} - \frac{\nabla p'}{\rho} + \nu_0\nabla^2\mathbf{u} + N\psi\hat{e}_3 \tag{5.1}$$

$$\frac{\partial \psi}{\partial t} + (\mathbf{u}\cdot\nabla)\,\psi = \theta - Nu_3 + \kappa_0\nabla^2\psi \tag{5.2}$$

with the incompressibility condition

$$\nabla\cdot\mathbf{u} = 0 \tag{5.3}$$

Here $\mathbf{u}(\mathbf{x},t)$, $\psi(\mathbf{x},t)$ and $p'(\mathbf{x},t)$ are the velocity, scalar and pressure fluctuations; ν_0 and κ_0 are the kinematic viscosity and molecular diffusivity respectively. The Gaussian random forces, $\mathbf{f}(\mathbf{x},t)$ and $\theta(\mathbf{x},t)$, are introduced in order to maintain turbulence in a statistically steady state. The Brunt-Väisälä frequency N is given by $N^2 = \beta g(dT_0/dx_3)$, in which g is the acceleration due to gravity, $\beta = -(1/\rho_0)\,(\partial\rho/\partial T)_p$, is the thermal expansion coefficient (assumed to be positive) with ρ_0 is the reference density; T_0 is the mean temperature whose vertical gradient is assumed to be along $\hat{e}_3$ (anti-parallel to gravity).

The scalar field $\psi(\mathbf{x},t)$ is related with the fluctuating temperature field T' as $\psi = (\beta g/N)T'$.

In Eqs. (5.1) and (5.2), the extra terms involving N represent the coupling of scalar field ψ with the velocity field $\mathbf{u}$. We write Eqs. (5.1) and (5.2) in Fourier space as

$$\left(\frac{\partial}{\partial t}+\nu_0 k^2\right) u_i(\mathbf{k},t) + \frac{i}{2}P_{ijl}(\mathbf{k}) \sum_{\mathbf{p}+\mathbf{q}=\mathbf{k}} u_j(\mathbf{p},t)u_l(\mathbf{q},t) = f_i(\mathbf{k},t) + NP_{i3}(\mathbf{k})\psi(\mathbf{k},t) \tag{5.4}$$

$$\left(\frac{\partial}{\partial t}+\kappa_0 k^2\right) \psi(\mathbf{k},t) + i\,k_j \sum_{\mathbf{p}+\mathbf{q}=\mathbf{k}} u_j(\mathbf{p},t)\psi(\mathbf{q},t) = \theta(\mathbf{k},t) - Nu_3(\mathbf{k},t) \tag{5.5}$$

where the summation sign represents integrations on $\mathbf{p}$ and $\mathbf{q}$ with triad relation $\mathbf{p}+\mathbf{q}=\mathbf{k}$, and

$$P_{ijl}(\mathbf{k}) = k_j P_{il}(\mathbf{k}) + k_l P_{ij}(\mathbf{k})$$

$$P_{ij}(\mathbf{k}) = \delta_{ij} - k_i k_j/\mathbf{k}^2$$

We write, for simplicity

$$F_i(\mathbf{k},t) = f_i(\mathbf{k},t) + NP_{i3}(\mathbf{k})\psi(\mathbf{k},t)$$

$$\Theta(\mathbf{k},t) = \theta(\mathbf{k},t) - Nu_3(\mathbf{k},t)$$

Now following Kraichnan's method, we introduce the full response functions determining the velocity and scalar fields as

$$u_i(\mathbf{k},t) = \int_{-\infty}^{t} ds G_{ij}(\mathbf{k};t,s)F_j(\mathbf{k},s) \tag{5.6}$$

$$\psi(\mathbf{k},t) = \int_{-\infty}^{t} ds \mathcal{G}(\mathbf{k};t,s)\Theta(\mathbf{k},s) \tag{5.7}$$

in which $G_{ij}(\mathbf{k};t,s)$ and $\mathcal{G}(\mathbf{k};t,s)$ are the response functions.

We define the isotropic background fields as

$$u_i^{(0)}(\mathbf{k},t) = \int_{-\infty}^{t} ds G_{ij}^{(0)}(\mathbf{k};t,s)\, f_j(\mathbf{k},s) \tag{5.8}$$

$$\psi^{(0)}(\mathbf{k},t) = \int_{-\infty}^{t} ds \mathcal{G}^{(0)}(\mathbf{k};t,s)\,\theta(\mathbf{k},s) \tag{5.9}$$

and we follow Leslie's [90] suggestion of replacing the full response by the isotropic response, so that the full velocity and scalar fields are

$$u_i(\mathbf{k},t) = u_i^{(0)}(\mathbf{k},t) + N\int_{-\infty}^{t} ds G_{ij}^{(0)}(\mathbf{k};t,s)P_{j3}(\mathbf{k})\psi(\mathbf{k},s) \tag{5.10}$$

$$\psi(\mathbf{k},t) = \psi^{(0)}(\mathbf{k},t) - N\int_{-\infty}^{t} ds \mathcal{G}^{(0)}(\mathbf{k};t,s)u_3(\mathbf{k},s) \tag{5.11}$$

The full correlation functions, namely, the velocity correlation tensor $Q_{ij}(\mathbf{k},t,t')$, the scalar correlation $\Psi(\mathbf{k},t,t')$, and current $J_i(\mathbf{k};t,t')$, are defined as

$$\langle u_i(\mathbf{k},t)u_j(\mathbf{k}',t')\rangle = Q_{ij}(\mathbf{k};t,t')[2\pi]^3\delta^3(\mathbf{k}+\mathbf{k}') \tag{5.12}$$

$$\langle \psi(\mathbf{k},t)\psi(\mathbf{k}',t')\rangle = \Psi(\mathbf{k};t,t')[2\pi]^3\delta^3(\mathbf{k}+\mathbf{k}') \tag{5.13}$$

$$\langle \psi(\mathbf{k},t)u_i(\mathbf{k}',t')\rangle = J_i(\mathbf{k};t,t')[2\pi]^3\delta^3(\mathbf{k}+\mathbf{k}') \tag{5.14}$$

Now we substitute Eqs. (5.10) and (5.11) in Eqs. (5.12), (5.13) and (5.14) iteratively and obtain the expansions to the leading order

$$Q_{ij} = Q_{ij}^{(0)} + Q_{ij}^{(1)} + Q_{ij}^{(2)} + \cdots$$

$$\Psi = \Psi^{(0)} + \Psi^{(1)} + \Psi^{(2)} + \cdots$$

$$J_i = J_i^{(0)} + J_i^{(1)} + \cdots$$

where the superscripts denote the order in powers of N.

The isotropic correlation functions are

$$[2\pi]^3\delta^3(\mathbf{k}+\mathbf{k}')Q_{ij}^{(0)}(\mathbf{k};t,t') = \langle u_i^{(0)}(\mathbf{k},t)u_j^{(0)}(\mathbf{k}',t')\rangle \tag{5.15}$$

$$[2\pi]^3\delta^3(\mathbf{k}+\mathbf{k}')\Psi^{(0)}(\mathbf{k};t,t') = \langle \psi^{(0)}(\mathbf{k},t)\psi^{(0)}(\mathbf{k}',t')\rangle \tag{5.16}$$

$$J_i^{(0)}(\mathbf{k};t,t') = 0 \tag{5.17}$$

and we find that $Q_{ij}^{(1)} = 0$ and $\Psi^{(1)} = 0$.

The isotropic tensors have the properties

$$Q_{ij}^{(0)}(\mathbf{k};t;t') = Q^{(0)}(k;t,t')P_{ij}(\mathbf{k})$$

$$G_{ij}^{(0)}(\mathbf{k};t;t') = G^{(0)}(k;t,t')P_{ij}(\mathbf{k})$$

Using these properties, we find the leading order corrections to the correlation functions, due to the anisotropy, as

$$\begin{aligned} & Q_{ij}^{(2)}(\mathbf{k};t,t') \\ &= N^2 P_{i3}(\mathbf{k})P_{j3}(\mathbf{k}) \int_{-\infty}^{t} ds \int_{-\infty}^{t'} ds' G^{(0)}(k;t,s)G^{(0)}(k;t',s')\Psi^{(0)}(k;s,s') \\ &- N^2 P_{j3}(\mathbf{k})P_{i3}(\mathbf{k}) \int_{-\infty}^{t'} ds \int_{-\infty}^{s} ds' G^{(0)}(k;t',s)\mathcal{G}^{(0)}(k;s,s')Q^{(0)}(k;t,s') \\ &- N^2 P_{i3}(\mathbf{k})P_{j3}(\mathbf{k}) \int_{-\infty}^{t} ds \int_{-\infty}^{s} ds' G^{(0)}(k;t,s)\mathcal{G}^{(0)}(k;s,s')Q^{(0)}(k;s',t') \end{aligned} \tag{5.18}$$

$$\begin{aligned} \Psi^{(2)}(k;t,t') &= N^2 P_{33}(\mathbf{k}) \int_{-\infty}^{t} ds \int_{-\infty}^{t'} ds' \mathcal{G}^{(0)}(k;t,s)\mathcal{G}^{(0)}(k;t',s')Q^{(0)}(k;s,s') \\ &- N^2 P_{33}(\mathbf{k}) \int_{-\infty}^{t'} ds \int_{-\infty}^{s} ds' \mathcal{G}^{(0)}(k;t',s)G^{(0)}(k;s,s')\Psi^{(0)}(k;t,s') \\ &- N^2 P_{33}(\mathbf{k}) \int_{-\infty}^{t} ds \int_{-\infty}^{s} ds' \mathcal{G}^{(0)}(k;t,s)G^{(0)}(k;s,s')\Psi^{(0)}(k;s',t') \end{aligned} \tag{5.19}$$

and

$$\begin{aligned} J_i^{(1)}(k;t,t') &= NP_{i3}(\mathbf{k}) \int_{-\infty}^{t'} ds G^{(0)}(k;t',s)\Psi^{(0)}(k;t,s) \\ &- NP_{i3}(\mathbf{k}) \int_{-\infty}^{t} ds \mathcal{G}^{(0)}(k;t,s)Q^{(0)}(k;t',s) \end{aligned} \tag{5.20}$$

Thus we see that the leading order anisotropic corrections to the velocity-velocity and temperature-temperature correlation functions, given by Eqs.

(5.18) and (5.19), acquire two new terms (bearing negative signs) in addition to those which were obtained in our previous Leslie-type calculations (Chapter 4). However, the correction to the velocity-temperature correlation function, given by Eq. (5.20) remains the same as that of Leslie-type calculation.

Now, as suggested in Chapter 4, we evaluate the time integrals by assuming an exponential decay of the response and correlation functions [38], namely

$$G^{(0)}(k;t,t') = \theta(t-t')e^{-\eta(k)(t-t')}, \qquad Q^{(0)}(k;t,t') = Q^{(0)}(k)e^{-\eta(k)|t-t'|}$$
$$\mathcal{G}^{(0)}(k;t,t') = \theta(t-t')e^{-\zeta(k)(t-t')}, \qquad \Psi^{(0)}(k;t,t') = \Psi^{(0)}(k)e^{-\zeta(k)|t-t'|}$$

where $\theta(t-t')$ is the Heaviside step-function, $\eta(k)$ and $\zeta(k)$ are the eddy damping factors.

In order to calculate the equal time correlations, we set $t = t'$ in Eqs. (5.18), (5.19) and (5.20), and then the integrations are performed by choosing the proper region in the s-s' space as shown in Fig. 5.1. In Fig. 5.1(a), the region of integration is $s > s'$, in which s' varies from $-\infty$ to s and s varies from $-\infty$ to t. Similarly, in Fig. 5.1(b), the region of integration is $s < s'$, in which s' varies from s to t and s varies from $-\infty$ to t.

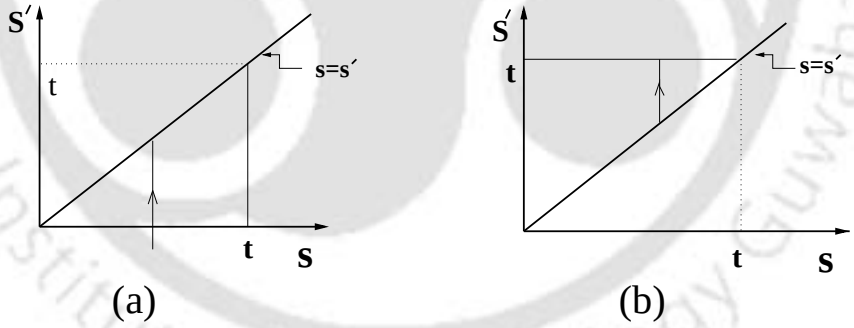

Figure 5.1: The region of integration for the time-integral expressions (5.18) and (5.19). The integration is performed (a) in the region $s > s'$ (the lower triangular region), ans (b) in the region $s < s'$ (the upper triangular region).

Thus, by evaluating the integrals, we obtain the equal-time leading order correction to the correlation functions from Eqs. (5.18), (5.19) and (5.20) as

$$Q_{ij}^{(2)}(k;t,t) = N^2 P_{i3}(\mathbf{k})P_{j3}(\mathbf{k})[2\pi]^3 a(k) \tag{5.21}$$

$$\Psi^{(2)}(k;t,t) = N^2 P_{33}(\mathbf{k})[2\pi]^3 b(k) \tag{5.22}$$

$$J_i^{(1)}(k;t,t) = N P_{i3}(\mathbf{k})[2\pi]^3 c(k) \tag{5.23}$$

with

$$a(k) = \frac{\Psi^{(0)}(k)}{\eta(k)\left[\eta(k)+\zeta(k)\right]} - \frac{Q^{(0)}(k)}{\eta(k)\left[\eta(k)+\zeta(k)\right]} \tag{5.24}$$

$$b(k) = \frac{Q^{(0)}(k)}{\zeta(k)\left[\zeta(k)+\eta(k)\right]} - \frac{\Psi^{(0)}(k)}{\zeta(k)\left[\zeta(k)+\eta(k)\right]} \tag{5.25}$$

$$c(k) = \frac{\Psi^{(0)}(k) - Q^{(0)}(k)}{\left[\eta(k)+\zeta(k)\right]} \tag{5.26}$$

Thus, under the present scheme of calculations, we see that the anisotropic corrections to the velocity-velocity and temperature-temperature correlations depend on the isotropic correlation functions in a more complicated fashion than in the earlier case of Leslie-type calculations (Chapter 4).

Now using the well known universal isotopic Kolmogorov Obukhov scaling [74, 121, 12, 33] for the energy and mean-square scalar, namely

$$E(k) = \frac{1}{[2\pi]^3} 4\pi k^2 Q^{(0)}(k) = C\varepsilon^{2/3}k^{-5/3}$$
$$\mathcal{E}(k) = \frac{1}{[2\pi]^3} 4\pi k^2 \Psi^{(0)}(k) = \mathrm{Ba}\ \chi\ \varepsilon^{-1/3}k^{-5/3}$$

and the eddy damping rates

$$\eta(k) = \alpha\ \varepsilon^{1/3}k^{2/3} \qquad \text{and} \qquad \zeta(k) = \beta\ \varepsilon^{1/3}k^{2/3}$$

we obtain

$$a(k) = \frac{1}{4\pi}\left[\frac{\mathrm{Ba}}{\alpha(\alpha+\beta)}\varepsilon^{-1}\chi - \frac{C}{\alpha(\alpha+\beta)}\right]k^{-5} \tag{5.27}$$

$$b(k) = \frac{1}{4\pi}\left[\frac{C}{\beta(\beta+\alpha)} - \frac{\mathrm{Ba}}{\beta(\alpha+\beta)}\varepsilon^{-1}\chi\right]k^{-5} \tag{5.28}$$

$$c(k) = \frac{1}{4\pi}\frac{\mathrm{Ba}\varepsilon^{-2/3}\chi - C\varepsilon^{1/3}}{\beta+\alpha}k^{-13/3} \tag{5.29}$$

Thus, we see once again that the scaling factors $a(k)$, $b(k)$ and $c(k)$, which are related with anisotropic parts of the velocity-velocity, temperature-temperature, and velocity-temperature correlations respectively, depend on ε, χ, and on the universal numbers C, Ba, α and β. The dependence, however, is now more complicated than that suggested by our previous Leslie-type calculations.

To evaluate these scaling factors, we use our previously calculated values of the universal numbers C, Ba, and σ (Chapter 3). As we calculated these numbers under two different schemes, namely with ϵ expansion and without ϵ expansion, here we carry out two sets of corresponding calculations for $a(k)$, $b(k)$ and $c(k)$.

Taking ϵ expansion values, namely $C = 1.4363$, Ba $= 1.031$, and $\sigma = 0.7179$, we get

$$\frac{\text{Ba}}{\alpha(\alpha+\beta)} = 1.9997, \quad \frac{C}{\beta(\beta+\alpha)} = 1.9997, \quad \frac{C}{\alpha(\beta+\alpha)} = 2.7855$$
$$\frac{C}{\alpha+\beta} = 1.2930, \quad \frac{\text{Ba}}{\alpha+\beta} = 0.9282, \quad \frac{\text{Ba}}{\beta(\alpha+\beta)} = 0.11418$$

When we substitute these values in Eqs. (5.27), (5.28), and (5.29), we finally obtain

$$a(k) = \left(0.15906\ \varepsilon^{-1}\chi - 0.22157\right) k^{-5} \tag{5.30}$$

$$b(k) = \left(0.15906 - 0.11418\ \varepsilon^{-1}\chi\right) k^{-5} \tag{5.31}$$

$$c(k) = \left(0.07383\ \varepsilon^{-2/3}\ \chi - 0.10285\ \varepsilon^{1/3}\right) k^{-13/3} \tag{5.32}$$

Further, with no ϵ expansion values, namely $C = 1.5618$, $\sigma = 0.61351$, and Ba $= 0.9583$, we obtain

$$\frac{\text{Ba}}{\alpha(\alpha+\beta)} = 2.0001, \quad \frac{C}{\beta(\beta+\alpha)} = 2.0001, \quad \frac{C}{\alpha(\beta+\alpha)} = 3.2594$$
$$\frac{C}{\alpha+\beta} = 1.3914, \quad \frac{\text{Ba}}{\alpha+\beta} = 0.8537, \quad \frac{\text{Ba}}{\beta(\alpha+\beta)} = 1.22718$$

which gives

$$a(k) = \left(0.15908\ \varepsilon^{-1}\chi - 0.25928\right) k^{-5} \tag{5.33}$$

$$b(k) = \left(0.15908 - 0.097618\ \varepsilon^{-1}\chi\right) k^{-5} \tag{5.34}$$

$$c(k) = \left(0.06790\ \varepsilon^{-2/3}\ \chi - 0.11067\ \varepsilon^{1/3}\right) k^{-13/3} \tag{5.35}$$

Thus, from our above analysis, it is obvious that the anisotropic part of the velocity-velocity and temperature-temperature correlations are

$$Q_{ij}^{(2)}(k;t,t) = a_1 N^2 P_{i3}(\mathbf{k}) P_{j3}(\mathbf{k}) k^{-5}$$

$$\Psi^{(2)}(k;t,t) = a_2 N^2 P_{33}(\mathbf{k}) k^{-5}$$

and velocity-temperature correlation is

$$J_i^{(1)}(k;t,t) = a_3 N P_{i3}(\mathbf{k}) k^{-13/3}$$

Here we note that the prefactors a_1, a_2, and a_3, which depend on ε, χ, C, Ba, and σ are radically different than C_1, C_2 and C_3 found in Leslie-type calculations in Chapter 4.

Further, similar to Chapter 4, the correlation functions reproduce the anisotropic energy and mean-square scalar spectra as k^{-3} and the anisotropic buoyancy spectrum as $k^{-7/3}$.

5.3 Conclusion

In this chapter, we make an effort to calculate the universal amplitudes associated with the three-dimensional stably stratified turbulence, by making a perturbative expansion similar to the Kraichnan's DIA. This allowed us to derive the leading order anisotropic corrections to the velocity-velocity, temperature-temperature, and velocity-temperature correlation functions as given in Eqs.

(5.18), (5.19), and (5.20). Here, we have seen that, unlike our previous Leslie-type perturbative treatment, the velocity-velocity and temperature-temperature correlations acquire new terms, indicating an improvements over the previous treatment. We evaluated these time integrals by choosing a proper region in s-s' space which yields the anisotropic corrections to the equal-time velocity-velocity, temperature-temperature, and the velocity-temperature correlation as given by Eqs. (5.21), (5.22), and (5.23). We have seen that, the scaling factors $a(k)$, $b(k)$, and $c(k)$ depend on the isotropic correlation functions in a more complicated fashion than in the earlier case of Leslie-type calculations. Moreover, we have also seen that, the correction to the velocity-temperature correlation function, given by Eq. (5.20) remains the same as that of Leslie-type calculation.

The prefactors a_1, a_2, and a_3 are found to depend on ε, χ, Batchelor constant Ba, Prandtl number σ, and Kolmogorov constant C. We further offered a set of calculation of the prefactors, based on our previous calculations of Batchelor constant, Kolmogorov constant and the turbulent Prandtl number. To our knowledge, neither experiments nor numerical simulations have been devoted so far to find out the universal functions, which can be compared directly with the present results. Further comparison with those data would be necessary to explore some important insight into the thermal and mechanical processes at work in the flow.

Since the correlation functions contain a rich information about the global and local structure of turbulent flows, our investigation of scaling behavior and estimation of anisotropy in terms of few scalar functions in stably stratified turbulence, seems to be useful for the parameter determinations in future DNS, experiments and stratified turbulence modeling.

It turns out that the above formalism provides a convenient way of disentangling isotropic and anisotropic effects in stratified turbulence. It can also be used to study other anisotropic numerically simulated or experimental flows. For this purpose, the buoyancy forcing terms in the equation of motion should be replaced by any appropriate anisotropic forcing mechanism. We

conclude by noting that this work can further be extended for more realistic case, namely rotating stratified turbulence [105, 73], in which the Coriolis effect is prominent. We leave it for further work in future.

Our calculations, within this framework, yield the anisotropic energy and mean-square scalar spectra as k^{-3} and the anisotropic buoyancy spectrum as $k^{-7/3}$. We note that, at sufficiently large scales, the anisotropic k^{-3} spectrum would dominate over the isotropic $k^{-5/3}$ spectrum. Thus we expect a k^{-3} power law behavior of energy spectrum at sufficiently large scales. It may be noted that this scenario is similar to the Nastrom and Gage [115, 116], who analyzed the atmospheric data, collected during the Global Atmospheric Sampling Program (GASP), and obtain a $k^{-5/3}$ spectrum in the mesoscale and k^{-3} in the synoptic scale. Following this, various hypothesis on the origin of the spectra have been proposed, such as 2D turbulence with two sources [92], internal gravity waves [35, 55]. Calculation of third order structure function [29] suggested a forward cascade of $k^{-5/3}$ spectrum in the mesoscale range. This also led to hypothesize about a direct energy cascade in a two-layer quasigeostrophic (QG) model [167], surface QG models [165, 150], stratified turbulence simulations [18], and spectral condensation of 2D turbulence [180, 181]. However, our calculation supports the additive spectrum previously proposed by Tung and Orlando [167].

Chapter 6

Dynamic Renormalization Group Analysis of Stably Stratified Turbulence

6.1 Introduction

Stratified flows encountered in the atmosphere, ocean and lakes, has long been treated as a challenging problem in geophysical or astrophysical applications, and has been extensively studied because of their relevance to engineering problems [155, 62, 54, 91, 157]. The dynamics of freely evolving turbulence under the influence of buoyancy forces is of great importance to the understanding of atmospheric and oceanic turbulence [96]. In the presence of gravity, the flow develops a preferred direction and exhibits anisotropy. The degree of anisotropy depends on the strength of the gravitational field. Density stratification in atmospheric boundary layers [147, 162] and salt stratification in oceanic mixed layers [54] may be considered to be stable which tends to reduce the vertical mixing leading to the development of spatial anisotropy.

Observations in the atmosphere and ocean have motivated a number of theories of stratified turbulence. The atmospheric mesoscale kinetic energy and temperature spectra, obtained from the atmospheric observation [115, 116], shows a $k^{-5/3}$ power law behavior. The cascade of energy from large to

small scales in stably stratified fluids has been confirmed by many independent studies [96, 72, 172, 135].

In this chapter, we are going to take the approach of renormalization group (RG) to the problem of stably stratified turbulence. The dynamic renormalization group theory was employed by Forster, Nelson and Stephen[43] in the case of Navier-stokes fluid along with the coupled problem of the advection of a passive scalar, the dynamics being driven by random stirring force fields. They were motivated by the RG treatment of Ma and Mazenko [103] in critical phenomena. A generalization of the randomly stirred model was subsequently offered by DeDominicis and Martin [34] which resembled the Kolmogorov turbulence more closely. Later this randomly stirred model was applied by Yakhot and Orszag [184, 183] which enabled them to calculate various universal amplitudes associated with high Reynolds number (Kolmogorov) turbulence (including the case of a passive scalar). The agreement of these numbers with the experimentally measured ones was very close.

Afterwards, extensive theoretical research on turbulence has been carried out similar to Yakhot-Orszag RG treatment. Carati and Brenig [22] studied the Navier-Stokes equations and the evolution of a scalar field for an anisotropically stirred fluid through RG scheme and evaluated the resulting corrections to the turbulent Prandtl number. Using an essentially different RG procedure than Yakhot and Orszag, Elperin and Kleeorin [39] studied the problem of passive scalar convection in turbulent fluid flow in the presence of an external gradient of passive scalar concentration, in which the passive scalar fluctuations are assumed to be excited by tangling of an external gradient of mean passive scalar field by a turbulent velocity field. In this analysis, the turbulent Prandtl number σ for large Reynolds number was estimated to be $\sigma \approx 0.792$. Buša et al. [19] performed an RG analysis of randomly stirred fluid with anisotropic distribution of random force, and thereby evaluated the Kolmogorov constant and the amplitude of longitudinal and transverse projection operators with respect to the preferred direction in the energy spectrum. Machiels [104] studied numerically the randomly forced turbulent systems with

hyperviscous dissipation, and computed the eddy viscosity and the correction to the forcing induced by scale elimination. This study suggested that there is an intermediate range for the energy spectrum in between inertial range and dissipative range characterized by a reduction of the eddy viscosity and a correction to the forcing representing a backward energy flux. Applying recursive RG scheme together with the quasinormal approximation, Lin et al. [93] investigated the thermal turbulent transport properties and offered an estimation for the Prandtl number and Batchelor constant which were shown to depend on several characteristic wavenumbers of the particular flow under consideration. Verma [169] performed a field theoretic RG calculation of renormalized viscosity, resistivity, and energy fluxes of non helical magneto hydrodynamic (MHD) turbulence, in which Kolmogorov $k^{-5/3}$ power law was shown to be a consistent solution for $d \geqslant d_c \approx 2.2$. In addition, various cascade rates and Kolmogorov constant were calculated within this framework by solving numerically the flux equation to first order in the perturbation series. Considering a simple hypothesis that large scale eddies are statistically independent of those of smaller eddies [107], Chang et al. [25] performed an RG analysis on Navier-Stokes equation and obtained an inhomogeneous ordinary differential equation for the invariant effective eddy-viscosity, the closed form solution of which yields the Kolmogorov constant in the ranges $C \approx 1.35 - 2.06$. Using field theoretic RG technique, Adzhemyan et al. [2] calculated the turbulent Prandtl number in a two-loop approximation of the ϵ expansion. It was shown that the difference between the one-loop and two-loop result for the Batchelor constant was small. However, the Kolmogorov constant and Skewness factor showed greater deviations between the one-loop and two-loop values.

Here we use a dynamic RG scheme up to one-loop order to achieve a coarse-grained description of turbulent flow field with a stable temperature stratification via successive elimination of small shells of modes from the ultraviolet (UV) end of wavenumbers. The scale elimination procedure generate corrections to the viscosity and diffusivity at successive stages of the procedure. Due to the presence of anisotropy, the perturbative RG treatment of this

problem involves many extra Feynman diagrams along with those of Yakhot and Orszag's [183]. We find that, apart from the usual isotropic viscosity and diffusivity terms ($\nu_0 k^2$ and $\kappa_0 k^2$), there appear different terms ($\nu_3 k_3^2$ and $\kappa_3 k_3^2$) corresponding to the vertical motion. This gives rise to a very complicated RG analysis. However, in the limit of weak stratification, the stability analysis of the flow equations can be performed with less difficulty. It is found that the Kolmogorov scaling regime exists and thus it is expected that the energy cascade at small scales would be Kolmogorovian as conjectured by Kolmogorov.

6.2 The Randomly Stirred Model

As we have seen previously, the dynamics of an incompressible randomly forced stably stratified turbulence in the Boussinesq approximation can be expressed as

$$\frac{\partial \mathbf{u}}{\partial t} + (\mathbf{u}\cdot\nabla)\,\mathbf{u} = \mathbf{f} - \frac{\nabla p'}{\rho} + \nu_0 \nabla^2 \mathbf{u} + N\psi \hat{e}_3 \tag{6.1}$$

$$\frac{\partial \psi}{\partial t} + (\mathbf{u}\cdot\nabla)\,\psi = \theta - N u_3 + \kappa_0 \nabla^2 \psi \tag{6.2}$$

with the incompressibility condition

$$\nabla\cdot\mathbf{u} = 0 \tag{6.3}$$

Here $\mathbf{u}(\mathbf{x},t)$, $\psi(\mathbf{x},t)$, and $p'(\mathbf{x},t)$ are the fluctuating velocity, temperature, and pressure fields with zero mean; ν_0 and κ_0 are the kinematic viscosity and molecular diffusivity respectively; as usual the Gaussian random forces $\mathbf{f}(\mathbf{x},t)$ and $\theta(\mathbf{x},t)$ are introduced in order to maintain turbulence in a statistically steady state. The Brunt-Väisälä frequency N is given by $N^2 = \beta g(dT_0/dx_3)$ in which T_0 is the mean temperature whose vertical gradient is assumed to be along $\hat{e}_3$ (anti-parallel to gravity), g is the acceleration due to gravity, and $\beta = -(1/\rho_0)\,(\partial\rho/\partial T)_p$, is the thermal expansion coefficient (assumed to be positive) with T and ρ are the temperature and density fields respectively. The scalar field $\psi(\mathbf{x},t)$ is related with the fluctuating temperature field T' as $\psi = (\beta g/N)T'$.

The corresponding $(d+1)$-dimensional Fourier transformed equations take the forms

$$\left(-i\omega+\nu_0 k^2\right) u_i(\mathbf{k},\omega) = f_i(\mathbf{k},\omega) + \alpha_0 N P_{i3}(\mathbf{k})\psi(\mathbf{k},\omega) - \frac{i\lambda_0}{2} P_{ijl}(\mathbf{k}) \int_0^\infty \frac{d^d\mathbf{q}}{[2\pi]^d} \int_{-\infty}^\infty \frac{d\omega'}{[2\pi]} u_j(\mathbf{q},\omega') u_l(\mathbf{p},\omega'') \quad (6.4)$$

and

$$\left(-i\omega+\mu_0 k^2\right) \psi(\mathbf{k},\omega) = \theta(\mathbf{k},\omega) - \beta_0 N u_3(\mathbf{k},\omega) - i\bar{\lambda}_0 k_j \int_0^\infty \frac{d^d\mathbf{q}}{[2\pi]^d} \int_{-\infty}^\infty \frac{d\omega'}{[2\pi]} u_j(\mathbf{q},\omega') \psi(\mathbf{p},\omega'') \quad (6.5)$$

along with the incompressibility condition

$$k_i u_i(\mathbf{k},\omega) = 0, \quad (6.6)$$

in which $P_{ijl}(\mathbf{k}) = k_j P_{il}(\mathbf{k}) + k_l P_{ij}(\mathbf{k})$, with the projection operator $P_{ij}(\mathbf{k}) = \delta_{ij} - k_i k_j/\mathbf{k}^2$, $\mathbf{p}+\mathbf{q} = \mathbf{k}$, $\omega'+\omega'' = \omega$, the formal parameter λ_0, $\bar{\lambda}_0$, α_0, and β_0 are introduced in order to construct perturbation expansions. An ultraviolet cutoff at a wavenumber Λ to the wave-vector integration is assumed, corresponding to the internal viscous cutoff. Here, both the velocity and temperature fields are modeled as being driven by the random stirring force fields $f_i(\mathbf{k},\omega)$ and $\theta(\mathbf{k},\omega)$, both of which are assumed to have Gaussian white-noise statistics with correlations

$$\langle f_i(\mathbf{k},\omega) f_j(\mathbf{k}',\omega')\rangle = F(k) P_{ij}(\mathbf{k}) [2\pi]^d \delta^d(\mathbf{k}+\mathbf{k}') [2\pi]\delta(\omega+\omega') \quad (6.7)$$

$$\langle \theta(\mathbf{k},\omega)\theta(\mathbf{k}',\omega')\rangle = \Theta(k) [2\pi]^d \delta^d(\mathbf{k}+\mathbf{k}') [2\pi]\delta(\omega+\omega') \quad (6.8)$$

in which $F(k)$ and $\Theta(k)$ are modeled as

$$F(k) = 2D_0 k^{-y} \quad (6.9)$$

$$\Theta(k) = 2\mathcal{D}_0 k^{-y'} \quad (6.10)$$

with $y > -2$ and $y' > -2$. The cases $y = -2$ and $y' = -2$ correspond to equilibrium situations where fluctuation-dissipation theorem holds [43].

6.3 Perturbative dynamic RG

The dynamic RG scheme, a self-consistent coarse-graining procedure, consists of eliminating the ultraviolet (UV) modes $u^>(\mathbf{k},\omega)$ and $\psi^>(\mathbf{k},\omega)$ from thin shells of wavenumbers (belonging to the range $\Lambda e^{-r} < k < \Lambda$) starting from the UV end, by means of integrating away these modes. This elimination process affects the infrared (IR) modes $u^<(\mathbf{k},\omega)$ and $\psi^<(\mathbf{k},\omega)$ (belonging to the range $0 < k < \Lambda e^{-r}$). The net effect is that the transport constants ν_0 and κ_0, and the coupling constants α_0 and β_0 acquire corrections due to the elimination process. For the present problem of stratified turbulence, we find that the elimination process generates additional viscosity and diffusivity corrections due to the anisotropy. These eddy viscosities and diffusivites are calculated analytically in the case of weak stratification.

We start RG treatment with eliminating the fast modes $u^>(\mathbf{k},\omega)$ and $\psi^>(\mathbf{k},\omega)$ lying in the band $\Lambda e^{-r} < k < \Lambda$ leading to an equation for slow modes $u^<(\mathbf{k},\omega)$ and $\psi^<(\mathbf{k},\omega)$ belonging to $0 < k < \Lambda e^{-r}$ given by

$$\left(-i\omega + \nu_0 k^2\right) u_i^<(\mathbf{k},\omega) = f_i^<(\mathbf{k},\omega) + \alpha_0 P_{i3}(\mathbf{k}) N \psi^<(\mathbf{k},\omega)$$
$$-\frac{i\lambda_0}{2} P_{ijl}(\mathbf{k}) \int_q \frac{d^d\mathbf{q}}{[2\pi]^d} \int_{-\infty}^{\infty} \frac{d\omega'}{[2\pi]} u_j^<(\mathbf{q},\omega') u_l^<(\mathbf{p},\omega'') + R_i(\mathbf{k},\omega) + S_{i3}(\mathbf{k},\omega) \tag{6.11}$$

and

$$\left(-i\omega + \kappa_0 k^2\right) \psi^<(\mathbf{k},\omega) = \theta^<(\mathbf{k},\omega) - \beta_0 N u_3^<(\mathbf{k},\omega)$$
$$-i\bar{\lambda}_0 k_j \int_q \frac{d^d\mathbf{q}}{[2\pi]^d} \int_{-\infty}^{\infty} \frac{d\omega'}{[2\pi]} u_j^<(\mathbf{q},\omega') \psi^<(\mathbf{p},\omega'') + R(\mathbf{k},\omega) + T(\mathbf{k},\omega) \tag{6.12}$$

with

$$R_i(\mathbf{k},\omega) = -\Sigma_{in}^A(\mathbf{k},\omega) u_n^<(\mathbf{k},\omega) \tag{6.13}$$

$$S_{i3}(\mathbf{k},\omega) = -\Sigma_{i3}^B(\mathbf{k},\omega)\ \psi^<(\mathbf{k},\omega) \tag{6.14}$$

$$R(\mathbf{k},\omega) = -\Sigma^C(\mathbf{k},\omega) \psi^<(\mathbf{k},\omega) \tag{6.15}$$

$$T(\mathbf{k},\omega) = -\Sigma_{n3}^D(\mathbf{k},\omega) u_n^<(\mathbf{k},\omega) \tag{6.16}$$

The terms $R_i(\mathbf{k},\omega)$ and $R(\mathbf{k},\omega)$, when taken on to the left-hand sides in Eqs. (6.11) and (6.12), gives correction to the bare viscosity ν_0 and bare diffusivity κ_0. These terms arise from the one-loop self energy terms $\Sigma^A_{in}(\mathbf{k},\omega)$ and $\Sigma^C(\mathbf{k},\omega)$ respectively. The terms $S_{i3}(\mathbf{k},\omega)$ and $T(\mathbf{k},\omega)$ give rise to corrections to the bare "vertices" α_0 and β_0. The corresponding Feynman diagrams for integral equations (6.11) and (6.12) are shown in Fig. 6.1 with the vertices $\lambda_0, \bar{\lambda}_0$, α_0, and β_0. We introduce the following diagrammatic notations:

$$-\frac{i\lambda_0}{2}P_{ijl}(\mathbf{k})\int\frac{d^dq}{[2\pi]^d} \equiv \bigcirc \qquad \alpha_0 N P_{i3}(\mathbf{k}) \equiv \bullet$$

$$-i\bar{\lambda}_0 k_j \int\frac{d^dq}{[2\pi]^d} \equiv \square \qquad -\beta_0 N \equiv \blacksquare$$

$$f_i(\mathbf{k},\omega) \equiv \times \qquad \theta(\mathbf{k},\omega) \equiv \mathsf{T}$$

$$G_0(\mathbf{k},\omega) \equiv \longrightarrow \qquad H_0(\mathbf{k},\omega) \equiv \cdots\!\!\rightarrow\!\!\cdots$$

There is a conservation of four-wave-vectors at each vertex so that $\mathbf{p}+\mathbf{q}=\mathbf{k}$ and $\omega'+\omega''=\omega$.

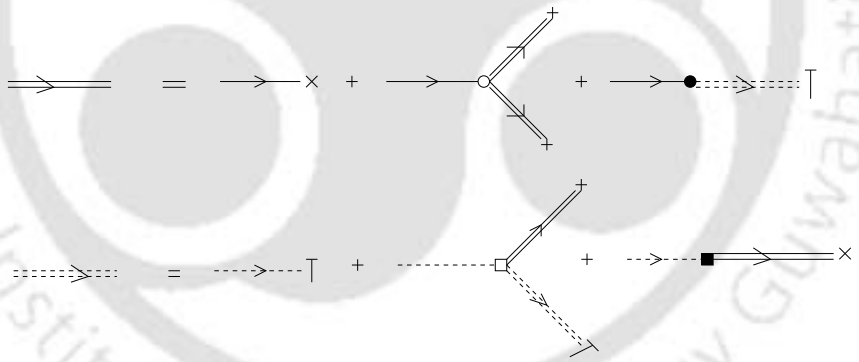

Figure 6.1: Diagrammatic representation of the equations (6.11) and (6.12).

As the calculation of the RG elimination process for Eqs. (6.4) and (6.5) is tedious, we follow standard diagrammatic procedures [43, 178], and here we only present the important results.

Fig. 6.2 shows the Feynman diagrams for self-energy, $\Sigma^A_{in}(\mathbf{k},\omega)$ which represent corrections to the bare viscosity. They consist of seven self energy diagrams out of which three involve velocity-velocity correlation and the other

four temperature-temperature correlation. They give rise to the self-energy term

$$\Sigma^A_{in}(\mathbf{k},\omega) = \lambda_0^2 P_{ijl}(\mathbf{k}) \int \frac{d\hat{q}}{[2\pi]^{d+1}} |G_0(\hat{q})|^2 G_0(\hat{p}) P_{lmn}(\mathbf{p}) P_{jm}(\mathbf{q}) F(q)$$
$$+ \lambda_0 \bar{\lambda}_0 \alpha_0^2 N^2 P_{ijl}(\mathbf{k}) \int \frac{d\hat{q}}{[2\pi]^{d+1}} G_0(\hat{q}) G_0(\hat{p}) |H_0(\hat{q})|^2 \times H_0(\hat{p})\ p_n P_{j3}(\mathbf{q}) P_{l3}(\mathbf{p}) \Theta(q)$$
$$- \lambda_0^2 \alpha_0 \beta_0 N^2 P_{ijl}(\mathbf{k}) \int \frac{d\hat{q}}{[2\pi]^{d+1}} |G_0(\hat{q})|^2 G_0(\hat{p}) H_0(\hat{q}) \times G_0(\hat{q}) P_{lmn}(\mathbf{p}) P_{j3}(\mathbf{q}) P_{m3}(\mathbf{q}) F(q)$$
$$+ \lambda_0^2 \alpha_0^2 N^2 P_{ijl}(\mathbf{k}) \int \frac{d\hat{q}}{[2\pi]^{d+1}} |G_0(\hat{q})|^2 G_0(\hat{p}) |H_0(\hat{q})|^2 \times P_{lmn}(\mathbf{p}) P_{j3}(\mathbf{q}) P_{m3}(\mathbf{q}) \Theta(q)$$
$$- \lambda_0 \bar{\lambda}_0 \alpha_0 \beta_0 N^2 P_{i3}(\mathbf{k}) H_0(\hat{k}) \int \frac{d\hat{q}}{[2\pi]^{d+1}} |G_0(\hat{p})|^2 G_0(\hat{q}) \times H_0(\hat{p}) k_j P_{jmn}(\mathbf{q}) P_{m3}(\mathbf{p}) F(p)$$
$$+ \bar{\lambda}_0^2 \alpha_0^2 N^2 P_{i3}(\mathbf{k}) H_0(\hat{k}) \int \frac{d\hat{q}}{[2\pi]^{d+1}} |H_0(\hat{q})|^2 G_0(\hat{q}) H_0(\hat{p}) k_j p_n P_{j3}(\mathbf{q}) \Theta(q)$$
$$+ \bar{\lambda}_0^2 \alpha_0^2 N^2 P_{i3}(\mathbf{k}) H_0(\hat{k}) \int \frac{d\hat{q}}{[2\pi]^{d+1}} |H_0(\hat{p})|^2 G_0(\hat{q}) \times H_0(\hat{q}) k_j q_n P_{j3}(\mathbf{q}) \Theta(p) \quad (6.17)$$

where

$G_0(\hat{q}) \equiv G_0(q,\omega) = \left(-i\omega + \nu_0 q^2\right)^{-1}$ and $H_0(\hat{q}) \equiv H_0(q,\omega) = \left(-i\omega + \kappa_0 q^2\right)^{-1}$

are bare propagators. It may be noted that we are considering terms up to $O(N^2)$ in our calculations.

In Fig.6.3 we show the Feynman diagrams for correction to "vertex" α_0 which can be expressed as

$$\Sigma^B_{i3}(\mathbf{k},\omega) = \lambda_0 \bar{\lambda}_0 \alpha_0 N P_{ijl}(\mathbf{k}) \int \frac{d\hat{q}}{[2\pi]^{d+1}} |G_0(\hat{q})|^2 G_0(\hat{p}) H_0(\hat{p})\ p_m P_{jm}(\mathbf{q}) P_{l3}(\mathbf{p}) F(q)$$
$$+ \bar{\lambda}_0^2 \alpha_0 N P_{i3}(\mathbf{k}) H_0(\hat{k}) \int \frac{d\hat{q}}{[2\pi]^{d+1}} |G_0(\hat{q})|^2 H_0(\hat{p})\ k_j\ p_l P_{jl}(\mathbf{q}) F(q) \quad (6.18)$$

The bare diffusivity κ_0 acquires correction from the four Feynman diagrams shown in Fig. 6.4. These corrections are found to be

$$\Sigma^C(\mathbf{k},\omega) = \bar{\lambda}_0^2\ k_j \int \frac{d\hat{q}}{[2\pi]^{d+1}} |G_0(\hat{q})|^2 H_0(\hat{p})\ p_l P_{jl}(\mathbf{q}) F(q)$$
$$- \bar{\lambda}_0^2 \alpha_0 \beta_0 N^2\ k_j \int \frac{d\hat{q}}{[2\pi]^{d+1}} |G_0(\hat{q})|^2 G_0(\hat{q}) H_0(\hat{q}) H_0(\hat{p})\ p_l P_{j3}(\mathbf{q}) P_{l3}(\mathbf{q}) F(q)$$

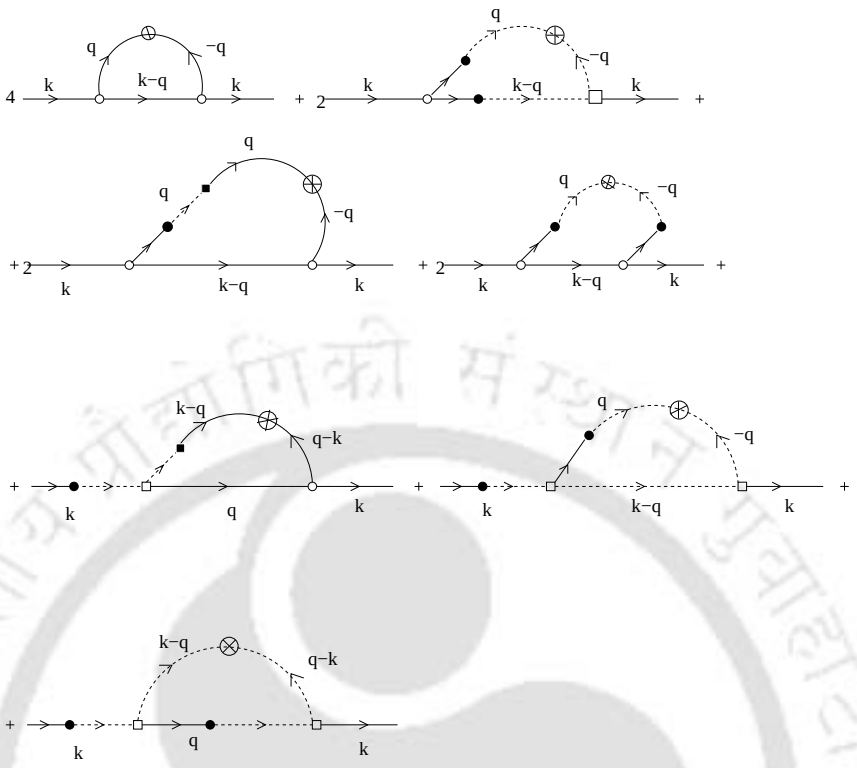

Figure 6.2: One-loop Feynman diagrams for self-energy $\Sigma^A_{in}(\mathbf{k},\omega)$, giving corrections to the bare viscosity. The curved solid lines represent the velocity correlation, and the curved dotted lines the temperature correlation. $\otimes$ represents noise-noise correlation. Note that the 4th and the last diagram are obtained by two iterations in the perturbation expansion. The analytical expressions are given in Eq. (6.17).

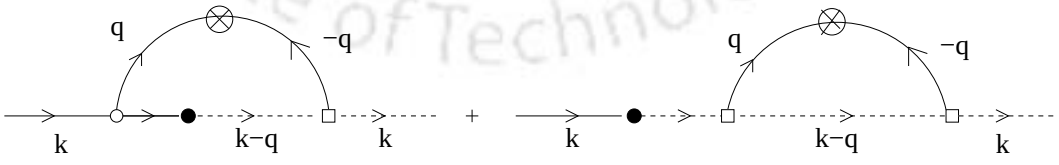

Figure 6.3: One-loop Feynman diagrams for self-energy $\Sigma^B(\mathbf{k},\omega)$, giving correction to the vertex, α_0. The analytical expressions are given in Eq. (6.18).

$$- \quad \bar{\lambda}_0^2 \alpha_0 \beta_0 N^2 \; k_j \int \frac{d\hat{q}}{[2\pi]^{d+1}} |G_0(\hat{p})|^2 G_0(\hat{q}) H_0(\hat{q}) H_0(\hat{p}) \; q_n P_{j3}(\mathbf{q}) P_{n3}(\mathbf{p}) F(p)$$

$$- \quad \bar{\lambda}_0^2 \alpha_0 \beta_0 N^2 \; k_j \int \frac{d\hat{q}}{[2\pi]^{d+1}} |G_0(\hat{q})|^2 G_0(\hat{p}) H_0^2(\hat{p}) \; p_n P_{jn}(\mathbf{q}) P_{33}(\mathbf{p}) F(q) \quad (6.19)$$

The vertex β_0 undergoes corrections due to the four Feynman diagrams in Fig. 6.5. These corrections take the form

$$\begin{aligned}
\Sigma_{i3}^D(\mathbf{k},\omega) = & \; \bar{\lambda}_0^2 \alpha_0 N \; k_j \int \frac{d\hat{q}}{[2\pi]^{d+1}} |H_0(\hat{q})|^2 G_0(\hat{q}) H_0(\hat{p}) \; p_n P_{j3}(\mathbf{q}) \Theta(q) \\
& + \quad \bar{\lambda}_0^2 \alpha_0 N \; k_j \int \frac{d\hat{q}}{[2\pi]^{d+1}} |H_0(\hat{p})|^2 G_0(\hat{q}) H_0(\hat{q}) \; q_n P_{j3}(\mathbf{q}) \Theta(p) \\
& - \quad \lambda_0 \bar{\lambda}_0 \beta_0 N \; k_j \int \frac{d\hat{q}}{[2\pi]^{d+1}} |G_0(\hat{q})|^2 G_0(\hat{p}) H_0(\hat{p}) P_{3ln}(\mathbf{p}) P_{jl}(\mathbf{q}) F(q) \\
& - \quad \lambda_0 \bar{\lambda}_0 \beta_0 N \; k_j \int \frac{d\hat{q}}{[2\pi]^{d+1}} |G_0(\hat{p})|^2 G_0(\hat{q}) H_0(\hat{p}) P_{jmn}(\mathbf{q}) P_{m3}(\mathbf{p}) F(p)
\end{aligned} \quad (6.20)$$

6.4 Effective Viscosities and Diffusivities

Due to the anisotropy introduced by stable temperature stratification, both the viscosity and diffusivity acquire corrections as shown in the previous section. In addition to the correction to the original terms $\nu_0 k^2$ and $\kappa_0 k^2$, two new correction terms, namely $\nu_3 k_3^2$ and $\kappa_3 k_3^2$ are generated.

By doing proper symmetrization [114] of self-energy integrals with respect to internal wave-vectors p and q, and taking large-scale long-time ($k \to 0$, $\omega \to 0$) limit, we simplify the self energy integrals which give rise to the relevant correction to the bare propagators, that, in turn, provide corrections to the bare viscosities, bare diffusivities, and the bare vertices α_0 and β_0. As a result, the bare propagator $G_{ij}^{(0)}(\mathbf{k},\omega)$ acquires correction

$$\Sigma_{ij}^A = \left(\Delta\nu k^2 + \Delta\nu_3 k_3^2\right) P_{ij}(\mathbf{k}) + \Delta s k^2 P_{i3}(\mathbf{k}) P_{j3}(\mathbf{k})$$

which, in addition to giving correction to the bare viscosity ν_0, it also gives rise to a vertical viscosity ν_3. Further, it turns out that, a correction Δs multiplied

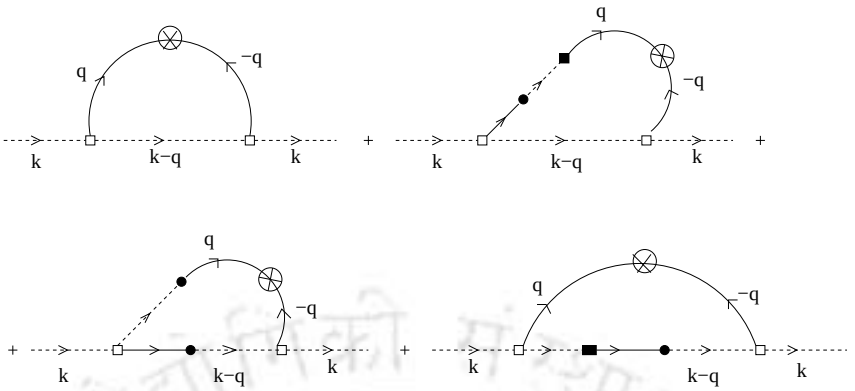

Figure 6.4: One-loop Feynman diagrams for self-energy $\Sigma^C(\mathbf{k},\omega)$ giving corrections to the bare-diffusivity κ_0. Note that the last diagram is obtained by iterating the perturbation expansion twice. The analytical expressions are given in Eq. (6.19).

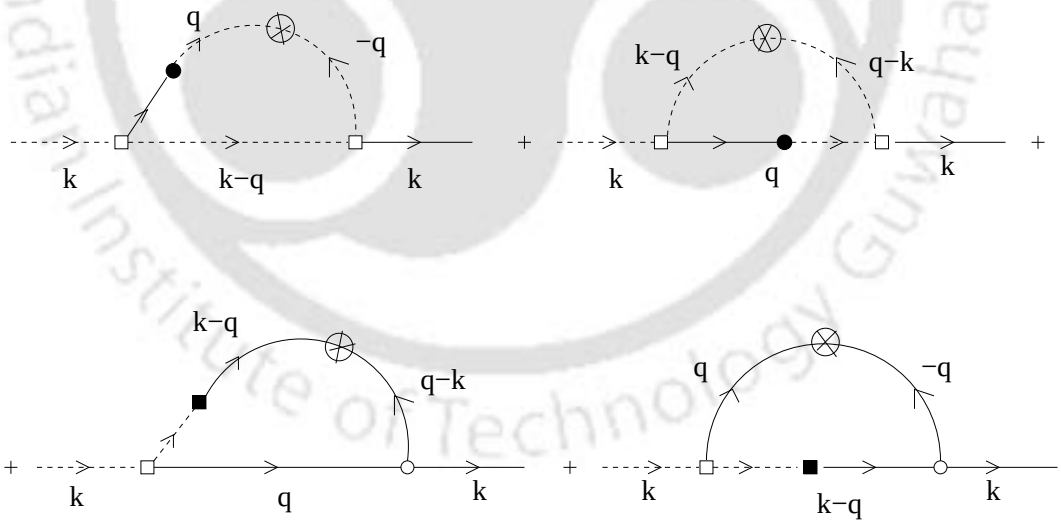

Figure 6.5: One-loop Feynman diagrams for self- energy, $\Sigma^D(\mathbf{k},\omega)$, giving correction to the vertex, β_0. The analytical expressions are given in Eq. (6.20).

by $k^2 P_{i3}(\mathbf{k}) P_{j3}(\mathbf{k})$ arises in our analysis which does not contribute directly to either ν_0 or ν_3. We shall neglect this term in the present study because its relevance is unknown. Thus, the relevant corrections to the bare propagator comes only from the first four diagrams of Fig. 6.2 because the last three diagrams contribute only to Δs.

The bare propagator $H_0(\mathbf{k}, \omega)$ gains correction from the self-energy $\Sigma^C(\mathbf{k}, \omega)$ which takes the form

$$\Sigma^C(\mathbf{k}, \omega) = \Delta\kappa k^2 + \Delta\kappa_3 k_3^2$$

where $\Delta\kappa$ and $\Delta\kappa_3$ are the leading order corrections to the bare diffusivity.

On integrating over the internal wavenumber $\Lambda e^{-r} \leq q \leq \Lambda$ in the corresponding Feynman diagrams, we obtain the corrections as

$$\Delta\nu = A_d \nu_0 \bar{\lambda}^2 \frac{e^{\epsilon r} - 1}{\epsilon} - \left(B_d + C_d f_\nu + D_d f_\nu^2 - C_d \frac{1}{f_\nu} \right) \nu_0 \bar{\lambda}_1^2 \frac{e^{\epsilon_2 r} - 1}{\epsilon_2} \tag{6.21}$$

$$\Delta\nu_3 = \left(E_d \frac{1}{l_\nu} - F_d \frac{f_\nu}{l_\nu} - G_d \frac{f_\nu^2}{l_\nu} + H_d \frac{1}{f_\nu l_\nu} - I_d \frac{1}{f_\nu^2 l_\nu} \right) \nu_3 \bar{\lambda}_1^2 \frac{e^{\epsilon_2 r} - 1}{\epsilon_2} \tag{6.22}$$

$$\Delta\kappa = M_d \kappa_0 \left(\frac{1}{f_\nu + f_\nu^2} \right) \bar{\lambda}^2 \frac{e^{\epsilon r} - 1}{\epsilon} - \left(J_d + K_d \frac{1}{f_\nu} + L_d \frac{1}{f_\nu^2} \right) \kappa_0 \bar{\lambda}_1^2 \frac{e^{\epsilon_2 r} - 1}{\epsilon_2} \tag{6.23}$$

$$\Delta\kappa_3 = - \left(N_d \frac{1}{g_\nu} + P_d \frac{f_\nu}{g_\nu} + Q_d \frac{1}{g_\nu f_\nu} \right) \kappa_3 \bar{\lambda}_1^2 \frac{e^{\epsilon_2 r} - 1}{\epsilon_2} \tag{6.24}$$

with

$$\bar{\lambda}^2 = \frac{\lambda_0^2 D_0}{\nu_0^3 \Lambda^\epsilon}, \quad \bar{\lambda}_1^2 = \frac{\lambda_0^2 \alpha_0 \beta_0 N^2 D_0}{\nu_0^2 (\nu_0 + \kappa_0)^3 \Lambda^{\epsilon_2}}, \quad f_\nu = \frac{\kappa_0}{\nu_0}, \quad l_\nu = \frac{\nu_3}{\nu_0}, \quad g_\nu = \frac{\kappa_3}{\nu_0},$$

$$A_d = \frac{S_d}{[2\pi]^d} \frac{d^2 - d - \epsilon}{2d(d+2)}, \quad B_d = \frac{S_d}{[2\pi]^d} \frac{2d - 24 + 2\epsilon_2}{2d(d+2)}, \quad C_d = \frac{S_d}{[2\pi]^d} \frac{2d - 6 + 2\epsilon_2}{d(d+2)},$$

$$D_d = \frac{S_d}{[2\pi]^d} \frac{4d - 9 + 4\epsilon_2}{4d(d+2)}, \quad E_d = \frac{S_d}{[2\pi]^d} \frac{d^2 - 3d - 2y - 21 - 2\epsilon_2}{2d(d+2)},$$

$$F_d = \frac{S_d}{[2\pi]^d} \frac{2d^2 - 2d - 4y - 39}{2d(d+2)}, \quad G_d = \frac{S_d}{[2\pi]^d} \frac{d^2 - d - 2y - 21}{2d(d+2)},$$

$$H_d = \frac{S_d}{[2\pi]^d}\frac{2d^2-5d+4y-25-3\epsilon_2}{2d(d+2)}, \quad I_d = \frac{S_d}{[2\pi]^d}\frac{d-6+\epsilon_2}{2d(d+2)},$$
$$J_d = \frac{S_d}{[2\pi]^d}\frac{d^2+10d+8+2y(d+1)}{2d(d+2)}, \quad K_d = \frac{S_d}{[2\pi]^d}\frac{d^2+32d+30+6y(d+1)}{2d(d+2)},$$
$$L_d = \frac{S_d}{[2\pi]^d}\frac{(d+1)(9+2y)}{d(d+2)}, \quad M_d = \frac{S_d}{[2\pi]^d}\frac{d-1}{d},$$
$$N_d = \frac{S_d}{[2\pi]^d}\frac{5d^2+5d-70-12y}{2d(d+2)},$$
$$P_d = \frac{S_d}{[2\pi]^d}\frac{d^2+d-18-4y}{2d(d+2)}, \quad Q_d = \frac{S_d}{[2\pi]^d}\frac{2d^2+2d-22-4y}{d(d+2)}$$

and

$$\epsilon = 4+y-d, \quad \epsilon_2 = 8+y-d$$

6.5 Vertex Renormalization

The lowest order correction to the α_0 and β_0 vertex due to self energy Σ^B_{i3} and Σ^D_{i3} from Figs. (6.3) and (6.5) are evaluated using a similar procedure as above and they are found to be

$$\begin{aligned}\Delta\alpha(k) &= -R_d\alpha_0\bar{\lambda}_2^2\frac{e^{\epsilon_1 r}-1}{\epsilon_1} - \frac{2}{3}M_d\alpha_0\frac{1}{f_\nu+2f_\nu^2}\bar{\lambda}_2^2\frac{e^{\epsilon_1 r}-1}{\epsilon_1} \\ &\quad - M_d\alpha_0\frac{1}{1+2f_\nu}\bar{\lambda}_2^2\frac{e^{\epsilon_1 r}-1}{\epsilon_1} \qquad (6.25)\end{aligned}$$

$$\begin{aligned}\Delta\beta(k) &= -T_d\beta_0\bar{\lambda}_3^2\frac{e^{\epsilon_1 r}-1}{\epsilon_1} + U_d\beta_0\frac{1}{f_\nu}\bar{\lambda}_3^2\frac{e^{\epsilon_1 r}-1}{\epsilon_1} + V_d\beta_0\frac{1}{f_\nu^2}\bar{\lambda}_3^2\frac{e^{\epsilon_1 r}-1}{\epsilon_1} + \\ &\quad - W_d\beta_0\bar{\lambda}_4^2\frac{e^{\epsilon_1 r}-1}{\epsilon_1} - X_d\beta_0 f_\nu\bar{\lambda}_4^2\frac{e^{\epsilon_1 r}-1}{\epsilon_1} - Y_d\beta_0 f_\nu^2\bar{\lambda}_4^2\frac{e^{\epsilon_1 r}-1}{\epsilon_1} \qquad (6.26)\end{aligned}$$

Here

$$\bar{\lambda}_2^2 = \frac{\lambda_0^2 D_0 k^2}{\nu_0^2\alpha_0(\nu_0+\kappa_0)\Lambda^{\epsilon_1}}, \quad \bar{\lambda}_3^2 = \frac{\lambda_0^2\alpha_0\mathcal{D}_0 k^2}{\beta_0(\nu_0+\kappa_0)^3\Lambda^{\epsilon_1}}, \quad \bar{\lambda}_4^2 = \frac{\lambda_0^2 D_0 k^2}{(\nu_0+\kappa_0)^3\Lambda^{\epsilon_1}},$$
$$R_d = \frac{S_d}{[2\pi]^d}\frac{d^2-2}{2d(d+2)}, \quad T_d = \frac{S_d}{[2\pi]^d}\frac{15+2y}{2d(d+2)}, \quad U_d = \frac{S_d}{[2\pi]^d}\frac{9+y}{2d(d+2)},$$
$$V_d = \frac{S_d}{[2\pi]^d}\frac{4+y}{2d(d+2)}, \quad W_d = \frac{S_d}{[2\pi]^d}\frac{d^2+4d-8}{2d(d+2)}, \quad X_d = \frac{S_d}{[2\pi]^d}\frac{d^2+3d-7}{2d(d+2)},$$
$$Y_d = \frac{S_d}{[2\pi]^d}\frac{d^2+2d-2}{2d(d+2)}, \quad \epsilon_1 = 6+y-d$$

As these lowest order correction terms are $O(k^2)$, these corrections vanish and hence they do not contribute in the IR limit ($k \to 0$).

Because of Galilean invariance, we shall assume that the other vertices λ_0 and $\bar{\lambda}_0$ do not undergo relevant corrections.

6.6 Noise Renormalization

Expanding the velocity field in a perturbation series, we have

$$u_i(\mathbf{k},\omega) = u_i^{(0)}(\mathbf{k},\omega) + \lambda u_i^{(1)}(\mathbf{k},\omega) + \cdots$$

with

$$u_i^{(0)}(\mathbf{k},\omega) = G_0(\mathbf{k},\omega) f_i(\mathbf{k},\omega) \tag{6.27}$$

as zeroth order perturbation, and

$$\begin{aligned} u_i^{(1)}(\mathbf{k},\omega) = & -\frac{i\lambda_0}{2} G_0(k,\omega) P_{ijl}(\mathbf{k}) \int \frac{d\hat{\mathbf{q}}}{[2\pi]^{d+1}} u_j^{(0)}(\mathbf{q},\omega') u_l^{(0)}(\mathbf{p},\omega'') \\ - & \; i\alpha_0\bar{\lambda}_0 \; N \; G_0(k,\omega) \; H_0(k,\omega) k_j P_{i3}(\mathbf{k}) \int \frac{d\hat{\mathbf{q}}}{[2\pi]^{d+1}} u_j^{(0)}(\mathbf{q},\omega') \psi^{(0)}(\mathbf{p},\omega'') \\ - & \; \alpha_0\beta_0 N^2 G_0(k,\omega) H_0(k,\omega) P_{i3}(\mathbf{k}) u_3^{(0)}(\mathbf{k},\omega) \end{aligned} \tag{6.28}$$

as first order perturbation. Using these relations, the velocity correlation tensor can be expanded perturbatively as

$$Q_{ij} = Q_{ij}^{(0)} + \lambda Q_{ij}^{(1)} + \lambda^2 Q_{ij}^{(2)} + \cdots$$

in which

$$\langle u_i^{(0)}(\mathbf{k},\omega) u_j^{(0)}(\mathbf{k}',\omega')\rangle = Q_{ij}^{(0)}(k,\omega) P_{ij}(\mathbf{k}) [2\pi]^d \delta^d(\mathbf{k}+\mathbf{k}') [2\pi]\delta(\omega+\omega') \tag{6.29}$$

as the isotropic part and

$$\begin{aligned} & \langle u_i^{(0)}(\mathbf{k},\omega) u_j^{(1)}(\mathbf{k}',\omega')\rangle + \langle u_i^{(1)}(\mathbf{k},\omega) u_j^{(0)}(\mathbf{k}',\omega')\rangle \\ & \qquad = Q_{ij}^{(1)}(k,\omega) P_{ij}(\mathbf{k}) [2\pi]^d \delta^d(\mathbf{k}+\mathbf{k}') [2\pi]\delta(\omega+\omega') \end{aligned} \tag{6.30}$$

and

$$\langle u_i^{(1)}(\mathbf{k},\omega) u_j^{(1)}(\mathbf{k}',\omega')\rangle = Q_{ij}^{(2)}(k,\omega) P_{ij}(\mathbf{k}) [2\pi]^d \delta^d(\mathbf{k}+\mathbf{k}') [2\pi]\delta(\omega+\omega') \tag{6.31}$$

are the anisotropic parts. We perform a similar expansion for the scalar field $\psi(\mathbf{k},\omega)$.

The corrections to D_0 and $\mathcal{D}_0$ appearing in Eqs. (6.9) and (6.10) are given by the Feynman diagrams shown in Fig. 6.6. When these diagrams are integrated over the internal wavenumbers in the range $\Lambda e^{-r} \leq q \leq \Lambda$, they yield corrections in the $k \to 0$ and $\omega \to 0$ limit as

$$\Delta D(k,0) = R_d \frac{\lambda_0^2 D_0^2}{\nu_0^3}\, k^{2+y}\, \frac{e^{(d-2+2\epsilon)r}-1}{(d-2+2\epsilon)\Lambda^{d-2+2\epsilon}} \tag{6.32}$$

$$\Delta \mathcal{D}(k,0) = M_d \frac{\lambda_0^2 D_0 \mathcal{D}_0}{\nu_0\kappa_0(\nu_0+\kappa_0)}\, k^{2+y'}\, \frac{e^{(d-2+\epsilon+\epsilon')r}-1}{(d-2+\epsilon+\epsilon')\Lambda^{d-2+\epsilon+\epsilon'}} \tag{6.33}$$

Thus ΔD and $\Delta\mathcal{D}$ give rise to k independent, and hence, relevant, corrections to the constants D_0 and $\mathcal{D}_0$ only when $y = -2$ (or $\epsilon = 2-d$) and $y' = -2$ (or $\epsilon' = 2-d$) respectively. In this case, the constant corrections to D_0 and $\mathcal{D}_0$ become

$$\Delta D(0,0) = R_d \frac{\lambda_0^2 D_0^2}{\nu_0^3}\, \frac{e^{(2-d)r}-1}{(2-d)\Lambda^{2-d}} \tag{6.34}$$

$$\Delta \mathcal{D}(0,0) = M_d \frac{\lambda_0^2 D_0 \mathcal{D}_0}{\nu_0\kappa_0(\nu_0+\kappa_0)}\, \frac{e^{\epsilon r}-1}{\epsilon\Lambda^{\epsilon}} \tag{6.35}$$

As we are interested in non-equilibrium case ($y > -2$ and $y' > -2$), the correction to the noise amplitudes become irrelevant, because in this case, the corresponding corrections, given by Eqs. (6.32) and (6.33), are found to be proportional to some positive power of k, and hence go to zero in the RG limit $k \to 0$.

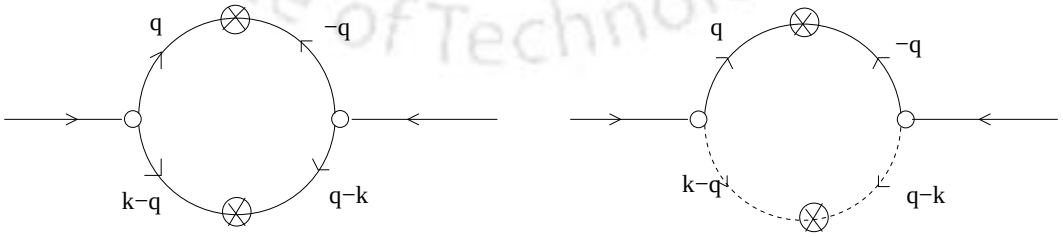

Figure 6.6: One-loop Feynman diagrams for noise correlation giving correction to the amplitudes D_0 and $\mathcal{D}_0$.

6.7 Rescaling

In order to keep invariant the form of the basic equations, the "reduced" range $0 < k < \Lambda e^{-r}$ is projected on to the "full" range $0 < k' < \Lambda$ by rescaling of $\mathbf{k}$, ω, $u(\mathbf{k},\omega)$, and $\psi(\mathbf{k},\omega)$ as

$$\mathbf{k}' = \mathbf{k}e^{r}, \qquad \omega' = \omega e^{\zeta(r)} \tag{6.36}$$

$$u^{>}(\mathbf{k},\omega) = \phi(r)u'(\mathbf{k}',\omega'), \quad \psi^{>}(\mathbf{k},\omega) = \xi(r)\psi'(\mathbf{k}',\omega') \tag{6.37}$$

where $\zeta(r)$, $\xi(r)$ and $\phi(r)$ are unknown functions.

After this rescaling, we must get the dynamical equations in covariant forms so that the form remains invariant under every iteration of the RG procedure. This condition of RG invariance leads us to get the equations in terms of the primed variables in the following forms

$$\begin{aligned}
&\left(-i\omega' + \nu(r)k'^2 + \nu_3(r)k_3'^2\right) u_i'(\mathbf{k}',\omega') \\
&= f_i'(\mathbf{k}',\omega') - \frac{i\lambda(r)}{2}\int \frac{d\hat{\mathbf{q}}'}{[2\pi]^{d+1}} u_j'(\hat{\mathbf{q}}')u_l'(\hat{\mathbf{p}}') + \alpha(r)N\psi'(\mathbf{k}',\omega')P_{i3}(\mathbf{k}')
\end{aligned}$$

$$\begin{aligned}
&\left(-i\omega' + \kappa(r)k'^2 + \kappa_3(r)k_3'^2\right) \psi'(\mathbf{k}',\omega') \\
&= \theta'(\mathbf{k}',\omega') - i\bar{\lambda}(r)k_j' \int \frac{d\hat{\mathbf{q}}'}{[2\pi]^{d+1}} u_j'(\hat{\mathbf{q}}')\psi'(\hat{\mathbf{p}}') - \beta(r)Nu_3'(\mathbf{k}',\omega')
\end{aligned}$$

where $\nu(r)$, $\nu_3(r)$, $\kappa(r)$, and $\kappa_3(r)$ are the scaled viscosity and diffusivity coefficients respectively, $\lambda(r)$, $\bar{\lambda}(r)$, $\alpha(r)$, and $\beta(r)$ are scaled couplings in the reduced wave number space.

Carrying out power counting in the above equations, we obtain

$$\begin{aligned}
&\nu(r) = \nu_r e^{\zeta(r)-2r}, \qquad \nu_3(r) = \nu_{3r}e^{\zeta(r)-2r} \qquad \lambda(r) = \lambda_0\phi(r)e^{-(d+1)}(r) \\
&\bar{\lambda}(r) = \bar{\lambda}_0\phi(r)e^{-(d+1)}(r), \qquad \kappa(r) = \kappa_r e^{\zeta(r)-2r}, \qquad \kappa_3(r) = \kappa_{3r}e^{\zeta(r)-2r} \\
&\alpha(r) = \alpha_0\phi(r)^{-1}\xi(r)e^{\zeta(r)} \qquad \beta(r) = \beta_0\phi(r)\xi(r)^{-1}e^{\zeta(r)}
\end{aligned}$$

where ν_r, κ_r, ν_{3r}, and κ_{3r} are the renormalized quantities. The new forcing terms are

$$f_i'(\mathbf{k}',\omega') = f_i^{>}(\mathbf{k},\omega)e^{\zeta(r)}\phi(r)^{-1}, \qquad \theta'(\mathbf{k}',\omega') = \theta^{>}(\mathbf{k},\omega)e^{\zeta(r)}\xi(r)^{-1} \tag{6.38}$$

Therefore,

$$D'(k') = D_r(k')exp[3\zeta(r) + (d+y)r]\phi(r)^{-2}$$

$$\mathcal{D}'(k') = \mathcal{D}_r(k')exp[3\zeta(r) + (d+y')r]\xi(r)^{-2}$$

Since $\frac{dD}{dr} = 0$ and $\frac{d\mathcal{D}}{dr} = 0$, we choose the functions $\xi(r)$ and $\phi(r)$ in such a way that $D' = D_0$ and $\mathcal{D}' = \mathcal{D}_0$ at each step of the RG procedure. Thus,

$$\phi(r) = exp\left[\frac{3\zeta(r) + (d+y)r}{2}\right], \qquad \xi(r) = exp\left[\frac{3\zeta(r) + (d+y')r}{2}\right]$$

Thus we obtain

$$\frac{d\lambda(r)}{dr} = \lambda(r)\left[\frac{3}{2}z - 1 - \frac{d-y}{2}\right], \qquad \frac{d\bar{\lambda}(r)}{dr} = \bar{\lambda}(r)\left[\frac{3}{2}z - 1 - \frac{d-y'}{2}\right]$$
$$\frac{d\alpha(r)}{dr} = \alpha(r)\left[z + \frac{y'-y}{2}\right], \qquad \frac{d\beta(r)}{dr} = \beta(r)\left[z + \frac{y-y'}{2}\right]$$

6.8 Flow Equations

We defining the (effective) scaled coupling constants as

$$\bar{\lambda}(r) = \frac{\lambda^2(r)D}{\nu^3(r)\Lambda^\epsilon}, \qquad f_\nu(r) = \frac{\kappa(r)}{\nu(r)}$$
$$l_\nu(r) = \frac{\nu_3(r)}{\nu(r)}, \qquad g_\nu(r) = \frac{\kappa_3(r)}{\nu(r)}$$

Differentiating these definitions with respect to r and using Eqns.(6.21)–(6.24) we get the complete RG flow at one-loop order

$$\frac{d\bar{\lambda}(r)}{dr} = \frac{1}{2}\bar{\lambda}(r)\left[\epsilon - 3A_d\bar{\lambda}^2 + 3\left(B_d + C_d f_\nu + D_d f_\nu - C_d\frac{1}{f_\nu}\right)\frac{\bar{\lambda}^2\alpha\beta N^2 D}{\nu^2\Lambda^4(1+f_\nu)^3}\right] \tag{6.39}$$

$$\frac{df_\nu(r)}{dr} = f_\nu(r)\left[-A_d\bar{\lambda}^2 + M_d\frac{1}{f_\nu(1+f_\nu)}\bar{\lambda}^2\right]$$
$$+f_\nu\left(B_d + C_d f_\nu + D_d f_\nu - C_d\frac{1}{f_\nu} - J_d - K_d\frac{1}{f_\nu} - L_d\frac{1}{f_\nu^2}\right)\frac{\bar{\lambda}^2\alpha\beta N^2 D}{\nu^2\Lambda^4(1+f_\nu)^3} \tag{6.40}$$

$$\begin{aligned}\frac{dl_\nu(r)}{dr} &= -l_\nu(r)A_d\bar{\lambda}^2 + \\ &+ l_\nu(r)\left(E_d\frac{1}{l_\nu} - F_d\frac{f_\nu}{l_\nu} - G_d\frac{f_\nu^2}{l_\nu} + H_d\frac{1}{f_\nu l_\nu} - I_d\frac{1}{f_\nu^2 l_\nu}\right)\frac{\lambda^2\alpha\beta N^2 D}{\nu^2\Lambda^4} + \\ &+ l_\nu(r)\left(B_d + C_d f_\nu + D_d f_\nu^2 - C_d\frac{1}{f_\nu}\right)\frac{\bar{\lambda}^2\alpha\beta N^2 D}{\nu^2\Lambda^4(1+f_\nu)^3} \qquad (6.41)\end{aligned}$$

$$\begin{aligned}\frac{dg_\nu(r)}{dr} &= -g_\nu(r)A_d\bar{\lambda}^2 + g_\nu(r)\left(B_d + C_d f_\nu + D_d f_\nu^2\right)\frac{\lambda^2\alpha\beta N^2 D}{\nu^2\Lambda^4} + \\ &+ g_\nu(r)\left(C_d\frac{1}{f_\nu} - N_d\frac{1}{g_\nu} - P_d\frac{f_\nu}{g_\nu}) - Q_d\frac{1}{g_\nu f_\nu}\right)\frac{\bar{\lambda}^2\alpha\beta N^2 D}{\nu^2\Lambda^4(1+f_\nu)^3} \qquad (6.42)\end{aligned}$$

6.9 Fixed Points and Stability Analysis

Without solving the flow equations exactly, we can perform an analysis of the RG flow equations of the previous section with the idea of a fixed point. We assume that as the RG iteration is carried out, i.e., as $r \to \infty$, the scaled coupling constants approach a set of constant values, called a fixed point, i.e., they cease to be r-dependent after infinitely many steps of RG iterations, so that the right-hand sides of equations (6.39)–(6.42) tend to zero as one approaches the fixed point. The existence of a fixed point depends on its linear stability with respect to infinitesimal perturbations around that point. Here we shall investigate the stability of the fixed points in the vanishing (or weak) stratification limit ($N \to 0$).

We shall investigate the behavior of the fixed point

$$\bar{\lambda} \to \bar{\lambda}^*, \quad f_\nu \to f_\nu^*, \quad l_\nu \to 0, \quad g_\nu \to 0 \qquad (6.43)$$

This fixed point is expected to correspond to the scaling laws for the Kolmogorov and Obukhov cascades of energy and mean square scalar. From Eqns. (6.39)–(6.42), we then obtain the fixed points as:

$$\bar{\lambda}^* = \left(\frac{\epsilon}{3A_d}\right)^{1/2}, \qquad f_\nu^*(1+f_\nu^*) = \frac{M_d}{A_d} \qquad (6.44)$$

We observe that the above fixed point is similar to that of Yakhot and Orszag [184], because the extra couplings which are not present in the Yakhot-Orszag theory, go to zero.

To investigate its stability, we assume

$$\bar{\lambda} \to \bar{\lambda}^* + \delta\lambda, \quad f_\nu \to f^* + \delta f_\nu, \quad l_\nu \to 0 + \delta l_\nu, \quad g_\nu \to 0 + \delta g_\nu$$

where $\delta\lambda$, δf_ν, δl_ν, and δg_ν are infinitesimal perturbations. Substituting them in Eqns. (6.39)–(6.42), and retaining only first-order terms we obtain the stability matrix as

$$\frac{d}{dr}\begin{pmatrix} \delta\bar{\lambda} \\ \delta f_\nu \\ \delta l_\nu \\ \delta g_\nu \end{pmatrix} = \begin{pmatrix} -\epsilon & 0 & 0 & 0 \\ 0 & -\epsilon/3 & 0 & 0 \\ 0 & 0 & -\epsilon/3 & 0 \\ 0 & 0 & 0 & -\epsilon/3 \end{pmatrix} \begin{pmatrix} \delta\bar{\lambda} \\ \delta f_\nu \\ \delta l_\nu \\ \delta g_\nu \end{pmatrix}$$

Thus the condition for stability is obtained as

$$\epsilon > 0.$$

6.10 Conclusions

Using the dynamic RG technique, we have investigated the influence of anisotropy on the behavior of the universal scaling laws governed by the stochastic Navier-Stokes equation. Stable stratification breaks the isotropy of the flow which is reflected in the renormalized viscosity and diffusivity. We calculated the corresponding corrections for both eddy-viscosity and eddy-diffusivity in one-loop approximation. We have also seen that vertices α_0 and β_0 do not acquire any relevant corrections in the IR limit. Further, we have found that the noise corrections becomes irrelevant in the non-equilibrium case ($y > -2$ and $y' > -2$).

The flow equations of the corresponding coupling constants are found to be of complicated nature. As such, they do not yield to the stability analysis of any arbitrary fixed points. However, the fixed point that is of interest to us is the one that would correspond to the Kolmogorov and Obukhov scaling laws. We have analysed one such fixed point in the limit of weak stratification. We find that such a fixed point exists with regard to its stability. Thus we

expect that the Kolmogorov and Obukhov scaling laws $E(k) \sim k^{-5/3}$ and $\mathcal{E}(k) \sim k^{-5/3}$ are realizable even in the presence of stratification. Since we have investigated their stability in the limit of weak stratification, we expect that these scaling laws would be observed at the smaller scales of motion where the effect of stratification decreases sufficiently.

Chapter 7

Summary and Conclusions

Throughout the work of this thesis we have made an effort to obtain a better understanding of the effect of anisotropy on Navier-Stokes dynamics. In particular, this study is primarily concerned with identifying and tackling some new and open problems of anisotropic turbulence, namely homogeneous shear flow and stratified turbulence of the atmospheric and oceanic motions. This dissertation mainly focuses on the theoretical treatments of these anisotropic turbulence problems in Chapters 2 to 6. In this chapter, a general review of the outcomes of this dissertation and comments on future studies is presented.

As presented in Chapter 2, the problem of homogeneous shear turbulence has been treated with the help of Leslie's perturbation method. We made a perturbation expansion of the velocity correlation tensor where the effect of anisotropy due to the mean flow is reflected in the leading order correction term. Through direct calculation, we found out the form of the leading order anisotropic equal-time velocity correlation tensor which was found to be consistent with previous investigations [61, 185, 112]. Using inputs from renormalization group calculations, we calculated the universal numbers, namely A and B associated with the scaling functions of equal-time velocity correlation tensor. Our theoretical calculation gave

$$A = -0.13 \quad \text{and} \quad B = -0.48$$

We compared our results with the experimental results, namely $A \approx -0.17$ and

$B \approx -0.45$ [164]. Previous theoretical attempts in Ref. [185] had produced $A = -0.12 \pm 0.002$ and $B = 0.009 \pm 0.014$ and $A = -0.10$ and $B = -0.37$ in [112]. Further our results are also comparable with the DNS values, namely $A = -0.16 \pm 0.03$ and $B = -0.40 \pm 0.06$ (with 512^3 grid points and Reynolds number $R_\lambda = 284$) [61] and $A = -0.15 \pm 0.01$ and $B = -0.48 \pm 0.02$ (with 1024^3 grid points and Reynolds number $R_\lambda = 480$) [185].

As noted earlier, the above method can be extended to investigate the anisotropic statistical properties of turbulent plasmas [161], the anisotropy often persists in the presence of mean magnetic and fluid velocity fields. This method can also be applied to find out the coefficients associated with the fragmentation of drift wave structures (a signature of the zonal flow generation), in anisotropic electrostatic turbulence [9, 118].

In order to extract the information about the effect of anisotropy on turbulence with stable stratification we have applied various perturbation methods. In the problem of stratified turbulence, inputs about the passive scalar dynamics being necessary, we studied the problem of turbulent convection using Heisenberg approximation [57] in Chapter 3. We calculated the universal numbers, namely Batchelor constant (Ba), turbulent Prandtl number (σ), and Kolmogorov constant (C), associated with the passive scalar dynamics. We presented our theoretical calculation under two different scheme, namely with ϵ expansion

$$C = 1.4363, \quad \sigma = \alpha/\beta = 0.7179 \quad \text{and} \quad \text{Ba} = 1.031$$

and without ϵ expansion

$$C = 1.5618, \quad \sigma = 0.61351 \quad \text{and} \quad \text{Ba} = 0.9583$$

These results are comparable with various experiments.

We also derived a relation between three-dimensional Batchelor spectrum and the corresponding one-dimensional spectrum, and thereby obtained a relation between 3D Batchelor constant Ba and 1D Batchelor constant Ba$'$ as

$$\text{Ba}' = \frac{3}{5}\,\text{Ba}$$

which yields for Ba = 1.031, Ba$'$ = 0.62. This value is comparable with the recent value obtained via numerical simulation on strongly stratified turbulence by Brethouwer and Lindborg [18], namely Ba$'$ $\approx$ 0.5. Within the same framework, we have also seen that with increasing value of space dimensions d, Prandtl number σ increases and approaches unity, while the Kolmogorov constant C and Batchelor constant Ba approach very close to each other. To investigate the behavior of these universal numbers at very large space dimensions, we made a large d expansion, and we found that, at very high space dimensions, the Kolmogorov constant C, Batchelor constant Ba, and Prandtl number σ go like

$$C = C_0\ d^{1/3}, \quad \mathrm{Ba} = \mathrm{Ba}_0\ d^{1/3}, \quad \text{and} \quad \sigma = \frac{\alpha}{\beta} = 1$$

in the leading order of the $1/d$ expansion. The constants C_0 and Ba_0, evaluated in the same scheme, were found to be

$$C_0 = \mathrm{Ba}_0 = \left(\frac{16}{27}\right)^{1/3} \approx 0.83995$$

In the dynamics of stratified flow, the scalar (temperature or density) field is coupled to the velocity field by an externally imposed buoyancy force in the absence of which the scenario reduces to the passive scalar case. Following Leslie, the extra terms can be treated as perturbation to the dynamics. In Chapter 4, we performed a Leslie-type perturbative treatment [90] on stably stratified turbulence, where the buoyancy terms $N\psi\hat{e}_3$ and $-Nu_3$ in the corresponding dynamical equations are treated as perturbations against the isotropic background fields and made perturbation expansions of the velocity and scalar fields. This enabled us to evaluate the corresponding corrections to various correlation functions, namely, velocity-velocity $C_1N^2P_{i3}(\mathbf{k})P_{j3}(\mathbf{k})k^{-5}$, temperature-temperature $C_2N^2P_{33}(\mathbf{k})k^{-5}$, and velocity-temperature correlations $C_3NP_{i3}(\mathbf{k})k^{-13/3}$. It was found that the prefactors C_1, C_2 and C_3 depend on Kolmogorov constant (C), Batchelor constant (Ba), turbulent Prandtl number (σ), energy flux ε, and the scalar flux χ. Using our calculated values of the universal numbers, namely C, Ba, and σ, as presented in Chapter

3, we were able to calculate the relevant numbers. Also we noted that the anisotropic part of energy and mean-square scalar spectra go like k^{-3} and the anisotropic buoyancy spectrum goes like $k^{-7/3}$. At sufficiently large scales, the anisotropic k^{-3} spectrum would dominate over the isotropic $k^{-5/3}$ spectrum. Thus we expect a k^{-3} power law behavior of energy spectrum at sufficiently large scales. This scenario is similar to the analysis of experimental investigations by Nastrom and Gage [115, 116], who analysed the atmospheric data (upper troposphere and lower stratosphere) collected by NASA instrumented commercial Boeing 747 airliners, and found that the atmospheric energy spectra follow the -3 power law in the synoptic scale and the $-5/3$ power law in the mesoscale with a smooth transition in between. Following this, various hypothesis on the origin of the spectra have been proposed, such as 2D turbulence with two sources [92], internal gravity waves [35, 55]. Calculation of third order structure function [29] suggested a forward cascade of $k^{-5/3}$ spectrum in the mesoscale range. This also led to hypothesize about a direct energy cascade in a two-layer quasigeostrophic (QG) model [167], surface QG models [165, 150], stratified turbulence simulations [18], and spectral condensation of 2D turbulence [180, 181]. However, our calculation supports the additive spectrum previously proposed by Tung and Orlando [167].

To carry out the problem further, we performed a perturbation expansion similar to the Kraichnan's direct interaction approximation (DIA) to investigate problem of stratified turbulence with stable temperature stratification, in Chapter 5. Within this framework, we evaluated the corresponding corrections to velocity-velocity, temperature-temperature, and velocity-temperature correlation functions up to the leading order terms, and found that, unlike the Leslie-type treatment of the same problem as presented in Chapter 4, the anisotropic corrections to the velocity-velocity and temperature-temperature correlations acquire two additional new terms, whereas the correction to the velocity-temperature correlation remained the same as obtained in the Leslie-type calculations. The prefactors associated with these universal scaling laws were calculated within this framework which were found to be dependent on ε,

χ, C, Ba, and σ in a more complicated fashion than our previous Leslie-type calculations.

Finally, in Chapter 6, we presented a dynamic renormalization group (RG) analysis of turbulent flow field with temperature stratification. We carried out our analysis up to one-loop order to achieve a coarse-grained description of turbulent flow field via successive elimination of small shell of modes, yielding the flow equations for the renormalized coupling constants. Due to the presence of anisotropy, the perturbative RG treatment of this problem involve many extra Feynman diagrams along with those of Yakhot and Orszag's [183, 43]. The small-scale elimination procedure leads to the emergence of vertical eddy- viscosity (ν_3) and eddy-diffusivity (κ_3) (corresponding to the vertical motions), in addition to the usual isotropic viscosity and diffusivity (ν_0 and κ_0). This gives rise to a very complicated RG analysis. We performed stability analysis of the flow equations in the limit of weak stratification and it was found that the Kolmogorov scaling regime exists and thus it was expected that the energy cascade at small scales would be Kolmogorovian and along the line conjectured by Kolmogorov.

Bibliography

[1] L. T. Adzhemyan, N. V. Antonov, M. V. Kompaniets, and A. N. Vasil'ev. *Int. J. Mod. Phys. B* **17**, 2137 (2003).

[2] L. T. Adzhemyan, J. Honkonen, T. L. Kim, and L. Sladkoff. *Phys. Rev. E* **71**, 056311 (2005).

[3] G. Ahlers, S. Grossmann, and D. Lohse. *Rev. Mod. Phys.* **81**, 503 (2009).

[4] N. V. Antonov. *Phys. Rev. E* **60**, 6691 (1999).

[5] N. V. Antonov, A. Lanotte, and A. Mazzino. *Phys. Rev. E* **61**, 6586 (2000).

[6] I. Arad, L. Biferale, and I. Procaccia. *Phys. Rev. E* **61**, 2654 (2000).

[7] I. Arad, B. Dhruva, S. Kurien, V. S. L'vov, I. Procaccia, and K. R. Sreenivasan. *Phys. Rev. Lett.* **81**, 5330 (1998).

[8] M. A. Baker and C. H. Gibson. *J. Phys. Oceanogr.* **17**, 1817 (1987).

[9] R. Balescu, I. Petrisor, and M. Negrea. *Plasma Phys. Control. Fusion* **47**, 2145 (2005).

[10] A. L. Barabási and H. E. Stanley. *Fractal Concepts in Surface Growth.* Cambridge University Press, Cambridge (1995).

[11] G. K. Batchelor. *The Theory of Homogeneous Turbulence.* Cambridge University Press (1953).

[12] G. K. Batchelor. *J. Fluid. Mech.* **5**, 113 (1959).

[13] D. Bernard, K. Gawedzcki, and A. Kupiainen. *Phys. Rev. E* **54**, 2624 (1996).

[14] A. Bhattacharya, S. C. Kassinos, and R. D. Moser. *Phys. Fluids* **20**, 101502 (2008).

[15] L. Biferale, I. Daumont, A. Lanotte, and F. Toschi. *Phys. Rev. E* **66**, 056306 (2002).

[16] L. Biferale and F. Toschi. *Phys. Rev. Lett.* **86**, 4831 (2001).

[17] N. E. J. Boston and R. W. Burling. *J. Fluid Mech.* **55**, 473 (1972).

[18] G. Brethouwer and E. Lindborg. *Geophys. Res. Lett.* **35**, L06809 (2008).

[19] J. Buša, M. Hnatich, J. Honkonen, and D. Horvath. *Phys. Rev. E* **55**, 381 (1997).

[20] C. Cambon, R. Rubinstein, and F.S. Godeferd. *New J. Phys.* **6**, 73 (2004).

[21] V. M. Canuto. *The Astro. Journ.* **508**, 767 (1998).

[22] D. Carati and L. Brenig. *Phys. Rev. A* **40**, 5193 (1989).

[23] C. M. Casciola, P. Gualtieri, B. Jacob, and R. Piva. *Phys. Rev. Lett.* **95**, 024503 (2005).

[24] S. Chandrasekhar. *Hydrodynamic and Hydromagnetic Stability.* Pergamon Press (1989), 2nd edition.

[25] C. C. Chang, B. S. Lin, and C.-T. Wang. *Phys. Rev. E* **67**, 047301 (2003).

[26] J. G. Charney. *J. Atmos. Sci.* **28**, 1087 (1971).

[27] M. Chertkov, C. Connaughton, I. Kolokolov, and V. Lebedev. *Phys. Rev. Lett.* **99**, 084501 (2007).

[28] M. Chertkov, G. Falkovich, I. Kolokolov, and V. Lebedev. *Phys. Rev. E* **52**, 4924 (1995).

[29] J. Y. N. Cho and E. Lindborg. *J. Geophys. Res.* **106**, 10223 (2001).

[30] P. Y. Chou. *Chin. J. Phys.* **4**, 1 (1940).

[31] A. Rai Choudhuri. *The Physics of Fluids and Plasmas.* Cambridge University Press, Cambridge (1998).

[32] I. Chunchuzov. *J. Atmos. Sci.* **59**, 1753 (2002).

[33] S. Corrsin. *J. Appl. Phys.* **22**, 469 (1951).

[34] C. DeDominicis and P. C. Martin. *Phys. Rev. A,* **19**, 419 (1979).

[35] E. Dewan. *Science* **204**, 832 (1979).

[36] C. Domb and M. S. Green. *Phase Transitions and Critical Phenomena, Vol. 2.* Academic Press, New York (1972).

[37] M. Van Dyke. *An Album of Fluid Motion.* Parabolic, Stanford (1982).

[38] S. F. Edwards. *J. Fluid. Mech.* **18**, 239 (1964).

[39] T. Elperin and N. Kleeorin. *Phys. Rev. E* **53**, 3431 (1996).

[40] A. Marenco et al. *J. Geophys. Res.* **103**, 25631 (1998).

[41] A. Fairhall, O. Gat, V. S. L'vov, and I. Procaccia. *Phys. Rev. E* **53**, 3518 (1996).

[42] G. Falkovich. *Phys. Rev. Lett.* **69**, 3173 (1992).

[43] D. Forster, D. R. Nelson, and M. J. Stephen. *Phys. Rev. A* **16**, 732 (1977).

[44] J. D. Fournier and U. Frisch. *Phys. Rev. A,* **28**, 1000 (1983).

[45] U. Frisch. *Turbulence—A Legacy of A. N. Kolmogorov.* Cambridge University Press (1999).

[46] J. Gaite. *Phys. Rev. E* **68**, 056310 (2003).

[47] S. Garg and Z. Warhaft. *Phys. Fluids* **10**, 662 (1998).

[48] O. Gat, V.S. L'vov, E. Podivilov, and I. Procaccia. *Phys. Rev. E* **55**, 3836 (1997).

[49] K. Gawedzki and A. Kupiainen. *Phys. Rev. Lett.* **75**, 3834 (1995).

[50] C. H. Gibson. *Appl. Mech. Rev.* **49**, 299 (1996).

[51] J. Glimm and D. H. Sharp. *J. Stat.Phys.* **62**, 415 (1991).

[52] M. Gonzalez. *Phys. Fluids* **12**, 2302 (2000).

[53] H. L. Grant, R. W. Stewart, and A. Moilliet. *J. Fluid Mech.* **12**, 241 (1962).

[54] M. C. Gregg. *J. Geophys. Res.* **92**, 5249 (1987).

[55] A. S. Gurvich and I. P. Chunchuzov. *Ann. Geophys.* **26**, 2037 (2008).

[56] K. Hamilton, Y.O. Takahashi, and W. Ohfuchi. *J. Geophys. Res.* **113**, D18110 (2008).

[57] W. Heisenberg. *Z. Phys.* **124**, 628 (1948).

[58] J. O. Hinze. *Turbulence.* McGraw-Hill, New York (1975).

[59] G. Holloway. *J. Phys. Oceranogr.* **16**, 2179 (1986).

[60] T. Ishida and Y. Kaneda. *Phys. Fluids* **19**, 075104 (2007).

[61] T. Ishihara, K Yoshida, and Y. Kaneda. *Phys. Rev. Lett.* **88**, 154501 (2002).

[62] E. C. Itswiere, K. N. Helland, and C. W. van Atta. *J. Fluid Mech.* **162**, 299 (1986).

[63] C. Itzykson and J. M. Drouffe. *Statistical Field Theory*, volume 1 and 2. Cambridge University Press (1989).

[64] C. Itzykson and J. B. Zuber. *Quantum Field Theory.* Mc-Graw Hill, New York (1980).

[65] M. N. Izakov. *Planet. Space Sci.* **49**, 47 (2001).

[66] Y. Kaneda. *J. Fluid Mech.* **107**, 131 (1981).

[67] M. Kardar, G. Parisi, and Y.-C. Zhang. *Phys. Rev. Lett.* **56**, 889 (1986).

[68] S. Kassinos, W. Reynolds, and M. Rogers. *J. Fluid Mech.* **428**, 213 (2001).

[69] L. V. Keldysh. *Sov. Phys. JETP* **20**, 1018 (1965).

[70] R. M. Kerr. *J. Fluid Mech.* **211**, 309 (1990).

[71] S. Kida and S. Goto. *J. Fluid Mech.* **345**, 307 (1997).

[72] Y. Kitamura and Y. Matsuda. *Geophys. Res. Lett.* **33**, L05809 (2006).

[73] N. Kleeorin and I. Rogachevskii. *Phys. Rev. E* **67**, 026321 (2003).

[74] A. N. Kolmogorov. *C. R. Acad. Sci. URSS* **30**, 301 (1941).

[75] R. H. Kraichnan. *Phys. Fluids* **10**, 1417 (1967).

[76] R. H. Kraichnan. *Phys. Fluids* **30**, 1583 (1987).

[77] R. H. Kraichnan. *Phys. Fluids* **30**, 2400 (1987).

[78] R. H. Kraichnan. *J. Fluid Mech.* **5**, 497 (1959).

[79] R. H. Kraichnan. *J. Fluid Mech.* **47**, 513 (1971).

[80] R. H. Kraichnan. *J. Fluid Mech.* **47**, 525 (1971).

[81] R. H. Kraichnan. *Phys. Fluids* **8**, 575 (1965).

[82] R. H. Kraichnan. *Phys. Fluids* **8**, 995 (1965).

[83] R. H. Kraichnan and J. R. Herring. *J. Fluid Mech.* **88**, 355 (1978).

[84] R.H. Kraichnan. *Phys. Fluids* **11**, 945 (1968).

[85] S. Kurien, V. L'vov, I. Procaccia, and K. Sreenivasan. *Phys. Rev. E* **62**, 2206 (2000).

[86] S. Kurien, V. S. L'vov, I. Procaccia, and K. R. Sreenivasan. *Phys. Rev. E* **61**, 407 (2000).

[87] L. D. Landau and E. M. Lifshitz. *Fluid Mechanics*. Pergamon Press, London (1989).

[88] J. P. Laval, J. C. McWilliams, and B. Dubrulle. *Phys. Rev. E* **68**, 036308 (2003).

[89] M. Lesieur. *Turbulence in Fluids*. Springer (2008), 4th edition.

[90] D. C. Leslie. *Developments in the Theory of Turbulence*. Clarendon Press, Oxford (1973).

[91] J. K. Lienhard and C. W. van Atta. *J. Fluid Mech.* **210**, 57 (1990).

[92] D. K. Lilly. *J. Atmos. Sci.* **46**, 2026 (1989).

[93] B.-S. Lin, C. C. Chang, and C.-T. Wang. *Phys. Rev. E* **63**, 016304 (2000).

[94] E. Lindborg. *J. Atmos. Sci.* **64**, 1017 (2007).

[95] E. Lindborg. *Phys. Rev. Lett.* **102**, 149401 (2009).

[96] E. Lindborg. *J. Fluid Mech.* **550**, 207 (2006).

[97] E. Lindborg. *J. Fluid Mech.* **388**, 259 (1999).

[98] E. Lindborg. *Geophys. Res. Lett.* **32**, L01809 (2005).

[99] E. Lindborg and J. Y. N. Cho. *Phys. Rev. Lett.* **85**, 5663 (2000).

[100] J. L. Lumley. *Phys.Fluids* **10**, 855 (1967).

[101] J. L. Lumley. *J. Atmos. Sci.* **21**, 99 (1964).

[102] V. S. L'vov, I. Procaccia, and V. Tiberkevich. *Phys. Rev. E* **67**, 026312 (2003).

[103] S. K. Ma and G. Mazenko. *Phys. Rev. B* **11**, 4077 (1975).

[104] L. Machiels. *Phys. Rev. E* **57**, 6191 (1998).

[105] A. Mahalov, B. Nicolaenko, and Y. Zhou. *Phys. Rev. E* **57**, 6187 (1998).

[106] P. C. Martin, E. D. Siggia, and H. A. Rose. *Phys. Rev. A* **8**, 423 (1973).

[107] W. D. McComb. *The Physics of Fluid Turbulence*. Oxford University Press, New York (1990).

[108] E. Medina, T. Hwa, M. Kardar, and Y.-C. Zhang. *Phys. Rev. A* **39**, 3053 (1989).

[109] P. K. Mishra and M. K. Verma. *Phys. Rev. E* **81**, 056316 (2010).

[110] S. D. Mobbs and G. P. Lucas. *Appl. Sci. Res.* **51**, 263 (1993).

[111] A. S. Monin and A. M. Yaglom. *Statistical Fluid Mechanics*, volume 1 and 2. MIT Press (1971).

[112] M. K. Nandy. *J. Phys. A: Math. Theor.* **40**, 2219 (2007).

[113] M. K. Nandy. *Phys. Rev. E* **61**, 2605 (2000).

[114] M. K. Nandy. *Phys. Rev. E.* **55**, 5455 (1997).

[115] G. D. Nastrom, K. S. Gage, and W. H. Jasperson. *Nature* **310**, 36 (1984).

[116] G.D. Nastrom and K. S. Gage. *J. Atmos. Sci.* **42**, 950 (1985).

[117] C. L. M. H. Navier. *Mem. de l'Acad. des Sciences* **6**, 389 (1822).

[118] M. Negrea, I. Petrisor, and B Weyssow. *Phys. Scr.* **77**, 055502 (2008).

[119] R. E. Newell, V. Thouret, J. Y. N. Cho, P. Stoller, A. Marenco, and H. G. Smit. *Nature* **398**, 316 (1999).

[120] A. M. Obukhov. *C. R. Acad. Sci. URSS* **32**, 19 (1941).

[121] A. M. Obukhov. *Izv. Akad. Nauk, SSSR, Geogr. i. Geofiz.* **13**, 58 (1949).

[122] S. A. Orszag. *J. Fluid Mech.* **41**, 363 (1970).

[123] Y. H. Pao. *Phys. Fluids* **8** , 1063 (1965).

[124] Y. H. Pao. *Phys. Fluids* **11**, 1371 (1968).

[125] J. E. Paquin and S. Pond. *J. Fluid Mech.* **50**, 257 (1971).

[126] J. Pedlosky. *Geophysical Fluid Dynamics*. Springer (1987).

[127] O. M. Phillips. In A. M. Yaglom and V. I. Tarasky, editors, *Atmospheric Turbulence and Radio Wave Propagation*, pages 121–128. Moscow (1965).

[128] S. B. Pope. *Turbulent Flows*. Cambridge University Press (2000).

[129] A. Pumir. *Phys. Fluids* **8**, 3112 (1996).

[130] A. Pumir and B. Shraiman. *Phys. Rev. Lett.* **75**, 3114 (1995).

[131] A. Pumir, B. I. Shraiman, and E. D. Siggia. *Phys. Rev. E* **55**, R1263 (1997).

[132] D. Ramsden and G. Holloway. *J. Geophys. Res.* **97**, 3659 (1992).

[133] O. Reynolds. *Phil. Trans. Roy. Soc. London A* **186**, 123 (1895).

[134] O. Reynolds. *Phil. Trans. Roy. Soc. London A* **174**, 935 (1883).

[135] J. J. Riley and S. M. deBruynKops. *Phys. Fluids* **15**, 2047 (2003).

[136] J. J. Riley and M. P. Lelong. *Annu. Rev. Fluid Mech.* **32**, 613 (2000).

[137] S. Saddoughi and S. V. Veeravalli. *J. Fluid Mech.* **268**, 333 (1994).

[138] J. Schumacher, K. Sreenivasan, and P. Yeung. *Phys. Fluids* **15**, 84 (2003).

[139] M. G. Shats, H. Xia, and H. Punzmann. *Phys. Rev. E* **71**, 046409 (2005).

[140] M. G. Shats, H. Xia, H. Punzmann, and G. Falkovich. *Phys. Rev. Lett.* **99**, 164502 (2007).

[141] X. Shen and Z. Warhaft. *Phys. Fluids* **12**, 2976 (2000).

[142] X. Shen and Z. Warhaft. *Phys.Fluids* **12**, 2976 (2000).

[143] X. Shen and Z. Warhaft. *Phys. Fluids* **14**, 370 (2002).

[144] B. Shivamoggi. *Theoretical Fluid Dynamics.* John Wiley (1998), 2nd edition.

[145] B. Shraiman and E. Siggia. *Nature (London)* **405**, 639 (2000).

[146] B. I. Shraiman and E. D. Siggia. *Phys. Rev. Lett.* **77**, 2463 (1996).

[147] C. Sidi and F. Dalaudier. *Adv. Space. Res.* **10**, 25 (1990).

[148] W. C. Skamarock. *Mon. Wea. Rev.* **132**, 3019 (2004).

[149] W. C. Skamarock and J. B. Klemp. *J. Comput. Phys.* **227**, 3465 (2008).

[150] K. S. Smith and R. Tulloch. *J. Atmos. Sci.* **66**, 1073 (2009).

[151] K. R. Sreenivasan. *Phys. Fluids* **8**, 189 (1996).

[152] A. Staicu, B. Vorselaars, and W. Water. *Phys. Rev. E.* **68**, 046303 (2003).

[153] A. Staicu and W. Water. *Phys. Rev. Lett.* **90**, 094501 (2003).

[154] C. Staquet and J. Sommeria. *Ann. Rev. Fluid Mech.* **34**, 559 (2002).

[155] D.C. Stillinger, K. N. Helland, and C. W. van Atta. *J. Fluid Mech.* **131**, 91 (1983).

[156] G. G. Stokes. *Trans. Camb. Phil. Soc.* **8**, 287 (1845); **9**, 8 (1845).

[157] S. Sukoriansky, B.Galperin, and I. Staroselsky. *Phys. Fluids.* **17**, 085107 (2005).

[158] Y. O. Takahashi, K. Hamilton, and W. Ohfuchi. *Geophys. Res. Lett.* **33**, L12812 (2006).

[159] T. Tatsumi. *Adv. Appl. Mech.* **20**, 39 (1980).

[160] H Tennekes and J. L. Lumley. *A First Course in Turbulence*. MIT Press, Cambridge (1972).

[161] P. W. Terry. *Rev. Mod. Phys.* **72**, 109 (2000).

[162] M. Tjernström. *J. Appl. Mateor.* **32**, 948 (1993).

[163] A. A. Townsend. *The Structure of Turbulent Shear Flow*. Cambridge University Press (1976).

[164] Y. Tsuji. In Y. Kaneda and T Gotoh, editors, *Statistical Theories and Computaional Approaches to Turbulence, Modern Perspectives and Applications to Global-scale Flows*. Springer (2002).

[165] R. Tulloch and K. S. Smith. *Proc. Nat. Acad. Sci.* **103**, 14690 (2006).

[166] R. Tulloch and K. S. Smith. *J. Atmos. Sci.* **66**, 450 (2009).

[167] K. K. Tung and W. W. Orlando. *J. Atmos. Sci.* **60**, 824 (2003).

[168] T. VanZadt. *Geophys. Res. Lett.* **9**, 575 (1982).

[169] M. K. Verma. *Phys. Rev. E* **64**, 026305 (2001).

[170] M. K. Verma. *Phys. Rep.* **401**, 229 (2004).

[171] M. K. Verma. *Int. J. Mod. Phys. B* **15**, 3419 (2001).

[172] M. L. Waite and P. Bartello. *J. Fluid Mech.* **517**, 281 (2004).

[173] M. L. Waite and P. Bartello. *J. Fluid Mech.* **546**, 313 (2006).

[174] M. L. Waite and C. Snyder. *J. Atmos. Sci.* **66**, 883 (2009).

[175] Z. Warhaft. *Annu. Rev. Fluid. Mech.* **32**, 203 (2000).

[176] J. Weinstock. *J. Phys. Oceanogr.* **15**, 475 (1985).

[177] K. G. Wilson and J. Kogut. *Phys. Rep.* **12**, 75 (1974).

[178] H. W. Wyld. *Ann. Phys. (N.Y.)* **14**, 143 (1961).

[179] J. C. Wyngaard and O. R. Cote. *J. Atmos. Sci.* **28**, 190 (1971).

[180] H. Xia, H. Punzmann, G. Falkovich, and M. G. Shats. *Phys. Rev. Lett.* **101**, 194504 (2008).

[181] H. Xia, M. Shats, and G. Falkovich. *Phys. Fluids* **21**, 125101 (2009).

[182] V. Yakhot. *Phys. Rev. E* **49**, 2887 (1994).

[183] V. Yakhot and S. A. Orszag. *Phys. Rev. Lett.* **57**, 1722 (1986).

[184] V. Yakhot and S. A. Orszag. *J. Sci. Computing* **1**, 3 (1986).

[185] K Yoshida, T. Ishihara, and Y. Kaneda. *Phys. Fluids* **15**, 2385 (2003).

[186] V. E. Zakharov and V. S. L'vov. *Radiophys. Quantum Electron.* **18**, 1084 (1975).

[187] Y. Zhou. *Phys. Rep.* **488**, 1 (2010).

[188] Y. Zhou and G. Vahala. *Phys. Rev. E* **48**, 4387 (1993).